8-30-2011

Short & long term properties of self-consolidating concrete incorporating fly ash and local aggregate

Jacob Hays

Jacob S. Hays
Candidate

Civil Engineering
Department

This thesis is approved, and it is acceptable in quality and form for publication:

Approved by the Thesis Committee:

Dr. Mahmoud Reda Taha , Chairperson

Dr. Arup K. Maji

Dr. Rafiqul Tarefder

SHORT & LONG TERM PROPERTIES OF SELF-CONSOLIDATING CONCRETE INCORPORATING FLY ASH AND LOCAL AGGREGATE

BY

Jacob Hays

B.S., Civil Engineering, University of New Mexico, 2009

THESIS

Submitted in Partial Fulfillment of the
Requirements for the Degree of
Master of Science

Civil Engineering

The University of New Mexico
Albuquerque, New Mexico

July, 2011

DEDICATION

To my mother Sylvia, my father Samuel, my brother Tyler, and to Tamar, I love you and appreciate everything that you have done for me.

ACKNOWLEDGMENTS

To my Master's Thesis advisor and committee chair Dr. Mahmoud Reda Taha, I am extremely grateful and would like to thank you for your support. Without your valuable insights, this work could not be achieved. I am more confident in life and will certainly use what I have learned in and out of the world of engineering. The skills that I have gained here will definitely help me in the future. I would also like to thank my committee members Dr. Arup K. Maji and Dr. Rafiqul A. Tarefder for their guidance and support throughout my time as a graduate student.

I would like to thank Rick Grahn, Andrew Griffin, and Aaron Reinhardt for assisting me in the actual batching and testing of SCC. Thank you Kenny Martinez for helping repair the freeze thaw apparatus. Thanks to Dr. John C. Stormont, Lary Lenke, and Anthony Cabrera for introducing me to research here at the University of New Mexico. I would like to extend a special thanks to Bryce Simons, Jimmy Camp, and Virgil Valdez for their technical advice.

Lastly, I want to acknowledge the New Mexico Department of Transportation (NMDOT) for funding my assistantship and this research.

SHORT & LONG TERM PROPERTIES OF SELF-CONSOLIDATING CONCRETE INCORPORATING FLY ASH AND LOCAL AGGREGATE

BY

Jacob Hays

ABSTRACT OF THESIS

Submitted in Partial Fulfillment of the
Requirements for the Degree of
Master of Science

Civil Engineering

The University of New Mexico
Albuquerque, New Mexico

July, 2011

SHORT & LONG TERM PROPERTIES OF SELF-CONSOLIDATING CONCRETE INCORPORATING FLY ASH AND LOCAL AGGREGATE

By

Jacob Hays

B.S., Civil Engineering, University of New Mexico, 2009
M.S., Civil Engineering, University of New Mexico, 2011

ABSTRACT

Self-consolidating concrete (SCC) is a high performance concrete that flows under its own weight so that filling forms containing congested reinforcement is possible without mechanical vibration within placements. There has been growing interest to use SCC for precast and prestressed concrete elements. Therefore, it is important to examine the mechanical and durability properties of SCC to gain insights for the design and implementation of SCC in structures.

This Thesis presents the mechanical and durability experiments used for characterization and acceptance of SCC. Because there are many normally vibrated concretes (NVC) used today for structural applications, comparisons between the mechanical and durability properties of SCC and an NVC typically used in New Mexico bridges are performed to evaluate the performance of SCC. Two sources of local aggregate in New Mexico were used to produce SCC and NVC mixes. Mechanical properties include compressive and flexural strength, and static and dynamic modulus of elasticity. Durability properties include chloride ion resistance, freeze-thaw durability, and potential for alkali-silica reaction (ASR).

Experimental investigations show that SCC can have similar strength characteristics compared to NVC. Lowering the water to total cementitious materials ratio causes SCC to gain significant strength properties without compromising the requirements for plastic properties. Furthermore, results show that chloride ion resistivity in SCC is adequate, and in many cases exceeded that of NVC. It is recommended that air void systems of

SCC are examined in the future due to discrepancies in freeze thaw durability results of SCC. Finally, it was found that SCC does not have higher potential to ASR compared with NVC in the presence of reactive aggregate even when high dosages of chemical admixtures are provided.

CONTENTS

List of Figures

List of Tables

CHAPTER 1. INTRODUCTION

Information regarding the short and long term mechanical and durability properties of Self-Consolidating Concrete (SCC) will be of great significance for its use in structural concrete. SCC is commonly used today for many applications because it is highly workable and flows through reinforcement under its own weight without the need for mechanical vibration. SCCs incorporating class F fly ash have been investigated in this Thesis. Fly ash as a supplementary cementitious material is commonly used in New Mexico. Therefore fly ash is used here in the SCC along with viscosity modifying admixture (VMA) to achieve the required flowability characteristics of SCC mixes.

1.1 The necessity for examining the long and short term properties of SCC

The main objective of this Thesis is to examine short and long term properties of (SCC). Class F fly ash is incorporated because it is important to mitigate the effects of ASR. ASR is a long term reaction which occurs in concrete between silicates present in some types of aggregate, and alkaline earth metals in cement. Products of this reaction cause the concrete to expand. Class F fly ash is rich in silicates, and providing it to concrete mixtures allows the reaction to happen in fresh state. This eliminates the problem of long term expansion in hardened concrete. Characteristics of a group of SCC mixes were examined, and were produced using local New Mexico materials. Local New Mexico aggregates are very reactive and it is important to evaluate whether SCC produced using these materials can be used for exposed structural applications. It is beneficial to use SCC for highway bridges in the form of prestressed/precast concrete elements, and for other miscellaneous placements which require highly flowable concrete. Information on the long and short term characteristics of SCC is still limited,

and it is crucial to examine these properties using local sources so SCC can be used for bridges in New Mexico. This Thesis will also provide information about durability characteristics of SCC that can be used in future projects. Properties of SCC will be compared to a standard normal vibrated concrete (NVC) mix typically used in highway bridges in New Mexico. This information is currently unavailable and contributes crucial information for the New Mexico department of transportation (NMDOT). The main contributions of this Thesis are researching strength characteristics for up to one year, and durability properties of SCC using class F fly ash for structural concrete mixes.

1.2 Summary of Work

To investigate the properties of SCC concretes incorporating fly ash and local New Mexico aggregate, seven concrete mixes have been cast and tested. Both mechanical and durability properties have been tested for comparisons between the seven SCC and NVC mixes. Final SCC mix designs were created by trial batching. The criteria for for accepting SCC mix designs were the freshly mixed, or plastic properties, and the characteristic strength (28-day strength) of the concrete. Of the seven mixes, two are normally vibrated concrete (NVC) mix designs. Two NVC mixes were produced. The two mixes vary by aggregate source, and have similar amounts of fly ash. The other five mixes produced were SCCs that vary by aggregate source, and fly ash content. Fly ash was provided as a percent of weight of cement. Concrete mix designs were produced by optimizing the aggregate structure and then by trial batching to meet NMDOT standard requirements. Admixtures used to make SCC were provided at consistent proportions for all mixes. The fresh properties of SCC mixes were tested to confirm their compliance to standard SCC performance. The European Federation for Specialist

Construction Chemicals and Concrete Systems (EFNARC) [1] has described in detail how to classify SCC based on plastic properties and was used to accept or reject trial mixes for final mix designs. North American specifications for classifying SCC include the NCHRP state of the art for SCC used in precast/prestressed applications.

Many mechanical tests on hardened SCC have been performed to examine SCC's behavior over a one year time period. The standard tests included uniaxial compression, flexural strength, and static and dynamic modulus of elasticity. As a result, strength gain is apparent and is expected as the concrete has been cured for this relatively long period. Constituents can be proportioned in SCC so that it has properties similar to that of conventional strength NVC. SCC can easily make the strength requirements of HPC by lowering the water cementitious materials ratio.

It has been established that class F fly ash is provided as a supplementary cementitious material in NVC that is used today for all concretes produced for highway projects in the state of New Mexico primarily to inhibit ASR. Fly ash is also used here in the SCC mixes to suppress aggregate reactivity in hardened concrete, but also as a filler material to increase flowability in plastic state. It appears that class F fly ash mitigates ASR equally well in SCC. Resistance to chloride ion penetration has been measured for the concretes produced in this Thesis. SCC has been deemed adequate by having good resistance to chloride ion. Freeze/thaw durability has been measured to examine the damage to concretes exposed to cyclic freezing and thawing. Adequate freeze/thaw durability relies on a reliable network of entrained air voids incorporated within the cement paste of the concrete matrix. The results of freeze-thaw testing were not very

conclusive due to some technical problems in operating the test at early time of testing. Further research on freeze-thaw of SCC is recommended.

1.3 Outline of Thesis

Chapter 2 of this Thesis provides a literature review about proportioning and testing of SCC. This includes guidelines for proportioning constituents to meet the requirements of SCC, the various methods that have been implemented to measure plastic properties of SCC, and both mechanical and durability results of SCC. Chapter 2 describes the efforts of other researchers who have measured properties of SCC that are similar to the research of this Thesis.

Chapter 3 explains the materials and methods used for producing and examining the properties of the SCC and NVC mixes. The method of proportioning and the final mixes can be observed in chapter 3. The concrete batching procedure, plastic tests implemented, and the strength and durability tests are outlined. Analysis of test results of SCC is presented.

The results of SCC and NVC are presented in chapter 4. Commentary of the results is available in this chapter. The experimental results by others from the literature are compared with the results of our mixes. Some ideas for the implementation of SCC in the state of New Mexico are also discussed.

Chapter 5 presents the conclusions of this study. Ideas that may be implemented for future work are also available in this chapter.

CHAPTER 2. LITERATURE REVIEW

2.1 Introduction to Self-Consolidating Concrete

Over the last two decades, there has been an increase in the use of Self Consolidating Concrete (SCC), also referenced as "self compacting concrete", as an alternative to normally vibrated concrete (NVC). The use of self consolidating concrete (SCC) for structural applications is common because of its high flowability. It reduces voids within placements and increases the homogeneity of concrete in congested forms. SCC must also meet specific workability and passability requirements. The first prototype mix was completed in 1988 in Japan by Ozawa et al.[2]. Since then, SCC has gained significant momentum and has been used successfully in both bridges and structures [3-5]. SCC is best characterized by its ability to flow under its own weight while maintaining strong resistance to aggregate segregation. This allows placing SCC without the need for mechanical consolidation. SCC can flow through congested reinforcement and fill all the corners of formwork without losing homogeneity. The development of SCC represents outstanding recent advances in concrete technology.

According to Okamura and Ouchi (1998), the conditions that need to be met in order to be considered as an SCC are self compactability in fresh state, avoidance of initial defects in early age, and protection against external factors in hardened state. Methods for achieving self compactability are limiting the aggregate content, providing a low water powder ratio, and by using superplasticizer. The water powder ratio is the ratio between the weight of water in the mixture by the weight of cement, filler, and sand particles finer than 0.125 mm. Limiting the coarse aggregate content reduces the number of collisions and the contact interval between coarse aggregate particles. High frequency

of contact and collision results in increasing internal stress and friction when the concrete is deformed, resulting in blockage of aggregate particles near obstacles. Limiting the amount of fine aggregate in the mix reduces the pressure transfer between coarse aggregate particles. A highly viscous paste reduces internal stress when coarse aggregates approach obstacles. Therefore a very low water cementitious materials ratio (*w/cm*) is needed to increase the viscosity. Having such a low water cementitious materials ratio with the high expected flowability requires the use of superplasticizers [6]. A simple mix proportioning method proposed by Okamura and Ozawa require that the aggregate grading is fixed, so that the water powder and superplasticizer is adjusted to achieve the desirable fresh concrete properties. The coarse aggregate is recommended to be fixed at 50% of the solid volume, fines should be at 40% of the mortar volume, water/powder by volume should be in between 0.9 and 1.0, and superplasticizer and final water/powder ratio are determined so as to ensure self compactability [7]. Adding superplasticizer to concrete mixes reduces the amount of water that is required for achieving workability requirements. There are electrical and chemical effects that result from providing superplasticizer to concrete. The electrical effect is important because like electrical charges are created in the mixture which results in the repulsion of the constituents making up the concrete. The chemical effect is achieved by modifying the structure of some early formations of hydrated cement by giving them less cohesive solid structures.

In the Specification and Guidelines for Self-Compacting Concrete produced by the European Federation for Specialist Construction Chemicals and Concrete Systems (EFNARC), design parameters and plastic testing methods are described in detail. The

typical content of cement for SCC is between 350-450 kg/m^3. It is mentioned that over 500 kg/m^3 can be dangerous due to increased shrinkage and below 350 kg/m^3 may not be suitable with the inclusion of fillers such as fly ash. All normal concrete sands are suitable for producing SCC, but it is realized that fines less than 0.125 mm are considered as powder and are very important for the rheology of self compacting concrete. All types of coarse aggregate are suitable for making SCC though the nominal maximum size is typically 16–20 mm. Superplasticizer is the most important chemical admixture because SCC requires a low water to total cementitious materials ratio, but viscosity modifying admixture (VMA) provides the ability to control segregation when the amount of powder is limited.

Two types of SCC can be produced using one of two different methods. The two types are powder type SCC, and viscosity modifying admixture (VMA) type SCC. A combination of powder and VMA type SCC is also possible. In fact, SCC used in the field is considered as being in between powder type and VMA type SCC [8-13]. Powder type SCC uses superplasticizer and it is absolutely necessary to have a low water to cementitious materials ratio. To achieve self compactability, the combined aggregate gradation is optimized until the desired properties are met. Because limiting the coarse aggregate content reduces the number of collisions, the levels of intermediate and fine aggregates shall dominate the grading to reduce the effects of blockage. Figure 1 shows both the mechanism of blockage and self compactability of concrete flowing under its own weight. Larger aggregate occupies volume in ordinary concrete mixes, and through this keeps the cost fairly low. SCC uses only smaller aggregate, so large amounts of cementitious fillers such as silica fume or fly ash are typically used to keep the cost of

SCC comparable. VMA type SCC incorporates VMA (also known as viscosity enhancing admixtures (VEA)). Typical VMAs are water-soluble polysaccharides that increase cement paste's ability to retain water [10]. Adding VMA changes the concrete's cohesion, while allowing the mix to retain the desired properties [14-16]. VMAs increase the viscosity of the concrete by decreasing the flow or kinetic energy. VMA eliminates need for having a low *w/cm* ratio. Because adding more water exponentially reduces the viscosity, it is advantageous to add VMAs to control problems such as bleeding and/or segregation. Since adding small amounts of water drastically effects viscosity, it is sometimes difficult to separate the low water cementitious mixes from the mixes produced with VMA [17].

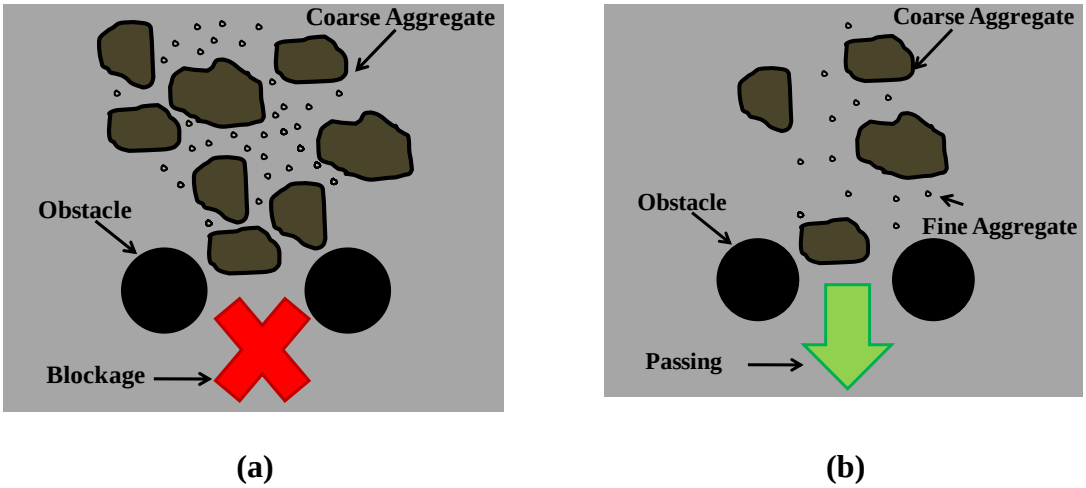

Figure 1: Schematic representation of (a) Mechanism of Blockage (b) Mechanism of self compactability produced in SCC mixes.

Khayat [10] showed that an optimal combination of superplasticizer and VMA produces a fluid mix with good segregation resistance. It has also been shown that the incorporation of a VMA results better filling capacity while resulting in the reduction of surface settlement [18-19]. Increasing the VMA content from 0.025% to 0.075% (by weight) in mixes containing silica fume and fly ash resulted in a substantial reduction in

settlement even though both mixes had similar flowability. It has also been reported that concretes with a high percentage of VMA showed up to a 61% increase in filling capacity [10, 20-21].

The National Cooperative Highway Research Program (NCHRP) has reported that SCC mixes with a *w/cm* of 0.4 and a low dose superplasticizer exhibited enhanced static stability when a VMA was introduced [3]. Slow development of early age properties result from adding VMA in concrete mixtures. The NCHRP report recommended the use of VMAs for concretes with a *w/cm* higher than 0.40, but VMA can be used in mixes below 0.40 to create a highly stable SCC. High dosages of VMAs greatly increases the need for superplasticizers [3].

2.2 SCC Fresh Properties

SCC mixes are mainly defined by their fresh state properties. The fresh characteristics that define SCC mixes include:

- **Flowability** – ability of fresh concrete to flow under its own weight.
- **Viscosity** – the resistance to flow once fluidity has been initiated.
- **Passability** – ability of the concrete to flow under its own weight through tightly spaced formwork and/or rebar without segregation or blocking.
- **Segregation Resistance** – ability of the concrete to sustain a homogenous composition in a fresh state [The European Guide lines for Self-Compacting Concrete 15].

Several different techniques to determine the behavior of SCC mixes in the fresh state have been developed. To measure flowability the slump flow test is commonly used. Plastic concrete tests implemented for SCC are also outlined in detail with specifications

in the Specification and Guidelines for Self-Compacting Concrete by the EFNARC. The slump flow test is used to assess the horizontal free flow of SCC without obstructions. It was first developed in Japan to evaluate underwater concrete acceptance. It is based on the test method to measure slump of normal concrete mixtures. The slump flow test requires the use of the same equipment required for a typical slump test except it requires no consolidation or tamping [22]. The diameter of the concrete circle is a measure of the filling ability of concrete.

The procedure for measuring slump flow is different from the ordinary slump test. To measure slump flow, the base plate and interior of the slump cone are moistened in a way that there will be no free water on the surfaces. The cone is then held to the center of the base plate on level ground, and filled in a single lift of SCC to the top. The top of the cone is then leveled, and all excess concrete around the cone is removed. The cone is lifted vertically to allow the concrete to flow free. The largest diameter and a diameter at a right angle to the largest diameter are then measured and the mean of these values is considered as the slump flow. Slump flow is a measure of concrete flowability. Figure 2 shows a set-up of a typical slump flow test with the two required measurements. This value of the slump flow test describes the ability of the concrete to flow under unconstrained conditions [3, 15, 23-24].

The measure of the slump flow diameter is required to be between 550 - 850 mm (21.5 – 33.5 inches). The three classifications of slump flow are SF1, SF2 and SF3 [1]. The slump flow for the SF1 class ranges between 550-650 mm (21.5–25.5 inch). Typical applications of SF1 mixes include concrete structures with little reinforcement, pump injecting systems and small sections that do not permit horizontal flow. SF2 describes

mixes with a slump flow in the range of 660-750 mm (26–29.5 inch). This range works for most conventional civil engineering applications such as walls and columns. The SF3 class describes SCC mixes with high slump flow. SF3 ranges between 760-850 mm (30–33.5 inch). Concretes within this class are typically used with highly congested reinforcement and structures with complicated shape. SF3 mixes are assumed to give a better finish than the other two classes. Segregation control of SF3 SCC is a big problem. SCCs with a slump flow higher than 850 mm are known to be unreliable in stability.

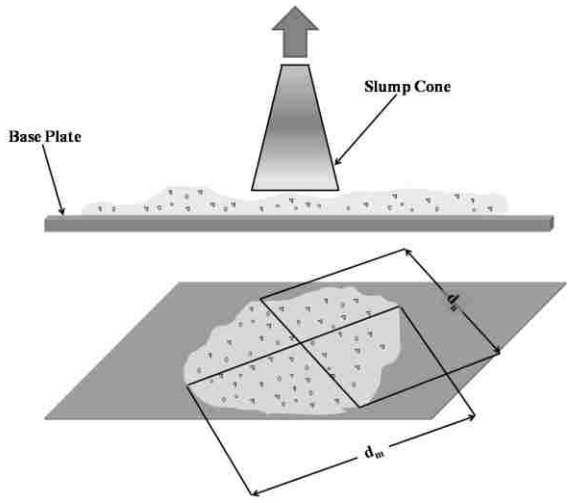

Figure 2: Schematic of the slump flow test set up showing the required measurements typically performed for SCC.

Another rheological property used to define SCC mixes is viscosity. While conducting the slump flow test, we can simultaneously measure viscosity. The time it takes for the freely flowing concrete to reach a diameter of 50 cm is known as T_{50} and is recorded in seconds. T_{50} is a secondary indication of flow where a low value indicates higher flowability. It is suggested that T_{50} is between 3-7 seconds for civil engineering applications. The value is related to the viscosity because it describes the rate of flow.

Low (VS1) or high (VS2) are the two categories that the T_{50} can be categorized as. VS1 represents concretes with a flow time of lower than two seconds and the VS2 represents concretes with a flow time higher than 2 seconds. VS1 mixes are used in applications with highly congested reinforcement and usually result in a good surface finish. Segregation is a problem for the VS1 mixture. VS2 mixes have a higher resistance to segregation than VS1 mixes, but perfect surface finishes are more difficult to achieve [1, 25].

Viscosity can also be measured using funnels to measure the time it takes for concrete to flow out. The o-shaped funnel and the v-shaped funnel are the two different types of funnels used for the funnel flow test. The time it takes for the concrete to flow out of the funnel gives an indication of its viscosity by correlating the flow rate to viscosity [18-19, 26-33]. Like the T_{50} viscosity test, the v-shaped funnel flow test shown in Figure 3 can be used to categorize SCC into high and low viscosity categories. VF1 represents concretes with a funnel flow of less than 8 seconds. VF2 represents v-funnel flow times within a range of 9 and 25 seconds [1, 19, 27, 34].

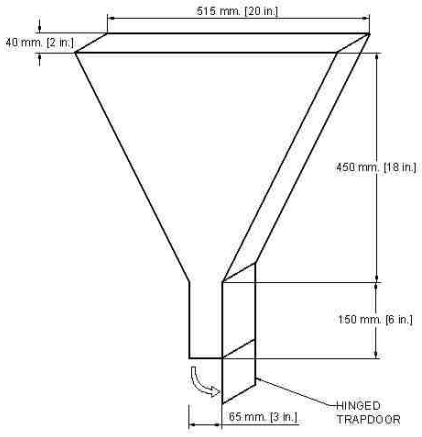

Figure 3: Schematic of V-Funnel Test [1].

Passability is another important freshly mixed concrete property for SCC. The most common tests to measure this are the J-Ring, U-box, and L-box tests. Passability is important as it is represents the ability of SCC to flow around obstacles such as reinforcement which is critical criterion for SCC. The J-ring test shown in Figure 4 is the slump flow test incorporating obstacles mimicking reinforcement. A ring with variable spaced rebar simulating a reinforcement configuration is placed over the cone to fence the concrete contained in the cone. The cone is raised and the concrete flows from the inside of the ring to the outside of the ring. The concrete diameters collected with and without the presence of the J-ring represent the level of passability [19, 26, 32, 34-35].

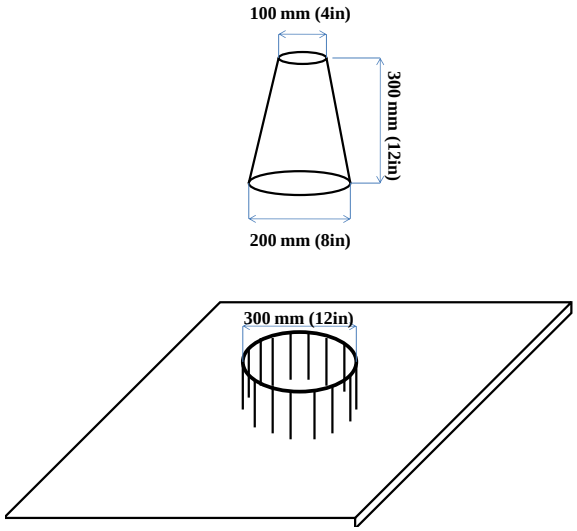

Figure 4: J-ring test setup.

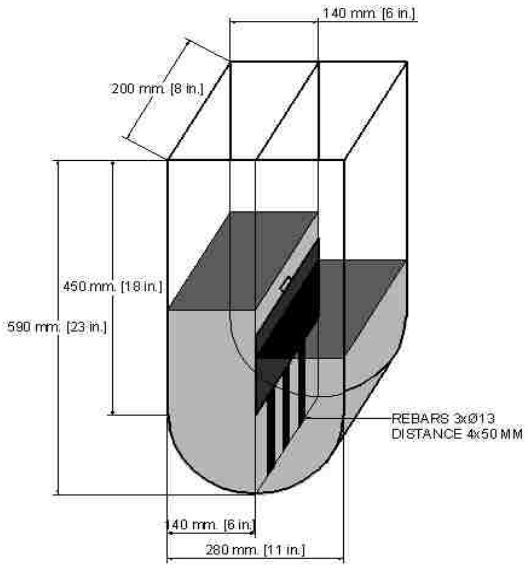

Figure 5: U-ring test setup and typical dimensions.

The U-box test involves a u-shaped box divided by a gate fixed with obstacles comparable to rebar. The difference in height of the concrete on the two sides of the box represents the passability [26, 33-36]. The U-ring test is shown schematically in Figure 5.

The L box test method is also a measure of passing ability, and consists of a rectangular section in the shape of an "L". The L-box test uses the same principles used in the U-box test except the apparatus has an L-shape. The vertical and horizontal sections are joined by a movable gate with vertical reinforcing bars directly in front of it. The L- box apparatus is placed on level ground, while the gate is in the closed position. The inside surfaces are moistened and surplus water is removed. The vertical column of the L shape is filled to the top with concrete, leveled at the top, and allowed to stand for one minute. The gate is lifted and the concrete is permitted to flow through the vertical reinforcing bars to the horizontal section of the L shape. Once the concrete stops flowing, the difference in elevation of the free concrete surface is evaluated at the furthest

point behind the reinforcement, and the furthest point beyond the reinforcement to get the blocking ratio. The blocking ratio is calculated as seen in Equation 1. Figure 6 shows the L box apparatus with the elevations required to calculate the blocking ratio.

$$Blocking\ Ratio = \frac{H2}{H1} \tag{1}$$

The blocking ratio would be unity if the test were conducted with water. Figure 6 shows a schematic of the L-box apparatus with a three bar obstacle representing a highly congested situation. The passability ratios are classified as either PA1 or PA2. PA1 represents concretes with an L-box ratio of 0.8 and above for tests performed with a 2 rebar obstacle and PA2 represents concretes with a ratio of 0.8 and above for tests with a 3 rebar obstacle [1].

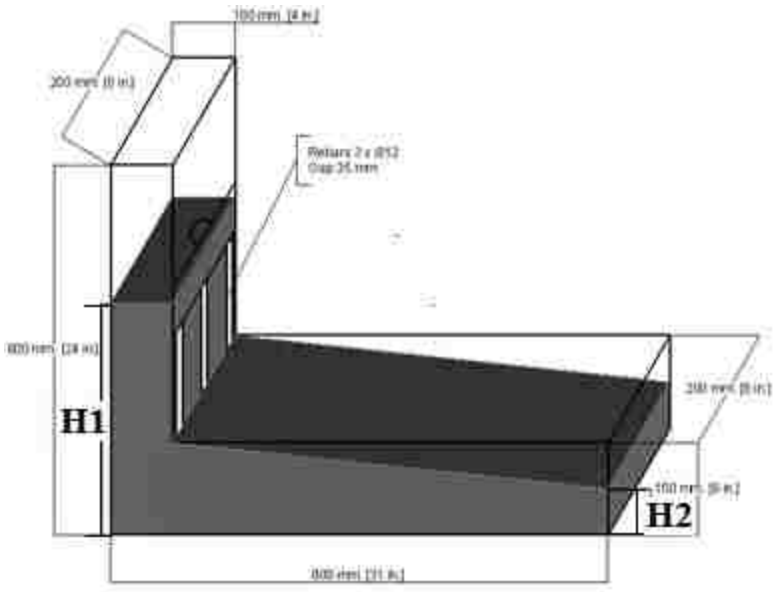

Figure 6: L-box test apparatus.

Segregation resistance of the fresh concrete mixes can be measured through penetration tests, a settlement column test, or a sieve segregation test. The sieve segregation test, shown below in Figure 7, involves pouring concrete over a 5 mm (#4)

sieve and measuring the amount of mortar passing through over a two-minute period. The percentage of mortar passing through the sieve represents the measure of segregation resistance [1, 33, 35-36]. The segregation resistance classes are SR1 for a segregation percentage less than or equal to 20% and SR2 for a segregation percentage less than or equal to 15%. SR1 is appropriate for applications with a confinement gap of less than 5 m (16.0 ft) and a flow distance of more than 80 mm (3 in). SR2 mixes are applicable for situations with a confinement gap of more than 5 m (16.0 ft) and a flow distance of less than 80 mm (3 in) [1, 33, 35-36].

Many researchers reported problems in obtaining target air content using conventional air-entrainment admixtures in SCC [37-40]. Flowability of SCC can cause air-bubbles to become unstable in an air entrained SCC. Superplasticizers of the new generation that are used to commonly achieve SCC fresh properties are shown to deteriorate air system stability [40]. It has been recommended to use anti-foaming admixtures in SCC mixes, to counteract the excessive air developed in SCC [37, 40].

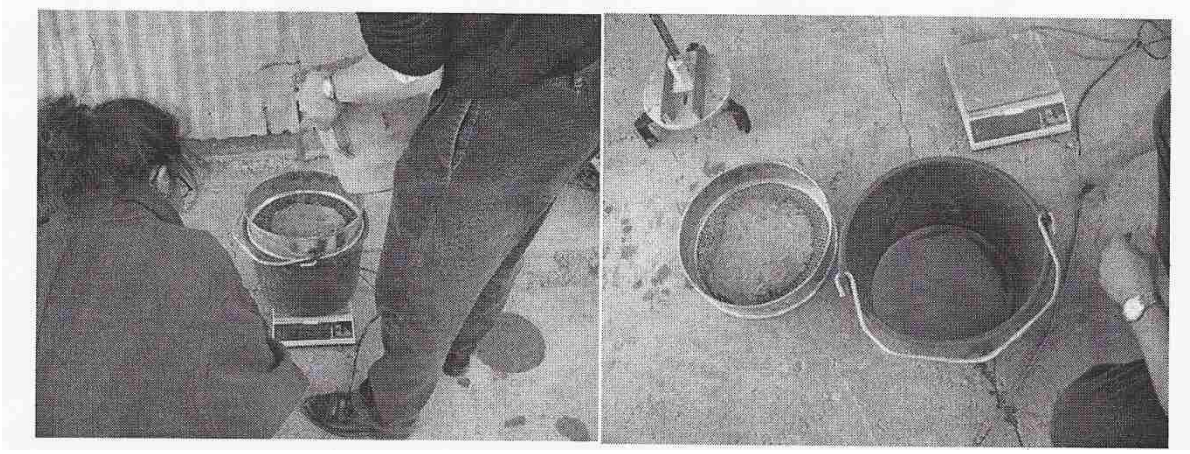

Figure 7: Sieve segregation test [1].

2.3 Strength Characteristics of SCC

Because of the differences in material proportioning and the fresh properties which characterize SCC, hardened properties are expected to be different from NVC. The SCC microstructure is enhanced and this is reflected in strength, but also improved durability properties and highly effective bondage to steel reinforcement. Some researchers have found strength improvements particularly in powder type SCC mixes. SCC mixes containing limestone based aggregate showed that early age compressive strength was significantly higher compared to NVC mixes with similar water to cementitious materials ratios [41-42]. On the other hand, SCC mixes show higher variation in hardened properties because of the mix proportions and wide range of materials used for producing SCC, and wide range of material [42].

Early strength gain relationships for various SCC mixes incorporating high volumes of fly ash were developed by Sukumar et al. [37] to account for the difference in comparison to NVC mixes. Andic-Cakir et al. [43] showed that when developing SCC mixes with light weight aggregate, a loss of strength greater than the reduction in unit weight is observed. The use of VMA has a negative impact on the compressive strength of superplasticized mortars. Because of this, it is recommended to assess the rheological properties and the strength the superplasticizer-VMA-cement system before its use in producing SCC [44].

It was reported that there is an average difference of 4 MPa between cube and cylinder strength of SCC whereas the observed difference between the two specimens for NVC is 8 MPa [42]. This was attributed to the smoother crack surfaces present in SCC because of the lower content of coarse aggregate when compared with NVC [42].

Experimental results on 70 recent SCC mixes showed that there is no significant difference between SCC and NVC mixes from the splitting tensile strength and the modulus of rupture [42] Because of the lack of large aggregate in SCC mixes, they are expected to have a lower Young's modulus of elasticity than NVC mixes. Domone [42] compared the elastic modulus of SCC mixes found from over the 70 recent studies with those of NVC mixes. In figure 8, the relationship between elastic modulus and compressive strength is displayed. At low strength levels it was found that lower strength SCC mixes have average stiffness that is approximately 40% less than NVC mixes of similar strength. It can be observed that at higher strength levels this difference is reduced to less than 5% [42]. Schindler et al. [45] reported modulus of elasticity as not being significantly different than that of NVC.

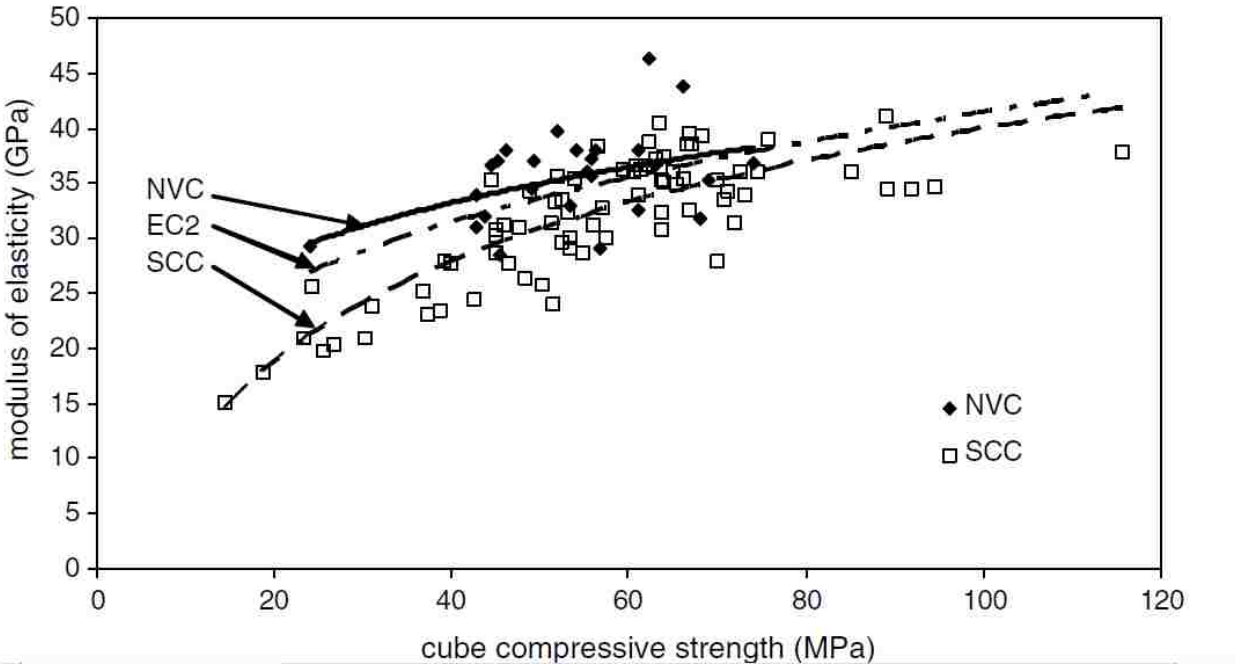

Figure 8: Elastic modulus vs. compressive strength in NVC and SCC [42]

2.4 Durability Characteristics of SCC

The high volume of powder filler incorporated into SCC and the admixtures used to achieve the workability required in SCC mixes result in varying pore volumes, ionic composition and chloride binding behavior [46]. Chloride ion experiments revealed that chloride diffusivity is dependent on the type of cement and the type of pozzolanic material supplemented. In experiments performed on SCC mixes with varying amounts of fly ash, Yazici showed that SCC mixes have sufficient chloride penetration resistance [47]. Other results suggested that chloride diffusivity of SCC mixes cannot be compared to NVC mixes based on solely strength and *w/cm*. Moreover, even with SCC mixes having a different microstructure in comparison with NVC mixes no indication has been given that suggest that standard chloride ion penetration tests are inadequate for SCC mixes [46]. Aisse showed that SCC has excellent durability characteristics with enhanced chloride ion permeability resistance [48-50].

Nehdi and Bassuoni explored the behavior of 21 different SCC mixes with a *w/cm* of 0.38 exposed to the dual action of sulfate attack and frost resistance [51]. These mixes contained varying sand to aggregate ratios, varying air entrainment admixtures, varied amounts of fibers and different binder combinations which included Portland cement, CSA Type 50 (ASTM Type V) sulfate resistant Portland cement, silica fume, Class F fly ash, slag and limestone filler. Figure 9 shows the results of specimens made with (a) 100% ordinary Portland cement (b) 100% sulfate resistant Portland cement, (c) 50% ordinary Portland cement + 15% limestone filler + 20% silica fume + 15% fly ash, and (d) 50% ordinary Portland cement + 15% limestone filler + 20% silica fume + 15% fly ash and fibers.

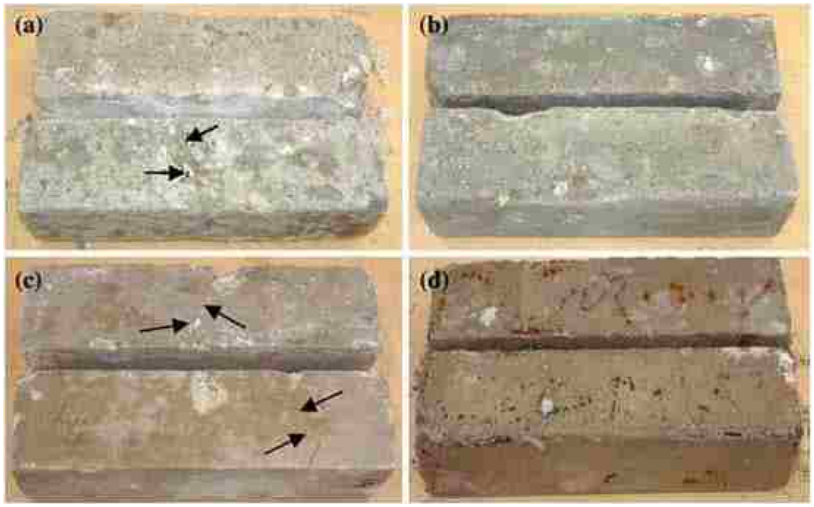

Figure 9: Visual results of SCC specimens subject to the dual action of frost resistance and sulfate attack [51].

It was found that all SCC mixes were able to resist sulfate attack when not combined with freeze-thaw cycles. However, the combined action of sulfate attack and frost action showed durability problems including surface scaling of mixes containing 100% ordinary Portland cement and incipient TSA of mixes containing limestone powder. Adding air-entrainment enhanced SCC mixes ability to resist the combined attack initially, although over time these mixes were shown not immune to degradation [51].

SCC was also shown to have similar internal frost resistant and salt scaling to that of NVC mixes, as long as the SCC mixes are made with a sound aggregate, meet strength requirements, do not exhibit excessive segregation or bleeding and have an adequate air void system [46]. For SCC mixes, the salt scaling resistance is sensitive to local variations in the air void system and bleeding or segregation that might occur when the concrete flows under its own weight. Persson compared the salt frost scaling and the internal frost resistance of SCC mixes of varying filler amounts, air contents and methods

of casting to an NVC mix of similar *w/cm* with an air content of 6% [52]. These tests indicated that the SCC mixes performed better than the NVC mixes in resisting internal frost action and that the mixes performed similarly in resisting salt scaling [52].

Little is known about the behavior of SCC with respect to alkali silica reaction (ASR) since field reports about damages do not yet exist [46]. However, since there is no indication that the link between moisture present, alkalinity of the pore solution, incidence of reactive aggregates and expansion of concrete is fundamentally different, the same measurements taken for NVC should be used for SCC [46]. Lowke et al. [53] showed SCC to have an adequate ASR resistance when appropriate volumes of fly ash were incorporated in the SCC mix. Shi and Wu [54] suggested the use of ground glass powder to produce SCC and showed that SCC mix to have adequate properties. SCC containing glass powder was reported not to exhibit deleterious expansion, even if alkali-reactive sand was used as fine aggregate of the concrete [54].

CHAPTER 3. EXPERIMENTAL METHODS

3.1 Materials Used for Concrete

All materials used to make these mixes were local New Mexico materials of interest to the Department of Transportation. Two aggregate sources were selected from the state of New Mexico. One of the sources is from Lafarge's pit in Placitas, New Mexico, and the other source used is from Griego and Sons Construction's pit in Ft. Sumner, New Mexico.

Figure 10: Locations of New Mexico's concrete material sources

Type I/II Portland cement [55] was used for this project and was produced in Tijeras, New Mexico by GCC Rio Grande Cement Company. Class F Fly ash [56] came from Salt River Materials Group's plant located at the coal burning power plant in Farmington, New Mexico. Fly ash is a product from coal burning in power plants for energy generation. It is a waste product available in the Rocky Mountain region of the US, so it is typically cheaper than other supplementary cementitious materials. There are two classes of fly ash: class C, and class F. They are different in chemical composition specifically silica oxide [56]. Class F fly ash has higher silica than class C fly ash, and tends to have less CaO by mass than class C. It is well known that class F is more suitable for mitigating ASR compared to class C fly ash. Admixtures used to make VMA types of SCC include high range water reducer (superplasticizer), and viscosity modifying admixture (VMA). To meet the New Mexico DOT standards, small amounts of air entraining admixture were provided to the mixes to produce the total required air to be 6-9% as in the NMDOT standard specification of highway and bridge construction. The types of admixtures used include BASF Glenium 3030 NS as superplasticizer, BASF Rheomac VMA 362 as VMA, and Grace Daravair AT-60 resin based air entrainment admixture. Finally, public potable water supply of the city of Albuquerque was used for the mixes.

Materials used to make the mixes were collected in bulk by estimating the required amount, and by doubling the quantity to ensure that a large enough sample size was collected. Aggregates were sampled from the rock quarries in the locations mentioned earlier. We were directed by authorized personnel to the stockpiles of aggregate classes requested, and the manufacturer scarified and blended a section of the

stockpile to be sampled. The aggregates were shoveled into 55 gallon sealable drums, or in some cases burlap sacks. These were separated into categories of coarse, intermediate, and fine aggregate. The drums containing the aggregate were then transported to the laboratory to be stored for future use. Fly ash was collected in a similar way, but cement was collected in 94 pound sacks directly from the producer. All admixtures used for the project were collected at the beginning, and enough was purchased for the entire project.

Figure 11: Aggregate stockpile in Ft. Sumner, New Mexico.

3.2 Aggregate Testing

Once the Aggregates were collected, tests were conducted to observe their properties. To replicate the grading for concretes that are used for NVC1 and NVC2, it was necessary to proportion the amounts of fine, intermediate, and coarse aggregate to resemble the existing mixes used for structural applications today. All necessary experiments on aggregate needed to make concrete have been performed. The

experiments included the grading tests [57], the specific gravity and absorption content tests on coarse and fine aggregate [58], and the moisture content tests [59]. Both aggregate sources included three different sizes (coarse aggregate, intermediate aggregate and fine aggregate). Each type of aggregate was sieved to determine the percentage passing.

The sieve analysis test is started by attaining a large sample from each type of aggregate in the storage location. In accordance with ASTM C702 [60], for Reducing Samples of Aggregate to Testing Size. The method of splitting was selected for this. In specification with ASTM C136, the required amounts for the types of aggregate collected were over 5000 grams for our coarse aggregate, over 1500 grams for our intermediate aggregate, and over 300 grams for fine aggregate after drying. Care was always taken to ensure that sample size conditions were satisfied in the dry condition. Once the new samples for sieve analysis were collected, each sample was washed over a #200 sieve according to ASTM C117 [61] to determine the content of particles finer than 75 micrometers. If the percent passing the #200 is greater than 3%, the aggregate cannot be used for concrete because of problems with water absorption rates and clay expansion. After washing, the sample is dried in a conventional oven at 110 degrees Celsius for 24 hours. Final grading was determined using all standard sieves, as individual weights retained on each sieve with a scale satisfying the requirements of the specification. The cumulative amount passing can be calculated based on retained weights of each individual sieve. Once the grading was known for each type of aggregate, attempts were made to proportion each type to match required grading for concrete mixes by trial and error. The proportioning of these three sizes to produce the final mixes was determined

using an optimization approach. Once this was attained, a sample of combined aggregate was mixed together in the laboratory, and a complete gradation was determined. The combined laboratory gradation compared with the proposed grading used for the NVC mixes can be seen in the results section. The results of mixing the three sizes of aggregate with these proportions are compared to the aggregate grading reported by the supplier of the concrete mixes. The combined optimal aggregate grading therefore meets the reference aggregate grading produced by Lafarge in NVC1, and Rivera's in NVC2. Comparisons of the two optimal gradations produced in the lab and those provided by the reference mixes are shown in the results section for NVC1 and NVC2. This is a necessary step such that the proposed NVC mixes can be used as a reference mixes. The equations used to calculate the percentage of particles passing certain sieve sizes can be seen below. In Equations 1 and 2, i = the value corresponding to a particular sieve size. Equation 3 is how the max density gradation for percentage passing is found using the 0.45 power curve. D_i = size of particle for the ith standard sieve, and D_{NM} represents the nominal maximum size aggregate for which 95% or more passes.

$$(Cumulative\ \%\ Retained)_{i+1} = (Cumulative\ \%\ Retained)_i + (\%\ Retained)_{i+1} \quad (2)$$

$$(Cumulative\ \%\ Passing)_i = 100\% - (Cumulative\ \%\ Retained)_i \quad (3)$$

$$Max\ Density\ Gradation = \left(\frac{D_i}{D_{NM}} \right)^{0.45} \quad (4)$$

(a) (b)

Figure 12: (a) Splitter used for attaining smaller aggregate samples, (b) Gilson Shaker used to determine combined grading of aggregate.

Specific gravity of all aggregate types was measured using ASTM C127 for coarse and intermediate aggregate, and ASTM C128 for fine aggregate. Samples for specific gravity were collected the same way that samples for sieve analysis were collected, and split down to required sample size using ASTM C702. The aggregate was sieved with a 5 mm (#4) standard sieve to eliminate finer particles in coarse aggregate and larger particles in fine aggregate. Following this, each aggregate type is soaked in water over night.

Coarse aggregates are removed from the water, and placed onto a damp towel to be dried to a condition that is saturated but surface dry (SSD). The specimen is immediately weighed at this point. To determine the volume of the sample weighed at SSD, the sample is weighed while it is submerged in water. The water used for all specific gravity tests must be 75.0 ^{o}F (23.0 ^{o}C). The mass of the sample in water

represents the mass of the water displaced. The sample is then oven dried, and the dry weight in air is found. Using the data collected from this experiment, the apparent, bulk saturated surface, and bulk dry specific gravities can be determined. The aggregate absorption can be determined by knowing the difference in weight between the aggregate at SSD, and the oven dried aggregate. The equations below are used to calculate specific gravity of coarse aggregate. A = weight of oven dried specimen in air, B = weight of saturated surface dry specimen in air, C = weight of saturated specimen in water.

$$Bulk\ Specific\ Gravity\ (Dry\ Basis) = \frac{A}{(B-C)} \tag{5}$$

$$Bulk\ Specific\ Gravity\ (SSD) = \frac{B}{(B-C)} \tag{6}$$

$$Apparent\ Specific\ Gravity = \frac{A}{(A-C)} \tag{7}$$

$$Absorption, \% = \frac{B-A}{A} \times 100\% \tag{8}$$

Determining the specific gravity of fine aggregate is more difficult, but the methodology is similar. SSD for fine aggregate is determined by understanding that absorbed water within the sand particles does not contribute to internal pore water pressure that will allow sand that is compacted into a mold to take shape of the mold when it is removed. The fine aggregate is removed from its saturation in the container, and spread out onto a table. A conventional fan is permitted to pass an air stream over the sample to assist in slow drying. The sample is constantly mixed so the drying is consistent. To determine whether or not the sample is at SSD, the sand is compacted into

a small cone with known compactive energy. When the cone is lifted vertically, the sand will not be able to assume the form of the mold if SSD condition is reached. The sample is immediately weighed, and the specimen is placed into a pycnometer of established weight when containing water only at its capacity. Once the sample is in the pycnometer, de-aerated water is poured over the sample to approximately half the capacity. The sample with water is agitated until there are no air bubbles left within the mixture. The remainder of pycnometer is carefully filled to capacity with water, and weighed. The difference between the weight of the pycnometer filled with soil and water at capacity, and the weight of the pycnometer filled with water only at capacity represents the volume of the sample within the pycnometer. Similarly, the specimen is then oven dried to collect the dry weight of the sample in air. By using the data collected the apparent, bulk saturated surface, and bulk dry specific gravities can be determined. The aggregate absorption is known by comparing the difference between the weight of the sand at SSD, and the oven dried sand. For purposes of research, the bulk specific gravity at saturated surface dry condition, and the absorption were required for all aggregate types. The following equations are used to calculate specific gravity of fine aggregates. A = weight of dry specimen in air, B = weight of pycnometer filled with water only, S = weight of saturated surface dry specimen, C = weight of pycnometer with specimen and filled with water.

$$Bulk\ Specific\ Gravity\ (Dry\ Basis) = \frac{A}{(B + S - C)} \tag{9}$$

$$Bulk\ Specific\ Gravity\ (SSD) = \frac{S}{(B + S - C)} \tag{10}$$

$$Apparent\,Specific\,Gravity = \frac{A}{(B + A - C)} \tag{11}$$

$$Absorption, \% = \frac{S - A}{A} \times 100\% \tag{12}$$

(a)

(b)

Figure 13: Specific gravity of coarse aggregate (a) submerging aggregate at SSD (b) determining the weight of water displaced.

Tables 1 and 2 show the optimized proportions of aggregate proposed to make the two NVC mixes with the aggregate sampled from the Placitas and Ft. Sumner locations to match the grading required by the NMDOT. Three types of aggregate from each source were used and have been classified using ASTM C33 to classify aggregates used for making concrete [62]. Figures 15 and 16 represent the combined gradation of the optimized proportions conducted in the laboratory.

(a) (b)

Figure 14: Specific gravity of fine aggregate (a) preparing sand to be at SSD (b) determining the volume of sand using calibrated pycnometer.

The proportion of the three components for the SCC mix was determined experimentally such that the proposed mix satisfies the flowability requirements of SCC. The final proportion for the SCC mixes using the Placitas aggregate (SCC1 and SCC2) is provided in Table 4. The gradation of the SCC1 and SCC2 mix aggregates is shown in Figure 17. The gradation of the SCC3, SCC4 and SCC5 mix aggregate is shown in Figure 18. It is confirmed that these proportions are required to achieve the required flowability of this type of SCC. It is important to note that the proposed SCC mix is pozzolanic-type SCC and not a powder type SCC. Therefore aggregate gradation that satisfies flow requirements with fly ash shall be the target and not through sole aggregate skeleton optimization.

Table 1: Optimal proportions of three aggregate sizes to produce NVC1

Aggregate Proportioning used from Optimization		
Aggregate Type	Designation	% of total Aggregate
Coarse	ASTM C33 #6	24%
Intermediate	ASTM C33 #8	40%
Fine	C33 fine/Lafarge 8515	36%

Table 2: Optimal proportions of three aggregate sizes to produce NVC2

Aggregate Proportioning used from Optimization		
Aggregate Type	ASTM Designation	% of total Aggregate
Coarse	C33 #6	40%
Intermediate	C33 #8	10%
Fine	C33 Fine Aggregate	50%

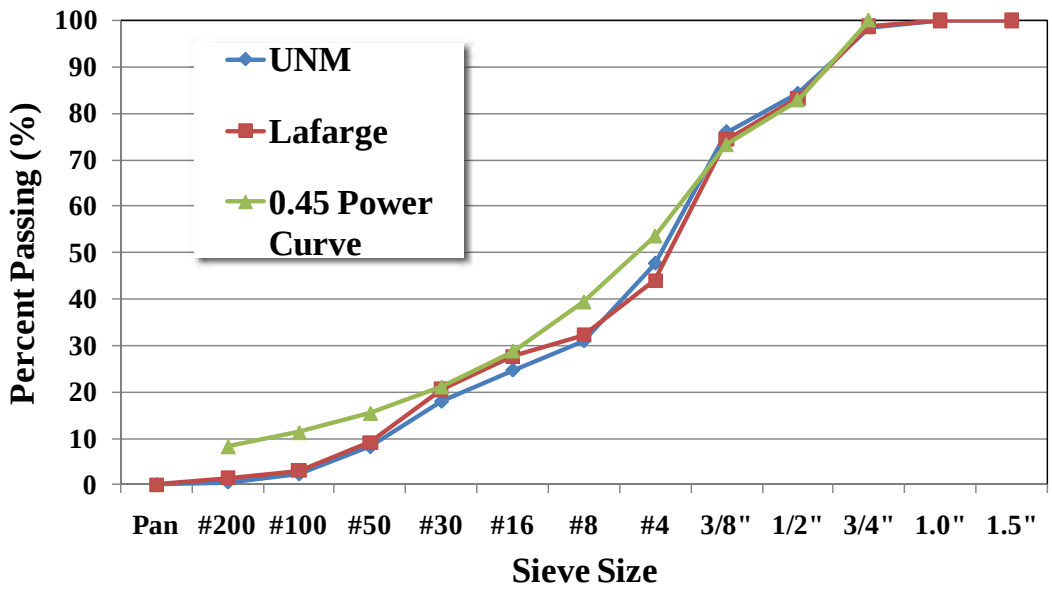

Figure 15: Optimal combined aggregate for NVC1 versus aggregate reported by Lafarge.

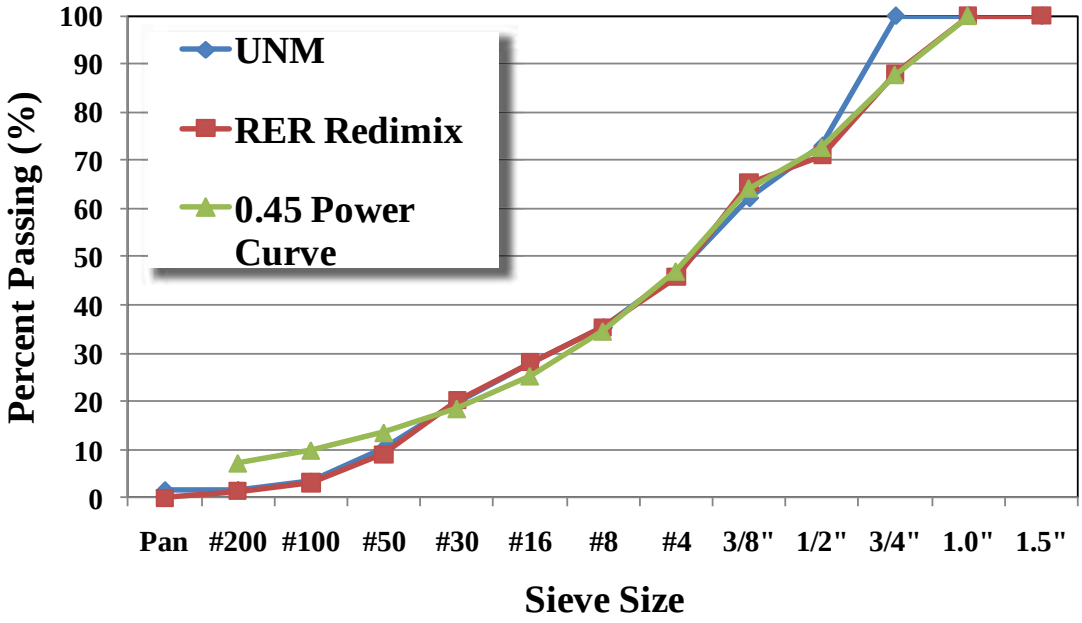

Figure 16: Optimal combined aggregate for NVC2 versus aggregate reported by Rivera. (Aggregates are supplied by Griego and Sons Construction)

Table 3: Optimal proportions of three aggregate sizes to produce SCC1-2 mixes

Aggregate Proportioning used from Optimization		
Aggregate Type	ASTM Designation	% of total Aggregate
Coarse	C33 #6	0%
Intermediate	C33 #8	45%
Fine	C33 fine/Lafarge 8515	55%

Table 4: Optimal Proportions of three aggregate sizes to produce SCC3-5 mixes

Aggregate Proportioning used from Optimization		
Aggregate Type	ASTM Designation	% of total Aggregate
Coarse	C33 #6	0%
Intermediate	C33 #8	33%
Fine	C33 Fine Aggregate	67%

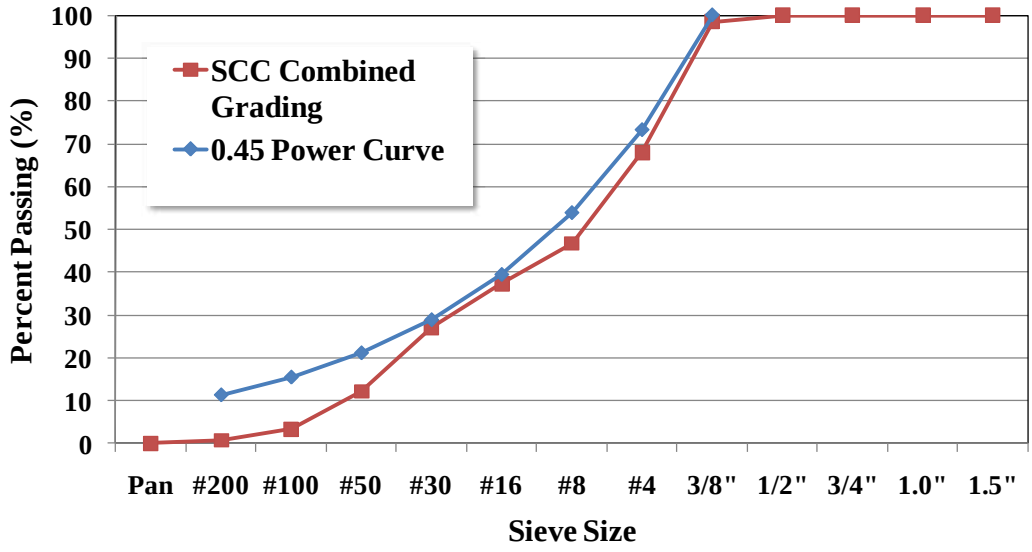

Figure 17: Optimal combined aggregate grading to produce SCC1 and SCC2 mixes.

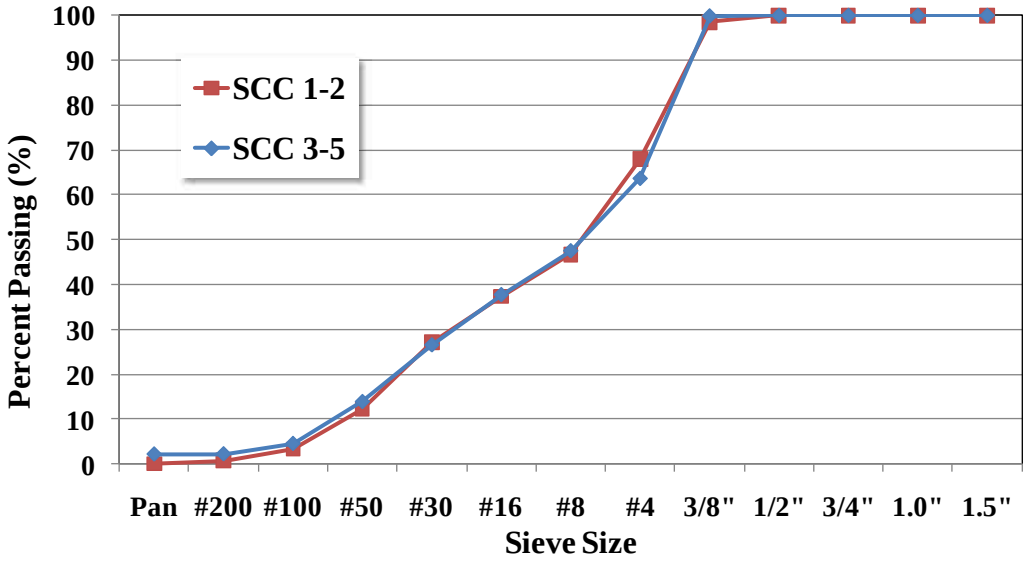

Figure 18: Optimal combined aggregate grading to produce SCC3, SCC4 and SCC5 mixes compared with SCC1 and SCC2.

3.3 Mix Design Proportioning

Constituents used to make the concretes were proportioned to meet requirements stated in the literature, and by the New Mexico Department of Transportation. Aggregate proportioning was designed to meet the combined grading fit the 0.45 Power Curve for the NVC mixes. This process was performed to produce NVC similar to that approved by the NMDOT. However, this was not the case for SCC mixes, the grading used for SCC closely fits the 0.45 Power Curve. The NVC mixes were designed by private organizations for the use in NMDOT structural applications. Mix designs were given, and were replicated for comparisons to the SCC mixes to be designed. All SCC mix designs incorporated fly ash. The percentages of fly ash by weight of cement were recommended by the DOT. Using the Placitas source of aggregate, SCC1 and SCC2 were designed to have respectively 25 and 40 percent fly ash by weight of cement. SCC3, SCC4, and SCC5 used the Griego and Sons aggregate source. The fly ash supplied respectively for these mixes incorporated 20, 30, and 40 percent by weight of cement. All fly ash was used as a supplementary cementitious material and not a replacement of cement. Table 5 presents the final mixes with varying fly ash content as a percentage of the weight of cement, water cementitious materials ratio expressed as water to total binder ratio (*w/b*) by weight, total volume of cement paste, and superplasticizer provided as a percentage by weight of cement. The water cement ratios of the Griego and sons SCC mixes are lower than the Placitas source concretes. This was done to raise the stability of the mixes in freshly mixed state.

The final mixes were found by trial and error, and the final concrete mixtures can be seen in Tables 9 – 15. The proportions can be seen with the 7 and 28 day compressive

strength that were found from each mix. The proportions are listed using English and metric units. Because there was no aggregate greater than ½" in SCC mixes, there was no need to add the coarse aggregate collected from either source. Admixtures for the NVC mixes were proportioned closely to the given mix designs supplied by the NMDOT, but it was necessary to adjust the proportion of air entraining admixture so that the percentage of air in the concrete mix is between 6% and 9%.

Results for specific gravity and absorption of the Lafarge source in Placitas, and the Griego and Sons Construction source in Fort Sumner are shown in Tables 6 and 7. The values of bulk specific gravity at SSD are provided as they were used for the mix designs to satisfy the unit volume condition. Moisture content was measured the day before batching concrete and used with the values of absorption to correct the amount of water provided to the mixtures for quality control purposes.

Table 8 displays a description of all other constituents used to make the concretes and the corresponding specific gravities implemented for the mix designs. The specific gravity of cement was estimated to be 3.150 as this is a commonly used value in the field. The specific gravity of fly ash ranges between 1.9 and 2 .3 with type F fly ash being less dense and regarded as 2.0. The specific gravities of the admixtures were determined by the manufacturers. They are typically not used in calculations of theoretical unit weight because so little is supplied in comparison with the other constituents.

Table 5: Mix proportioning of SCC Mixes

Mix Design	Cement Content (kg/m^3)	Fly Ash (%)	*w/b*	V_{cp} (%)	HRWR (%)	Fine : Coarse Aggregate Ratio
SCC1	309	25	0.411	36.1	2.47	11 : 9
SCC2	297	40	0.401	38.5	2.58	11 : 9
SCC3	334	20	0.356	34.8	2.29	2 : 1
SCC4	312	30	0.357	35.6	2.45	2 : 1
SCC5	302	40	0.336	36.5	2.53	2 : 1

Table 6: Bulk specific gravity at saturated surface dry (SSD), and absorption of aggregates from Lafarge.

Material Description	Bulk Specific Gravity (SSD)	Absorption (%)
Placitas ASTM C33/Lafarge 8515 Fine Aggregate	2.593	1.5
Placitas ASTM C33 Intermediate Aggregate	2.564	1.7
Placitas ASTM C33 Coarse Aggregate	2.597	1.1

Table 7: Bulk specific gravity at saturated surface dry (SSD), and absorption of aggregates from Griego and Sons' Construction.

Material Description	Bulk Specific Gravity (SSD)	Absorption (%)
Griego and Sons' ASTM C33 Fine Aggregate	2.634	1.05
Griego and Sons' ASTM C33 Intermediate Aggregate	2.661	1.36
Griego and Sons' ASTM C33 Coarse Aggregate	2.673	0.95

Table 8: Bulk specific gravity of all other constituents used to make SCC.

Material Description	Bulk Specific Gravity
Water (City of Albuquerque)	1.000
GCC Type I/II Portland Cement	3.150
Fly Ash SRMG Type F Fly Ash	2.000
Grace Daravair AT-60 AE	1.000
BASF Glennium 3030 NS Superplasticizer	1.050
BASF Rheomac VMA 362	1.000

Table 9: Final mix NVC1

Ingredient	**lb/yd^3**	**kg/m^3**
Rio Grande type I/II cement	566	338.0
SRMG Class F Fly Ash	168	100
Placitas Fine Agg.	960	573
Placitas Int Agg. #8	1067	636
Placitas Coarse Agg. #6	640	382
Water	270	161
Superplasticizer	44 oz	1709 mL
Viscosity modifying agent	0	0
Air entertainer	18 oz	699 mL
Characteristics		
Water/cementitious ratio	0.37	0.37
Slump (in) > 3 in	3.2 in	81 mm
Slump flow (in) – Target > 25.5 in	---	---
Unit weight	138.2 lb/ft^3	2213 kg/m^3
Yield	7.56 ft^3	0.214 m^3
Gravimetric air entrained %	4.9%	4.9%
Volumetric air entrained % (target > 6.5%)	6.5%	6.5%
Temperature (^{o}F)	71.0	21.6 ^{o}C
Compress strength (7 days) psi (target > 3000	3871 (±122)	27.1 (±0.8)
Compress strength (28 days) psi (target > 4000	4467 (±124)	31.3 (±0.9)

Table 10: Final mix SCC1

Ingredient	**lb/yd^3**	**kg/m^3**
Rio Grande type I/II cement	516.7	309.0
SRMG Class F Fly Ash	129.2	77.1
Placitas Fine Agg.	1521.3	908.3
Placitas Int. Agg.	1241.8	741.4
Placitas Coarse Agg.	0.0	0.0
Water	265.3	158.4
Superplasticizer	197 oz	7650 mL
Viscosity modifying agent	106 oz	4140 mL
Air entertainer	0.44 oz	17 mL
Characteristics		
Water/cementitious ratio	0.411	0.411
Slump (in) > 3 in	---	---
Slump flow (in) – Target > 25.5 in	30.7 in	780 mm
Unit weight	133.8 lb/ft^3	2143 kg/m^3
Yield (ft^3)	7.84 ft^3	0.222 m^3
Gravimetric air entrained %	7.4%	7.4%
Volumetric air entrained % (target > 6.5%)	8.2%	8.2%
Temperature	73.8 ^{o}F	23.2 ^{o}C
Compress strength (7 days) psi (target > 3000	3861 (±89) psi	27 (±0.6) MPa
Compress strength (28 days) psi (target > 4000	4795 (±159)	33.5 (±0.6)

Table 11: Final mix SCC2

Ingredient	**lb/yd^3**	**kg/m^3**
Rio Grande type I/II cement	496.8	295.0
SRMG Class F Fly Ash	198.7	118.6
Placitas Fine Agg.	1462.7	872.9
Placitas Int. Agg.	1194	712.6
Placitas Coarse Agg.	0	0.0
Water	278.8	166.4
Superplasticizer	197 oz	7650 mL
Viscosity modifying agent	106 oz	4140 mL
Air entertainer	0.36 oz	17 mL
Characteristics		
Water/cementitious ratio	0.40	0.40
Slump (in) > 3 in	---	---
Slump flow (in) – Target > 25.5 in	28.8 in	730 mm
Unit weight	134.6 lb/ft^3	2156 kg/m^3
Yield	4.4 ft^3	0.124 m^3
Gravimetric air entrained %	5.7%	5.7%
Volumetric air entrained % (target > 6.5%)	7.8%	7.8%
Temperature	71.6 ^{o}F	22.0 ^{o}C
Compress strength (7 days) psi (target > 3000 psi)	3362 (±213) psi	23.5 (±1.5) MPa
Compress strength (28 days) psi (target > 4000 psi)	4340 (±163) psi	30.4 (±1.1) MPa

Table 12: Final mix NVC2

Ingredient	**lb/yd^3**	**kg/m^3**
Rio Grande type I/II cement	466	276.0
SRMG Class F Fly Ash	116	69
Griego's Fine Agg.	1497	888
Griego's Coarse Agg.	1197	710
Griego's Intermediate Agg.	299	177
Water	241	143
Superplasticizer	56 oz	2176 mL
Viscosity modifying agent	0	0
Air entertainer	12 oz	490 mL
Characteristics		
Water/cementitious ratio	0.414	0.414
Slump (in) > 3 in	2.75 in	70 mm
Slump flow (in) – Target > 25.5 in	---	---
Unit weight	140.33 lb/ft^3	2247 kg/m^3
Yield	5.128 ft^3	0.145 m^3
Gravimetric air entrained %	7.1%	7.1%
Air using pressure method % (target > 6.5%)	7.8%	7.8%
Temperature	74.8 ^{o}F	23.7 ^{o}C
Compress strength (7 days) psi (target > 3000 psi)	3126 (±17) psi	22 (±0.1) MPa
Compress strength (28 days) psi (target > 4000	4266 (±7) psi	29.9 (±0.0) MPa

Table 13: Final mix SCC3

Ingredient	**lb/yd^3**	**kg/m^3**
Rio Grande type I/II cement	561	334
SRMG Class F Fly Ash	113	67
Griego's Fine Agg.	1929	1148
Griego's Coarse Agg.	0	0.0
Griego's Intermediate Agg.	965	574
Water	240	143
Superplasticizer	197 oz	7650 mL
Viscosity modifying agent	106 oz	4140 mL
Air entertainer	0.44 oz	17 mL
Characteristics		
Water/cementitious ratio	0.356	0.356
Slump (in) > 3 in	---	---
Slump flow (in) – Target > 25.5 in	26 in	660 mm
Unit weight	139.2 lb/ft^3	2230 kg/m^3
Yield	4.783 ft^3	0.135 m^3
Gravimetric air entrained %	7.5 %	7.5%
Air using pressure method % (target > 6.5%)	7.4 %	7.4%
Temperature	78.9 ^{o}F	26 ^{o}C
Compress strength (7 days) psi (target > 3000 psi)	5900 (±300) psi	41 (±2.1) MPa
Compress strength (28 days) psi (target > 3000 psi)	7576 (±200) psi	53 (±1.4) MPa

Table 14: Final mix SCC4

Ingredient	**lb/yd^3**	**kg/m^3**
Rio Grande type I/II cement	526.7	312
SRMG Class F Fly Ash	158.0	94
Griego's Fine Agg.	1912.2	1134
Griego's Coarse Agg.	0	0
Griego's Intermediate Agg.	955.6	567
Water	244.2	145
Superplasticizer	197 oz	7650 mL
Viscosity modifying agent	106 oz	4140 mL
Air entertainer	0.51 oz	17 mL
Characteristics		
Water/cementitious ratio	0.357	0.357
Slump (in) > 3 in	---	---
Slump flow (in) – Target > 25.5 in	28 in	711 mm
Unit weight	139.6 lb/ft^3	2236 kg/m^3
Yield	4.956 ft^3	0.140 m^3
Gravimetric air entrained %	6.6 %	6.6%
Air using pressure method % (target > 6.5%)	7.6 %	7.6%
Temperature	75.2 ^{o}F	24 ^{o}C
Compress strength (7 days) psi (target > 3000 psi)	3960 psi	27.7 MPa
Compress strength (28 days) psi (target > 4000 psi)	6681 (±400)	46.8 (±2.8) MPa

Table 15: Final mix SCC5

Ingredient	**lb/yd^3**	**kg/m^3**
Rio Grande type I/II cement	509.0	302
SRMG Class F Fly Ash	204	120.8
Griego's Fine Agg.	1887	1119
Griego's Coarse Agg.	0	0
Griego's Intermediate Agg.	943	559
Water	240	142
Superplasticizer	197 oz	7650 mL
Viscosity modifying agent	106 oz	4140 mL
Air entertainer	0.44 oz	17 mL
Characteristics		
Water/cementitious ratio	0.336	0.336
Slump (in) > 3 in	---	---
Slump flow (in) – Target > 25.5 in	28 in	711 mm
Unit weight	139.8 lb/ft^3	2240 kg/m^3
Yield	5.135 ft^3	0.145 m^3
Gravimetric air entrained %	6.2%	6.2%
Air using pressure method % (target > 6.5%)	6.6 %	6.6%
Temperature	78.1 ^{o}F	25.6 ^{o}C
Compress strength (7 days) psi (target > 3000 psi)	5073 (±300) psi	35.5 (±2.1) MPa
Compress strength (28 days) psi (target > 4000	7047 (±150) psi	49.3 (±1.0) MPa

The slump of NVC was required to be 4" plus or minus 1" according to NMDOT criteria. Slump flow of SCC was required to be greater than 25.5". L- box passability was required to be greater than 80%, and the T50 must be within the range of from 3 to 7 seconds. Air entrainment provided to SCC mixes was small in comparison to the proportion of air entrainment provided to NVC mixes partially because the entrapped air has been found to be higher in SCC. This is also due to air entrainment being very effective in highly flowable concrete.

3.4 Concrete Batching Procedure

Once the final mix designs were developed, batching for test specimens began. In all batching for both trial mixes, and final mixes, materials were proportioned by mass to the nearest 0.05 kilogram. Aggregates were proportioned the day before batching so that moisture content could be determined so the batch water could be adjusted to account for variable moisture of the aggregate in storage. Proportioning of aggregate was accomplished by adding 50 – 60 kg of aggregate into multiple 55 gallon sealable drums. A known amount of extra aggregate was always provided to each drum because it was known that samples for moisture content would be collected, and corrections to the weight would have to be made for the batch once moisture was known. Each drum was laid onto its side on the floor and rolled around to mix the aggregate. Moisture content of each drum was collected and a weighted average of moisture content was determined for water adjustments. Cement and fly ash were proportioned on the same day of batching. Water and admixtures were proportioned by mass just before making the concrete.

The Standard Practice for Making and Curing Concrete Test Specimens in the Laboratory [63] was followed with the exception of the batch procedure in making SCC

mixes. In the standard, the coarse aggregate is added first, and approximately half of the batch water combined with all superplasticizer and air entraining admixtures are added to it in the mixer before any other finer aggregates or binders can follow. When making the SCCs, the order of materials added to the mixer was coarse aggregate, fine aggregate, cement, fly ash, then water, superplasticizer, VMA, and air entrainment provided simultaneously toward the end. The mixing procedure was done the same at all times. The coarse and fine aggregates were allowed to mix together for two minutes. The cement and fly ash were added to the mix afterward, and allowed to mix for an additional two minutes. Once the bulk materials were mixed together homogeneously, half of the water, superplasticizer, VMA, and air entrainment admixture were added and allowed to mix for three to five minutes. The remainder of the water and admixtures were provided after this time and the mixing progressed for another three to five minutes. Once all the materials were added, the concrete was directly discharged into wheel barrels and taken to designated locations so specimens for testing could be cast. The first wheel barrel was always designated for freshly mixed concrete tests. The target mixing time from start to finish was fifteen minutes, where more than twenty minutes was considered as unacceptable for usage. Once concrete was discharged from the mixer, the time to cast all specimens was never allowed to exceed fifteen minutes.

Figure 19: Mixing SCC

3.5 Freshly Mixed Concrete Testing

Freshly mixed concrete properties were measured for every batch of a particular mix design. For NVC, the slump test [22] was required to be 3 inches plus or minus 1 inch. Slump is a measure of consistency but is used to describe workability. Once the concrete sample is collected, the slump cone is clamped to a level surface. Concrete is placed into the mold in three layers of equal volume to the top. Between successive volumes, the concrete in the cone is consolidated with a 5/8" diameter rounded stainless steel tamper 25 times. The rod penetrates 1 inch into the layer of concrete beneath with the exception of the first layer. After the final layer is consolidated, the top is leveled, all debris surrounding the outside of the cone is removed, and the cone is lifted vertically where contact between the mold and the concrete within must be terminated in five plus or minus two seconds once lifting begins. The concrete slumps under its own weight without the presence of the mold. Temperature was measured at the same time as the slump test using ASTM C1064, as shown in Figure 20-b [64].

(a) (b)

Figure 20: Slump test (a) and temperature using thermal-couple (b)

The air content was required to be between 6.5 and 9 percent. Two methods of measuring air were implemented. The air was measured by pressure method [65] and by the gravimetric method using actual and theoretical unit weights [66]. Essentially, the two methods are measured simultaneously. For both methods, a measuring bowl is filled with three equal layers of concrete and tamped the same way as the slump test. In between layers, the bowl is hit with a rubber mallet to consolidate the voids left behind from tamping. After completing the final layer, the top is leveled with a plate, and the bowl is cleaned on its outside. The weight of the concrete contained with the measuring bowl is recorded. The weight and volume of the bowl are known because they were determined when the air pressure meter was purchased, and recalibrated every 6 months thereafter.

The gravimetric air content can now be calculated using relationships between the calculated unit weight (theoretical unit weight), and the measured actual unit weight.

$$Gravimetric\ Air\ Content = \frac{Theoretical\ Unit\ Weight - Actual\ Unit\ Weight}{Theoretical\ Unit\ Weight} \qquad (13)$$

The type B pressure meter was used to measure the air content. The pressure meter is clamped to the measuring bowl, and water is provided to the cavity between the lid and the concrete surface within the apparatus. A pressure equivalent to one atmosphere is developed behind a closed controllable valve connected to the chamber where fresh concrete is present. The system is then isolated from the outside world by sealing all valves used to provide water to the gap, now containing water, between the lid and the concrete. When the controllable valve is opened, the pressure released downward on the fresh concrete causes it to compress. The difference in height due to compression gives an indication of the volumetric change due to the applied pressure. The main compressible component is air. Aggregates also compress and therefore aggregate correction factors are typically deducted from the apparent air reading in practice (ASTM C231).

For SCC mixes, the slump flow [23] was required to be in between 650 mm-850mm (25.75 and 33.5 inches). Slump flow test differs from the slump test because there is one lift of concrete to fill the cone to the top and there is no tamping. Once the cone is filled, the top is leveled, and all surplus concrete around the base of the cone is removed, the cone is lifted vertically and the concrete is permitted to flow. The time between the instant the cone is lifted and the time for the flow to reach a diameter of 50 cm is recorded. The average between the longest diameter and the diameter perpendicular to it is recorded and is the slump flow. The time to flow to 50 cm is known as T_{50} and is a measure of flowability and viscosity. The visual stability index (VSI) is determined at the end. On a scale from 0 to 3, the stability of the concrete is qualitatively rated. 0 is the most stable. 1 is stable, but some water may bleed outward from the flow

circle creating what is called a mortar halo. If the halo is less than 2 mm thick, and the rest of the concrete is still homogeneous, it can be denoted as 1. VSI 2 is approaching unstable SCC and VSI 3 is the most unstable, where one will actually notice aggregate segregation in the large scale placement. SCC mixes for this research are prohibited from having VSI 2 or VSI 3.

Fig 21: L-box, slump flow, and air pressure meter to test fresh properties of SCC.

Also exclusively for SCC mixes, the L-box was used to determine passability. The blockage ratio must be greater than 80%. The vertical column is filled without tamping or consolidation, and allowed to rest for 1 minute after leveling the top. The gate is opened, and the SCC passes through three vertical number 3 bars spaced equally. As the SCC vacates the column of the L, it fills the horizontal part. The blocking ratio is determined by evaluating the difference in height beyond the reinforcement, and behind the reinforcement.

3.6 Casting Test Specimens

The different types of concrete specimens were cast and consolidated according to ASTM C192. The types of specimens made include 4 x 8 inch cylindrical specimens, 6 x

6 x 22 inch beams, and 4 x 3 x 16 inch prismatic beams. Specimens were made by filling the molds in two equal layers of concrete. The molds were lubricated with form oil so the specimens can be removed from the molds more easily. Each layer was tamped with either a 3/8" or 5/8" diameter rounded stainless steel rod. The size of the rod depended on the size of the sample. The cylinders required the 3/8" diameter rod with 25 tamps per layer, and the beams and prisms required the 5/8" diameter rod with one tamp every two square inches. Each tamp shall penetrate through the concrete surface to the bottom of the mold for the first layer, and for the top layer, from the top to one inch into the layer beneath it. After each layer the specimens were tamped slightly on the sides to eliminate the pores left behind solely due to the tamping. These types of pores were never observed in SCC, but slight tamping was necessary for consistency between casting different types of concrete. The specimens were leveled at the top, finished with a trowel, and covered with plastic to be left in a stable level place for 24 hours to set. Once 24 hours had passed, the molds were removed. The specimens were labeled and then submerged in lime saturated water at constant temperature of 75^{o} Fahrenheit (23^{o} Celsius). They were allowed to cure in this condition until the time of testing.

Figure 22: Casting 4” x 3” x 16” prismatic concrete beams.

Figure 23: Casting 4” x 8” cylindrical concrete specimens.

3.7 Final Mixes

The final mixes were produced in two to three batches to cast all required specimens. Batch A was the first batch and it was used to make cylinders and smaller prismatic specimens. Batch B represents the second batch of a particular mix design, and was utilized to make larger specimens such as beams. For all batches, some cylinders were cast to measure consistency of hardened concrete between batches by testing the compressive strength. All concrete specimens were cured in 23^{o} C water bath of controlled temperature using heaters until the day of testing.

3.8 Strength Testing

Hardened tests performed include Compressive Strength of Cylindrical Concrete Specimens [67], Static Modulus of Elasticity and Poisson's Ratio of Concrete in Compression [68], and Flexural Strength of Concrete Using a Simple Beam with Third-Point Loading [69]. Pulse Velocity Through Concrete [70] was also measured to calculate the dynamic modulus of elasticity. Some data for pure tension was also collected for research. Strength tests were conducted on 7, 28, 90, 180, and 365 days after casting the specimens for Placitas source concretes, and on 7, 28, 90, and 180 days for Griego and Sons source concretes.

The compression test consists of applying an axial load to the cylinders at a constant rate until failure occurs. The strength σ is determined by dividing the ultimate load by the cross sectional area of the specimen. F = the ultimate load (lb), and A = cross sectional area measured at the middle of the specimen (in).

$$\sigma = \frac{F}{A} \tag{14}$$

A minimum of three specimens were used to give an average strength. The cylindrical specimens are removed from curing on the day before testing, and kept moist while measurements of weight, length, and diameter are recorded. They are moistened through this simply by covering the specimens with wet towels. The ends of the cylinders are dried using pressurized air, and then capped using ASTM C569 [71]. Sulfur mortar for capping compound requires that the caps cure for two hours when the concrete strength is lower than 5000 psi, and sixteen hours when the concrete strength is greater than 5000 psi. Sulfur compound cannot be used if concrete strength exceeds 11,000 psi. Grinding is recommended for concretes having greater strength. Once the specimens are capped, they are submerged back into the curing tanks so that the sulfur is allowed to strengthen until the next day. After this, the cylinders are removed and one by one tested in the compression testing machine. The load rate corresponding to compression of cylinders is 35 plus or minus 7 psi/s.

Figure 24: Compression of a 4" x 8" cylindrical concrete specimen.

Modulus of Rupture (MOR) has been determined to represent flexural strength of concrete. The standard test method for determining Flexural Strength of Concrete Using

Simple Beam with Third Point Loading (ASTM C78) was employed. The title implies three points, but it can actually be interpreted as having four – two creating the span for the beam to rest, and two positioned symmetrically about the center of the beam for downward force to be applied. This method is advantageous because the type of failure theoretically involves no shear stress. The stress causing failure is resulting from pure bending. The beam specimens were removed from the curing tanks, and grinded on all surfaces to eliminate burrs and sharp corners developed when the specimens were cast. The beam was rinsed, and surface dried. The weight was determined, and the specimen was placed into the compression testing machine on top of the supports making it simply supported. The side that is the top, designated from the day the specimen was cast, was never in contact with point loads. This face was always perpendicular to the point loads. The span length for this test is 18 inches and the beam is placed so that it is symmetrical on the supports. The loading apparatus was set on top of the beam and positioned so that the first point is 6 inches from the bottom support. As the downward loads are six inches apart, it is centered with respect to the span of the beam. Checks were made so that the dimensions of the experiment were correct, and leather sheaths were placed between the points and the specimen. After completion, the specimen was loaded consistently at a load rate that was between 125 - 175 psi/min at the tension face. Dimensions of base and height to calculate the modulus of rupture were collected close to the face of rupture after the specimen was failed. F = ultimate load applied (lb), L = the span length (in), b = the base of the beam (in), h = the height of the beam (in), and MOR = the bending stress at failure (psi).

$$MOR = \frac{FL}{bh^2} \tag{15}$$

(a) (b)

Figure 25: Modulus of rupture test: loading (a) after fracture (b).

Static Modulus of Elasticity and Poisson's Ratio of Concrete in Compression (ASTM C469) was determined to observe the stiffness develop. The same type of cylindrical specimen to measure compressive strength was used to measure the stiffness. Essentially, this test is conducted by compressing a concrete cylinder with dial gauges fixed to the specimen to record displacements. The specimens are capped as they are for compression testing. Four to five specimens were required for this test. Three cylinders were tested to find the ordinary compressive strength, and typically two were used to determine modulus of elasticity. It is first required to measure the ultimate strength of the concrete. This is because modulus of elasticity and Poisson's ratio values are applicable within the working stress range between 0 – 40 percent of the ultimate concrete strength. After the strength has been determined, a new specimen of the same mix and age is placed into the compressometer. The compressometer is clamped to the specimen by embedding a series of screws into it. Dial gauges are connected to the compressometer and record displacement in the longitudinal and transverse directions as the cylinder is

compressed. The specimen and compressometer assembly is aligned into the compression testing machine and checked for flaws and to ensure that no bracing from the compressometer itself is intact to yield untrue readings as we seek purely the stiffness of concrete. Also, the dial gauges are verified to be in steady contact with a datum, and reading zero. The load rate for this test is the same as the compression test load rate (37 psi/s). The specimen within the compressometer is loaded to 20 percent of ultimate load, and immediately released from this pressure. The gauges are checked to be zero. If the gauges are not reading zero once the specimen is decompressed, they are adjusted to be. We repeat this one more time to verify that the dial gauges are working properly and that the gauges read zero while the specimen is unloaded. This process is known as seating, and is used to eliminate faulty connections and is a trial before collecting real data used to calculate modulus of elasticity and Poisson's ratio. The test is conducted by reading displacements at increments of 2000 pounds up to 40 percent of the ultimate load. Through geometric relations, the longitudinal and transverse displacements are found at the center of the cylindrical specimen. The stress and strain used to calculate the modulus of elasticity are the stress and strain corresponding to 40 percent of the ultimate load, and the stress corresponding to longitudinal strain of 0.00005 in/in. The strains used to calculate Poisson's ratio are the final and initial transverse strain, and the final longitudinal strain and 0.00005in/in. Modulus of elasticity was calculated using equation 16 where S_2 = stress corresponding to 40% of ultimate load (psi), S_1 = stress corresponding to ε of 50 millionths (psi), ε_2 = longitudinal strain corresponding to S_2 (in/in), ε_{t2} = transverse strain produced by S_2 (in/in), ε_{t1} = transverse strain corresponding

to longitudinal strain of 50 millionths (in/in), E = static modulus of elasticity (psi), and ν = Poisson's Ratio.

$$E = \frac{S_2 - S_1}{\varepsilon_2 - 0.00005} \tag{16}$$

$$\upsilon = \frac{(\varepsilon_{t2} - \varepsilon_{t1})}{\varepsilon_2 - 0.00005} \tag{17}$$

Figure 26: Compressometer and cylinder assembly used to measure static modulus of elasticity and Poisson's ratio

Dynamic modulus of elasticity was measured using Pulse Velocity Through Concrete (ASTM 597). The test can assess the uniformity and relative quality of concrete, and indicate the presence of voids and cracks. The specimen was dried at the ends and dimensions of diameter, and length were collected. The reference bar was tested prior to each series of concrete tests to ensure that the transducers were calibrated. Once calibrated, the cylindrical specimens were tested by applying the transmitting transducer and receiving transducer at opposite ends of the cylinder. Vacuum grease was

supplied to the interface between the transducer and concrete specimen. The transit time can be observed, and the length of the specimen divided by the time for the pulse wave to travel the distance is the pulse velocity and can be used to calculate dynamic modulus of elasticity. The velocity = v (m/s), length of the specimen = L (m), transit time = T (sec), density of the concrete specimen = ρ (kg/m^3), and dynamic modulus of elasticity = E (Pa).

$$v = \frac{L}{T} \tag{18}$$

$$E = \rho v^2 \tag{19}$$

Figure 27: Pulse velocity apparatus

3.9 Durability Testing

Since SCC requires the implementation of high amounts of chemical admixtures, volume of cementitious materials, and sand to total aggregate ratio, it is important to verify that the durability is adequate when compared to NVC. Durability tests that were performed included chloride ion penetration test, freeze thaw durability on concrete, and alkali-silica reaction of mortars with combinations of cement and fly ash. Durability tests were conducted once for each mix.

The Rapid Chloride Ion Penetration Test (RCPT) [72] determines electrical conductance of concrete to provide an indication of its resistance to the chloride ion's penetration. The method consists of measuring the amount of electrical current passed through a two inch thick slice of a four inch diameter cylindrical specimen for a six hour time interval. The RCPT was performed on specimens that were 90 days of age. A cylindrical specimen is removed from curing and sawed into two 2" thick cylinders. It was required that three specimens be tested, so two cylinders were used mostly for safety reasons. The specimens were then dried at the surface, and epoxy was used to coat the outside surface of the cylinder excluding the top and bottom. The epoxy was allowed to dry, and the specimens were positioned into a vacuum desiccator to be under vacuum pressure for three hours.

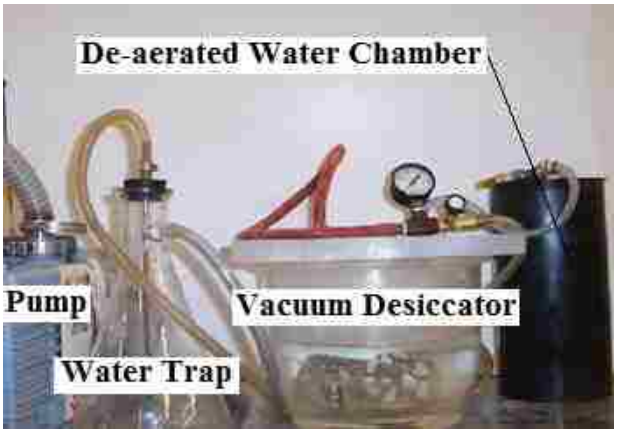

Figure 28: Schematic of Vacuum Desiccator

At the end of three hours, while still undergoing vacuum pressure, de-aerated water was allowed to enter the desiccator to completely submerge the specimens within. The vacuum was permitted to stay for an additional hour after this, and then the pressure was relieved allowing the submerged specimens to be at atmospheric pressure. The specimens would be soaked without vacuum in this condition for 18 hours. The following day, the specimens were removed from the water, and glued with silicon to the prescribed cells to conduct this test. The cells were sealed to be air tight, and the glue was allowed to dry. When the glue was dried, one of the cells was filled with 0.3 normal solution of sodium hydroxide. The opposite cell on the specimen was filled with a 3% by mass sodium chloride solution. A special RCPT device was developed at UNM. A 60 Volt potential difference is applied across the specimen by connecting a power supply having the negative terminal immersed in a sodium chloride solution and the positive terminal immersed in sodium hydroxide solution. The suspended chloride ions migrate through the saturated pores of the concrete specimen to the positive terminal as they are negatively charged. A current is created by the moving negatively charged ions. This current is measured every second for six hours. The total charge passed in coulombs is

related to the resistance of the specimen to chloride ion penetration. Once the charge on the specimen is known, it can be classified as having negligible to high chloride ion penetrability according to (ASTM C1202). To calculate the charge (Q) deposited on any specimen, the function of current (I) is integrated over the time interval.

$$Q = \int I(t)dt \tag{20}$$

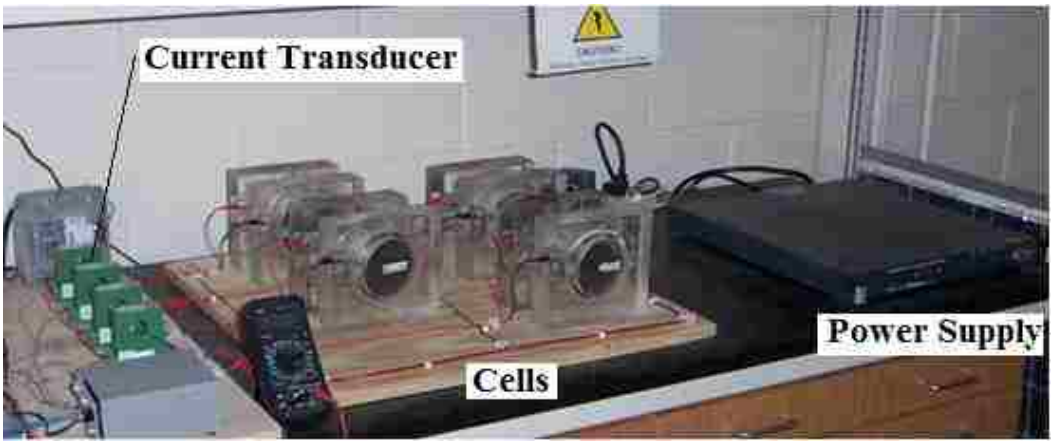

Figure 29: Rapid chloride ion penetration device.

Figure 30: Rapid Chloride Ion Penetration test on SCC**.**

The freeze-thaw test following ASTM C 666 was performed to compare freeze-thaw durability properties of SCC mixtures. Rapid freezing and thawing in water was the procedure selected for this experiment [73]. The fundamental transverse frequency of the concrete specimens was measured prior to, and after exposure freeze-thaw cycles. This was used to calculate dynamic Young's modulus of elasticity, and the level of damage due to freeze-thaw cycles. Measurements of fundamental transverse frequency were collected before starting freeze-thaw cycles, and every 36th cycle thereafter. The age of specimens at the start of the test was 120 days.

Freeze-thaw experiments were performed for all mixes. It was a goal to begin the testing after 120 days of curing. This was the case for SCC3, SCC4, SCC5, and NVC2. However, SCC1, SCC2, and NVC1 were frozen at 120 days but were not tested until the

freeze-thaw apparatus was operational. Figure 31 shows the freeze-thaw test equipment. Figure 32 shows some of the SCC specimens inside the freeze-thaw equipment.

Figure 31: Freeze-thaw equipment to test freeze-thaw resistance of SCC**.**

Figure 32: SCC specimens placed in freeze-thaw apparatus**.**

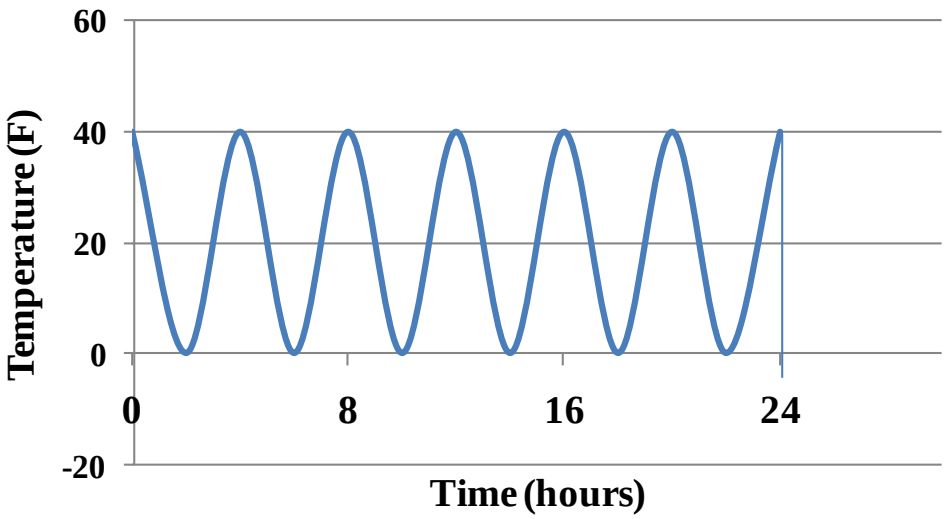

Figure 33: Freeze-thaw temperature cycling for one day.

One freeze-thaw cycle takes 4 hours, and the range of temperature is 0 to 40 ^{o}F. The relationship between time and temperature cycling can be seen in figure 33. The specimen was therefore subjected to 6 cycles per day or 42 freeze-thaw cycles per week. Each specimen was stored in a metal container which permitted 1/32" to 1/8" of water to be on each surface of the specimens. The specimens rested on wire supports located at the bottom of the container to ensure that the bottoms of the specimens met this criterion. The specimens were brought to 40 ^{o}F and surface dried when fundamental transverse frequency was measured. The cycling of temperature was permitted in this way until the relative dynamic modulus of elasticity reached 60% of the initial dynamic modulus, or 300 cycles. Figure 34 shows a prismatic specimen exposed to 108 freeze thaw cycles.

Figure 34: Prismatic specimen exposed to 108 freeze thaw cycles

The standard test method for "Fundamental Transverse Resonant Frequency of Concrete Specimens" [74] was implemented to measure dynamic modulus of elasticity. In this method, the forced resonance method is implemented to measure dynamic modulus of elasticity. The frequency test apparatus consists of a driver to provide mechanical vibrations, and a pickup to detect the vibrating displacement. The specimen is supported in transverse mode on rubber beam supports located at 0.224 times the length of the specimen measured from the ends. The driver is centered from every dimension of the beam and is placed in a way which is normal to the short cross sectional dimension and touching the beam. The pickup is positioned at the edge of the beam and is resting on the surface normal to the long cross sectional dimension. The test set-up is shown in Figure 35.

Figure 35: Prismatic concrete specimen positioned to determine transverse resonant frequency.

Once the beam is positioned the frequency of the driver is increased. A built in AC voltmeter is observed as the frequency is adjusted. The range of the voltmeter is adjusted until it is possible to read the maximum voltage while simultaneously increasing the frequency. An oscilloscope is used to verify resonance when the maximum voltage and frequency coincide. Such shape on the oscilloscope is shown in Figure 35. The dynamic modulus of elasticity is determined using Equations 21 and 22

$$E_{dynamic} = C\ M\ n^2 \tag{21}$$

$$C = 0.9464\left(\frac{L^3 T}{b\ t^3}\right) \tag{22}$$

Where M = mass (kg), n = fundamental transverse frequency, (Hz), L = length (m), b = long cross sectional dimension (m), t = short cross sectional dimension (m), T = 1.24

(constant based on *r/L* and Poisson's ratio). Two freeze thaw durability indices denoted *FTDI-1* and *FTDI-2* were calculated based on the reduction of the dynamic modulus of elasticity with freeze thaw cycles. The first freeze-thaw durability index *FTDI-1* was calculated as the ratio of the number of cycles where the modulus of elasticity reached 60% of its original value (N_{60}) to the total number of cycles of the test N_{total} = 300 cycles as described by Equation 23. The second freeze- thaw durability index *FTDI-2* was calculated as the ratio of the dynamic modulus of elasticity at 300 cycles to the original dynamic modulus of elasticity before starting freeze-thaw cycles as described by Equation 24.

$$FTDI-1 = \frac{N_{60}}{N_{total} = 300} \tag{23}$$

$$FTDI-2 = \frac{E_{300}}{E_0} \tag{24}$$

There have been essentially two laboratory test methods for evaluating the expansion of ASR of a given aggregate: the concrete prism test [75] and the accelerated mortar bar test [76]. A modified approach [77] for mortar bars incorporating supplementary cementitious materials has been used to measure the ASR reactivity of the SCC mixes for this Thesis. The test can be performed over a 14 day period. If the expansion is more than 0.10% for the AMBT (per ASTM C1260), the aggregate is considered as reactive.

Seven different mortars were made using the two sources of aggregate. Fly ash (Class F) was provided by replacing the same percentages of cement to mortar as in the SCC concrete mixes designed for this Thesis. One mortar was produced for each

aggregate source, and no fly ash was added to those mixes so that the reactivity of each source could be measured. One mortar was also produced using superplasticizer, and VMA to examine their significance on ASR reactivity as these admixtures are provided to SCC.

The aggregate was prepared according to ASTM C1260. A large sample of fine aggregate was collected from each source. This large sample was then split down to approximately 50 lb, and then oven dried. Once dried, the sample was weighed, and graded using large sieves on a Gilson shaker. The particles retained on the #8, #16, #30, #50, and #100, were stored into separate containers as seen in Figure 36, washed over a #200 sieve, and oven dried separately. After 24 hours of oven drying, the aggregate sizes were blended to make mortar sand. The combination of particle sizes for the mortar sand is specified as being 10% retained on the #8, 25% retained on #16, #30, and #50, and 15% retained on the #100 sieve. The blended mortar sand was then stored in a sealed 5 gallon bucket until the mortars were produced.

For all purposes, the water/cementitious ratio was fixed at 0.47 neglecting aggregate absorption. A total of 440 grams of cementitious material, and 990 grams of sand were used in each mortar. It was recommended by the standard to proportion the material like this in order to make three mortar bar specimens. The mixing procedure for making mortar in the lab was used. After all materials required to make mortar were collected, all the mixing water was poured into the mixer. Following this step, the cement mixture was added and mixed at low speed for 30 seconds. The sand was then added over a 30 second period also mixing on low. The sides of the bowl and the mixer paddle were then scraped, and then the mortar was mixed using medium speed for one

minute. The mortar samples were then cast, covered, and placed in the curing room for 24 hours.

Figure 36: Proportioned aggregate for making mortar sand.

Figure 37: Mortar bars used for measuring length change due to ASR.

After the 24 hour curing period the molds were carefully removed from the mortar bars, and an initial reading was collected. The specimens were submerged in water that was prepared to be 80 degree Celsius, and placed in an oven that was

controlled to be 80 degrees Celsius. After 24 hours, the specimens were measured for an initial length reading. The water in the containers was then replaced by 1 Normal sodium hydroxide (NaOH) solution and placed back into the oven. Subsequent readings followed over the next 16 day time period to monitor the expansion of the samples due to ASR. The expansion of the mortar bars is found using equation 25.

$$\Delta L = \frac{L}{L_0} - 1 \tag{25}$$

(a)

(b)

Figure 38: ASR testing (a) Specimens in storage for temperature control, (b) specimens measured for length using length comparator.

CHAPTER 4. RESULTS AND DISCUSSION

4.1 Fresh Concrete Properties

Plastic properties of the SCC mixes can be seen in Table 16. Results of air content for NVC and SCC can be observed in Figure 41 with variation between the batches being high in SCC compared to NVC. Stability of SCC was qualitatively determined for all mixes using visual stability index (VSI). The compressive strength at 7 days was intended to be greater than 3000 psi, and required to be greater than 4000 psi at 28 days. The 7 day strength of concrete can be seen by batches of a given mix design in Figure 42 as a measure of quality control.

Table 16: SCC plastic properties for final mixes

Mix Design	Slump Flow (in)	Visual Stability Index (VSI)	Passability L_{box} (%)	T_{50} (sec)	Air Content (%)
SCC1	31.75	1	94	1.8	8.2
SCC2	30.75	1	93	2.6	7.8
SCC3	26.5	0	81	4.5	7.4
SCC4	27.75	1	86	3.6	7.6
SCC5	27.25	0	83	4.2	6.6

SCC 1 and 2 were highly flowable, passable, and both had low viscosity. This can be attributed to the higher water to total cementitious materials ratios. However, it was not necessary to provide a higher water binder ratio for the Griego and Sons aggregate source concretes, SCC 3, 4, or 5, to attain the requirements of flowability, passability or viscosity. Figure 39 shows slump flow results for all SCC mixes, and the variation of results as the mixes were repeated in batches to make the specimens required for testing. Figure 40 compares L- box passability among SCC mixes.

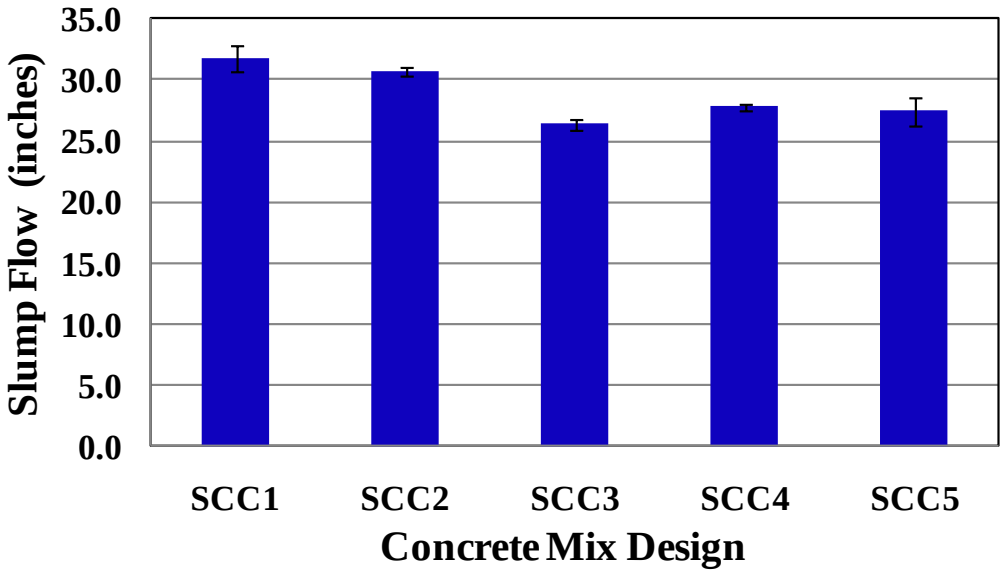

Figure 39: Slump flow comparison represents the mean value of three batches.

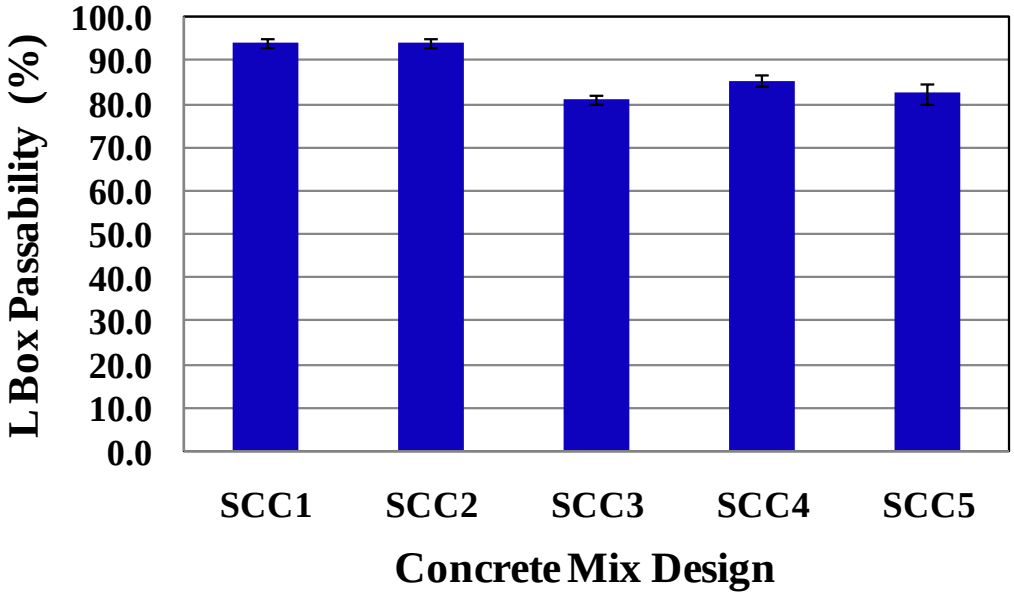

Figure 40: L- Box comparison represents the mean value of three batches

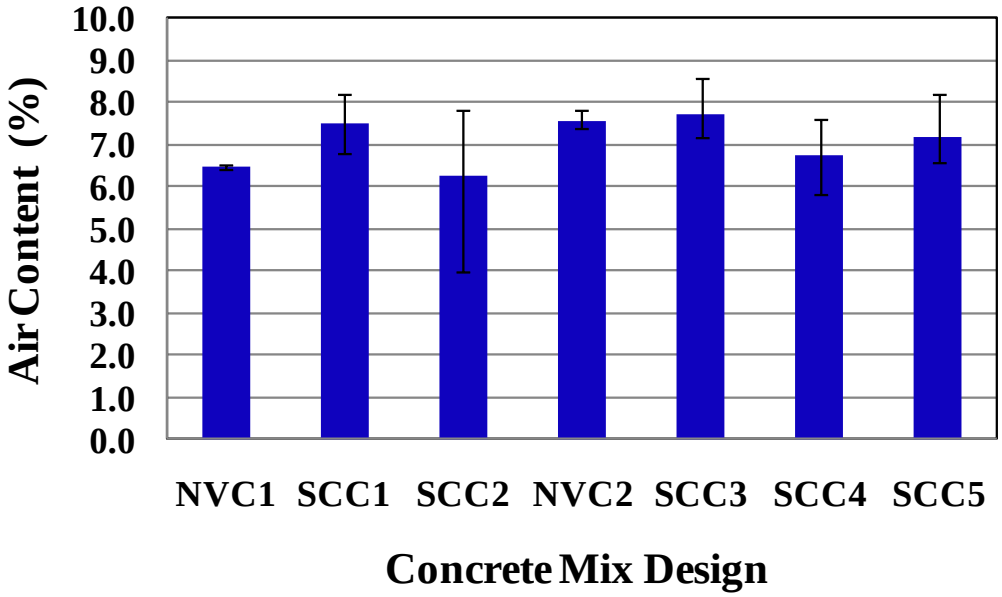

Figure 41: Comparison of air content measured by pressure meter represents the mean value of three batches.

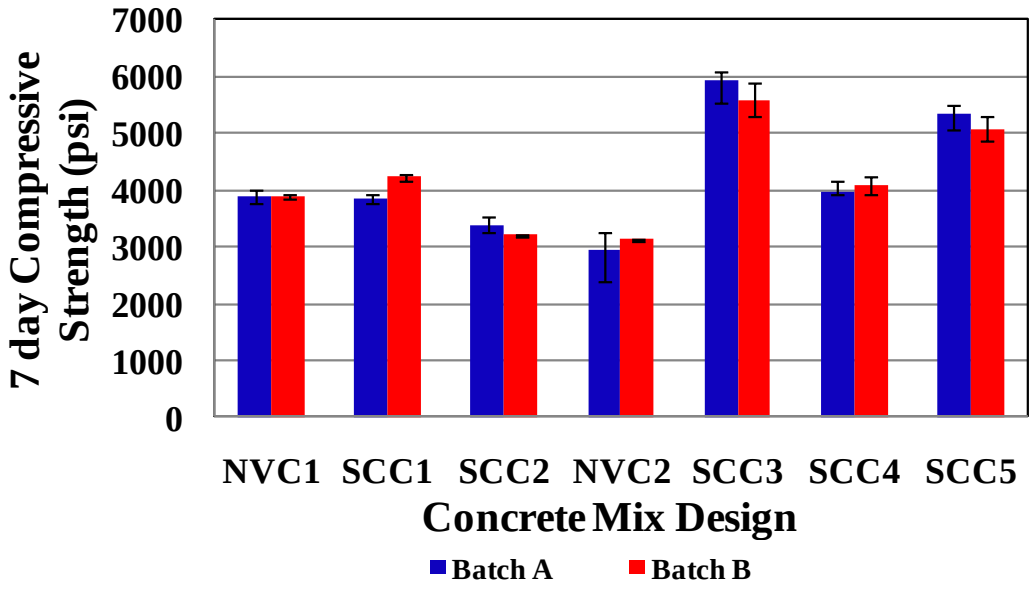

Figure 42: Comparison of 7 day compressive strength between batches of the same mix design.

4.2 Mechanical Test Results

Tables 17, 18, 19, 20, 21, 22, and 23 provide the major mechanical properties of NVC1, SCC1, SCC2, NVC2, SCC3, SCC4, and SCC5 determined at 7 and 28, 90, 180, and up to 365 days of age. Comparisons between the mixes NVC1, SCC1 and SCC2 are shown in Figure 43: compressive strength, Figure 45: modulus of rupture, Figure 47: modulus of elasticity, Figure 49: Poisson's ratio, and Figure 51: dynamic modulus of elasticity. Comparisons between the mixes NVC2, SCC3, SCC4, and SCC5 are shown in Figure 44: compressive strength, Figure 46: modulus of rupture, Figure 48: modulus of elasticity, Figure 50: Poisson's ratio, and Figure 52: dynamic modulus of elasticity. Final mix results are presented with detailed testing information for all mixes in the Appendix.

Table 17: Properties of mix NVC1

Criteria	**Mean (±Std. Dev) psi**	**Mean MPa**
Compress strength (7 days)	3871 (±122)	27.1
Compress strength (28 days)	4467 (±124)	31.3
Compress strength (90 days)	5663 (±114)	39.6
Compress strength (180 days)	7074 (±72)	49.5
Compress strength (360 days)	7045 (±385)	49.3
Tensile strength (7 days)	277 (±37)	1.9
Tensile strength (28 days)	253 (±2)	1.8
Tensile strength (90 days)	416 (±12)	2.9
Modulus of rupture (7 days)	530 (±25)	3.7
Modulus of rupture (28 days)	706 (±14)	4.9
Modulus of rupture (90 days)	803 (±8)	5.6
Modulus of rupture (180 days)	812 (±5)	5.7
Modulus of rupture (365 days)	866 (±NA)	6.1
Static modulus of elasticity (28 days)	4.2 E6 (±0.59E6)	29.4 GPa
Static modulus of elasticity (90 days)	4.8 E6 (±0.19E6)	33.6 GPa
Static modulus of elasticity (180 days)	5.4 E6 (N/A)	37.8 GPa
Static modulus of elasticity (360 days)	4.51 E6 (±0.108E6)	31.5 GPa
Dynamic modulus of elasticity (28	6.6 E6 (±0.09E6)	46.2 GPa
Dynamic modulus of elasticity (90	6.7 E6 (±0.013E6)	46.9 GPa
Dynamic modulus of elasticity (180	6.9 E6 (±0.001E6)	48.3 GPa
Dynamic modulus of elasticity (360	7.5 E6 (±0.529E6)	52.5 GPa
Poisson's ratio (28 days)	0.20 (±0.029)	0.2
Poisson's ratio (90 days)	0.22 (±0.035)	0.22
Poisson's ratio (180 days)	0.26 (N/A)	0.26
Poisson's ratio (360 days)	0.165 (±0.007)	0.165
Rapid Chloride ion permeability	1167 (±109)	1167
Rapid Chloride ion permeability Class	LOW	LOW

Table 18: Properties of mix SCC1

Criteria	**Mean (±Std. Dev) psi**	**Mean MPa**
Compress strength (7 days)	3861 (±89)	27.0
Compress strength (28 days)	4795 (±139)	33.6
Compress strength (90 days)	6198 (±320)	43.4
Compress strength (180 days)	7321 (±125)	51.2
Compress strength (360 days)	7755 (±501)	54.3
Tensile strength (7 days)	354 (±25)	2.5
Tensile strength (28 days)	359 (±4)	2.5
Tensile strength (90 days)	373 (±22)	2.6
Modulus of rupture (7 days)	446 (±30)	3.1
Modulus of rupture (28 days)	558 (±14)	3.9
Modulus of rupture (90 days)	687 (±42.4)	4.8
Modulus of rupture (180 days)	736 (±6)	5.2
Modulus of rupture (360 days)	761 (±NA)	5.3
Static modulus of elasticity (28 days)	4.8 E6 (±0.59E6)	33.6 GPa
Static modulus of elasticity (90 days)	6.8 E6 (±0.019E6)	47.6 GPa
Static modulus of elasticity (180 days)	5.3 E6 (±0.044E6)	37.1 GPa
Static modulus of elasticity (360 days)	5.5 E6 (±0.0019E6)	38.5 GPa
Dynamic modulus of elasticity (28	6.4 E6 (±0.16E6)	44.8 GPa
Dynamic modulus of elasticity (90	6.8 E6 (±0.2E6)	47.6 GPa
Dynamic modulus of elasticity (180	6.9 E6 (±0.18E6)	48.3 GPa
Dynamic modulus of elasticity (360	7.55 E6 (±0.25E6)	52.85 GPa
Poisson's ratio (28 days)	0.19 (±0.011)	0.19
Rapid Chloride ion permeability	1288 (±87)	1288
Rapid Chloride ion permeability Class	LOW	LOW

Table 19: Properties of mix SCC2

Criteria	**Mean (±Std. Dev) psi**	**Mean MPa**
Compress strength (7 days)	3362 (±213)	23.5
Compress strength (28 days)	4340 (±163)	30.4
Compress strength (90 days)	5847 (±158)	40.9
Compress strength (180 days)	6733 (±435)	47.1
Compress strength (360 days)	6410 (±269)	44.9
Tensile strength (7 days)	326 (±2)	2.3
Tensile strength (28 days)	347 (NA)	2.4
Tensile strength (90 days)	356 (±18)	2.5
Modulus of rupture (7 days)	485 (±32)	3.4
Modulus of rupture (28 days)	645 (±48)	4.5
Modulus of rupture (90 days)	727 (±2.5)	5.1
Modulus of rupture (180 days)	681 (±32)	4.8
Modulus of rupture (360 days)	745 (±79)	5.2
Static modulus of elasticity (28 days)	4.76 E6 (±0.23E6)	33.3 GPa
Static modulus of elasticity (90 days)	4.93 E6 (NA)	34.5 GPa
Static modulus of elasticity (180 days)	4.90 E6 (±0.88E6)	34.3 GPa
Static modulus of elasticity (360 days)	4.51 E6	31.6 GPa
Dynamic modulus of elasticity (28	5.7 E6 (±0.3E6)	39.9 GPa
Dynamic modulus of elasticity (90	6.3 E6 (±0.51E6)	44.1 GPa
Dynamic modulus of elasticity (180	6.87 E6 (±0.54 E6)	48.1 GPa
Dynamic modulus of elasticity (360	6.53 E6 (±0.283)	45.7 GPa
Poisson's ratio (28 days)	0.21 (±0.004)	0.21
Poisson's ratio (90 days)	0.184 (N/A)	0.184
Poisson's ratio (180 days)	0.22 (±0.035)	0.22
Poisson's ratio (360 days)	0.195 (±0.02)	0.195
Rapid Chloride ion permeability	1297 (±163)	1297
Rapid Chloride ion permeability Class	LOW	LOW

Table 20: Properties of mix NVC2

Criteria	**Mean (±Std. Dev) psi**	**Mean MPa**
Compress strength (7 days)	3126 (±17)	21.9
Compress strength (28 days)	4226 (±7)	29.6
Compress strength (90 days)	4963 (±338)	34.7
Compress strength (180 days)	5041 (±242)	35.3
Modulus of rupture (7 days)	469 (±7)	3.3
Modulus of rupture (28 days)	589 (±15)	4.1
Modulus of rupture (90 days)	638 (±45)	4.5
Modulus of rupture (180 days)	757 (±N/A)	5.3
Static modulus of elasticity (7 days)	3.26 E6 (±0.091	22.8 GPa
Static modulus of elasticity (28 days)	4.45 E6 (±0.112 E6)	31.2 GPa
Static modulus of elasticity (90 days)	4.35 E6 (±0.063 E6)	30.5 GPa
Static modulus of elasticity (180 days)	4.74 E6 (±0.352 E6)	33.2 GPa
Dynamic modulus of elasticity (7 days)	6.4 E6 (±0.298 E6)	44.8 GPa
Dynamic modulus of elasticity (28	7.0 E6 (±0.138 E6)	49.0 GPa
Dynamic modulus of elasticity (90	6.82 E6 (±0.053 E6)	47.7 GPa
Dynamic modulus of elasticity (180	7.34 E6 (±0.070E6)	51.4 GPa
Poisson's ratio (7 days)	0.15 (±0.0003)	0.15
Poisson's ratio (28 days)	0.16 (±0.0003)	0.16
Poisson's ratio (90 days)	0.175 (±0.021)	0.175
Poisson's ratio (180 days)	0.195 (±0.007)	0.195
Rapid Chloride ion permeability	1032 (±131)	1032
Rapid Chloride ion permeability Class	LOW	LOW

Table 21: Properties of mix SCC3

Criteria	**Mean (±Std. Dev) psi**	**Mean MPa**
Compress strength (7 days)	5918 (±298)	41.4
Compress strength (28 days)	7542 (±202)	52.8
Compress strength (90 days)	8780 (±215)	61.5
Compress strength (180 days)	7879 (±328)	55.2
Modulus of rupture (7 days)	690 (±32)	4.8
Modulus of rupture (28 days)	842 (±36)	5.9
Modulus of rupture (90 days)	899 (±30)	6.3
Modulus of rupture (180 days)	1094 (±41)	7.7
Static modulus of elasticity (7 days)	4.1 E6 (±0.28 E6)	28.7 GPa
Static modulus of elasticity (28 days)	4.8 E6 (±0.37 E6)	33.6 GPa
Static modulus of elasticity (90 days)	5.01 E6 (±0.148	35.1 GPa
Static modulus of elasticity (180 days)	5.45 E6 (±0.099	38.2 GPa
Dynamic modulus of elasticity (7 days)	7.2 E6 (±0.044 E6)	50.4 GPa
Dynamic modulus of elasticity (28	7.8 E6 (±0.034 E6)	54.6 GPa
Dynamic modulus of elasticity (90	(N/A)	(N/A)
Dynamic modulus of elasticity (180	8.34 E6 (±0.165	58.4 GPa
Poisson's ratio (7 days)	0.16 (±0.015)	0.16
Poisson's ratio (28 days)	0.18 (±0.006)	0.18
Poisson's ratio (90 days)	0.175 (±0.0071)	0.175
Poisson's ratio (180 days)	0.17 (±0.0001)	0.17
Rapid Chloride ion permeability	1003 (±104)	1003
Rapid Chloride ion permeability Class	LOW	LOW

Table 22: Properties of mix SCC4

Criteria	**Mean (±Std. Dev) psi**	**Mean MPa**
Compress strength (7 days)	3958 (±156)	27.7
Compress strength (28 days)	6681 (±411)	46.8
Compress strength (90 days)	8022 (±314)	56.2
Compress strength (180 days)	8101 (±298)	56.7
Modulus of rupture (7 days)	696 (±72)	4.9
Modulus of rupture (28 days)	769 (±39)	5.4
Modulus of rupture (90 days)	983 (±NA)	6.9
Modulus of rupture (180 days)	1330 (±128)	9.3
Static modulus of elasticity (28 days)	4.6 E6 (±0.31 E6)	32.2 GPa
Static modulus of elasticity (90 days)	4.5 E6 (±0.026 E6)	31.5 GPa
Static modulus of elasticity (180 days)	5.3 E6 (±0.31 E6)	37.1 GPa
Dynamic modulus of elasticity (7 days)	7.1 E6 (±0.20)	49.7 GPa
Dynamic modulus of elasticity (28	7.7 E6 (±0.22)	53.9 GPa
Dynamic modulus of elasticity (180	8.43 E6 (±0.15)	59.0 GPa
Poisson's ratio (28 days)	0.21 (±0.016)	0.21
Poisson's ratio (90 days)	0.17 (±0.015)	0.17
Poisson's ratio (180 days)	0.18 (±0.014)	0.18
Rapid Chloride ion permeability	831 (±150)	831
Rapid Chloride ion permeability Class	VERY LOW	VERY LOW

Table 23: Properties of mix SCC5

Criteria	**Mean (±Std. Dev) psi**	**Mean MPa**
Compress strength (7 days)	5327 (±224)	37.3
Compress strength (28 days)	7047 (±146)	49.3
Compress strength (90 days)	8283 (±600)	58.0
Compress strength (180 days)	9606 (±727)	67.2
Modulus of rupture (7 days)	707 (±20)	4.9
Modulus of rupture (28 days)	1021 (±37)	7.1
Modulus of rupture (90 days)	1069 (±155)	7.5
Modulus of rupture (180 days)	1253 (±68)	8.8
Static modulus of elasticity (28 days)	4.51 E6 (±0.345	31.6 GPa
Static modulus of elasticity (90 days)	4.40 E6 (±0.0759	30.8 GPa
Static modulus of elasticity (180 days)	5.60 E6 (±0.068	39.2 GPa
Dynamic modulus of elasticity (7 days)	7.2 E6 (±0.092 E6)	50.4 GPa
Dynamic modulus of elasticity (28	7.4 E6 (±0.028 E6)	51.8 GPa
Dynamic modulus of elasticity (180	8.41 E6 (±0.0168	58.9
Poisson's ratio (28 days)	0.19 (±0.016)	0.19
Poisson's ratio (90 days)	0.19 (±0.010)	0.19
Poisson's ratio (180 days)	0.195 (±0.021)	0.195
Rapid Chloride ion permeability	631 (±114)	631
Rapid Chloride ion permeability Class	VERY LOW	VERY LOW

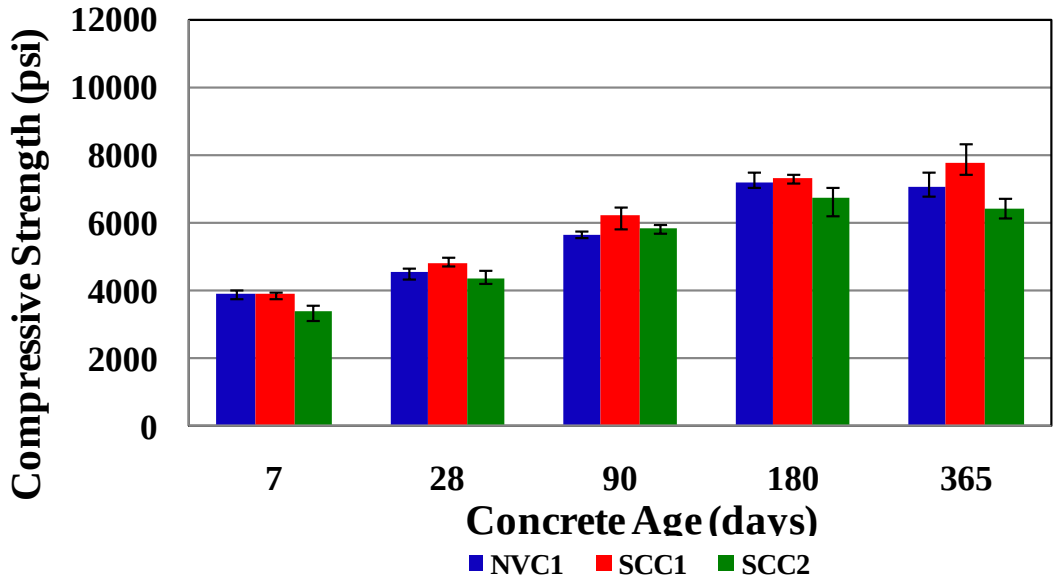

Figure 43: Comparison between the compressive strength of NVC1, SCC1 and SCC2.

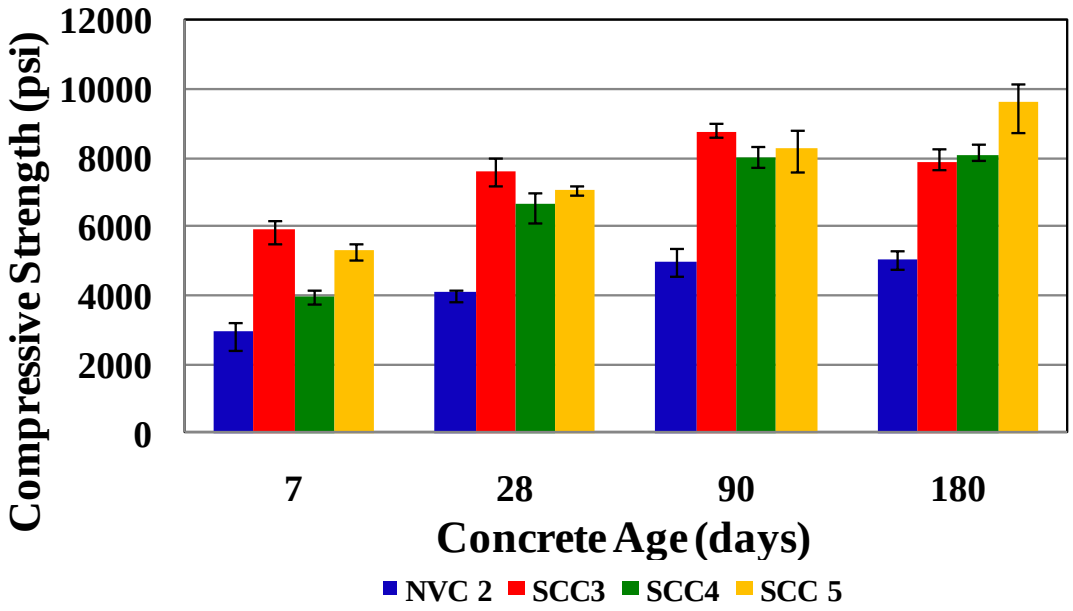

Figure 44: Comparison between the compressive strength of NVC2, SCC2, SCC4 and SCC5.

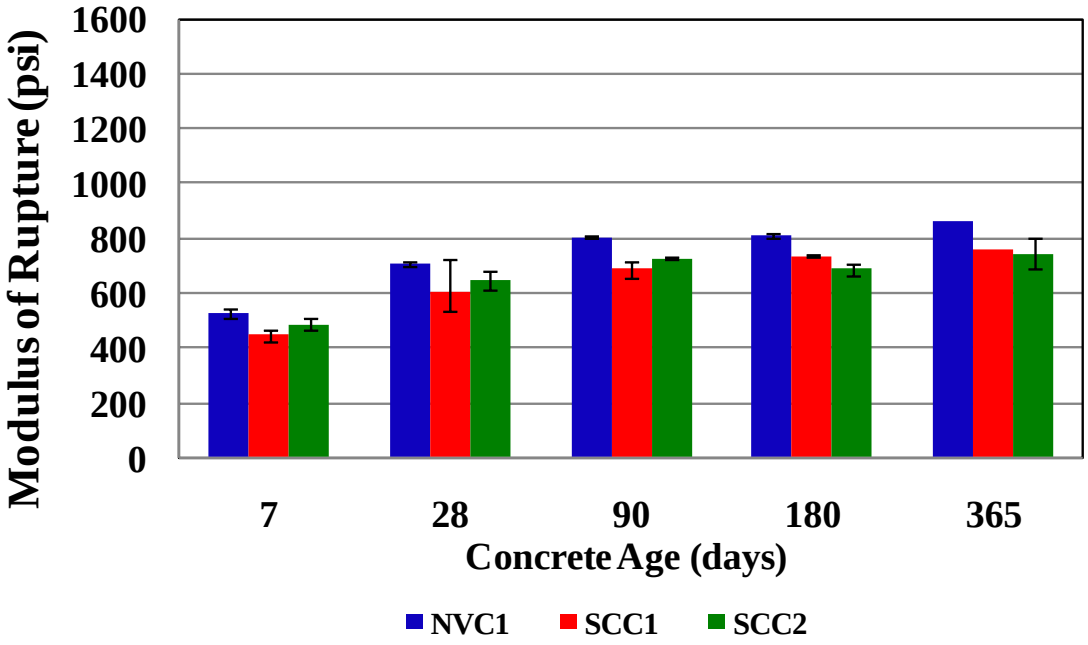

Figure 45: Comparison between the modulus of rupture of NVC1, SCC1 and SCC2.

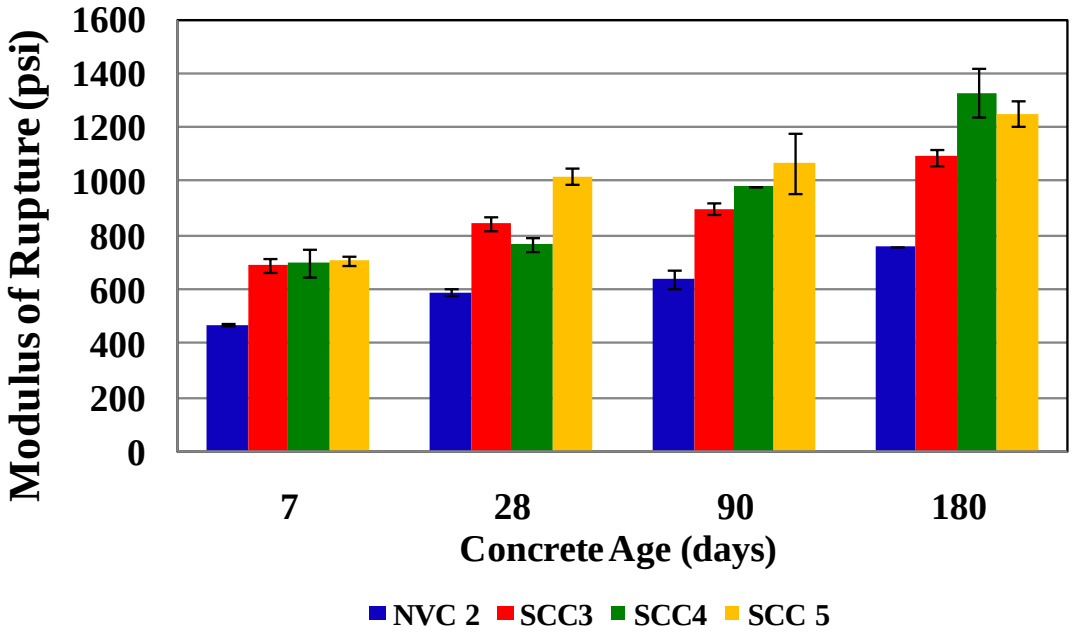

Figure 46: Comparison between the modulus of rupture of NVC2, SCC3, SCC4 and SCC5.

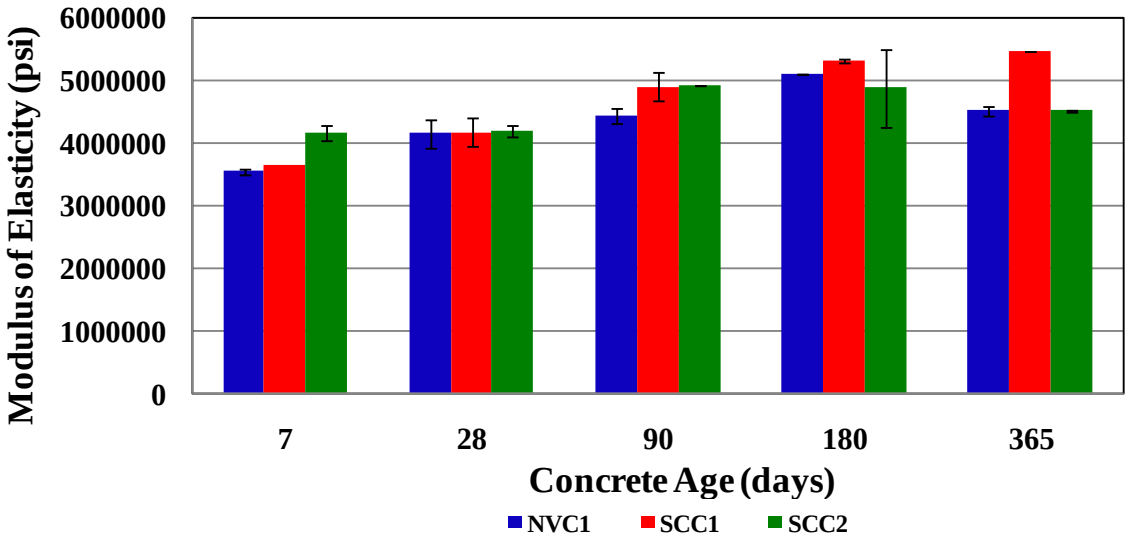

Figure 47: Comparison between the modulus of elasticity of NVC1, SCC1 and SCC2.

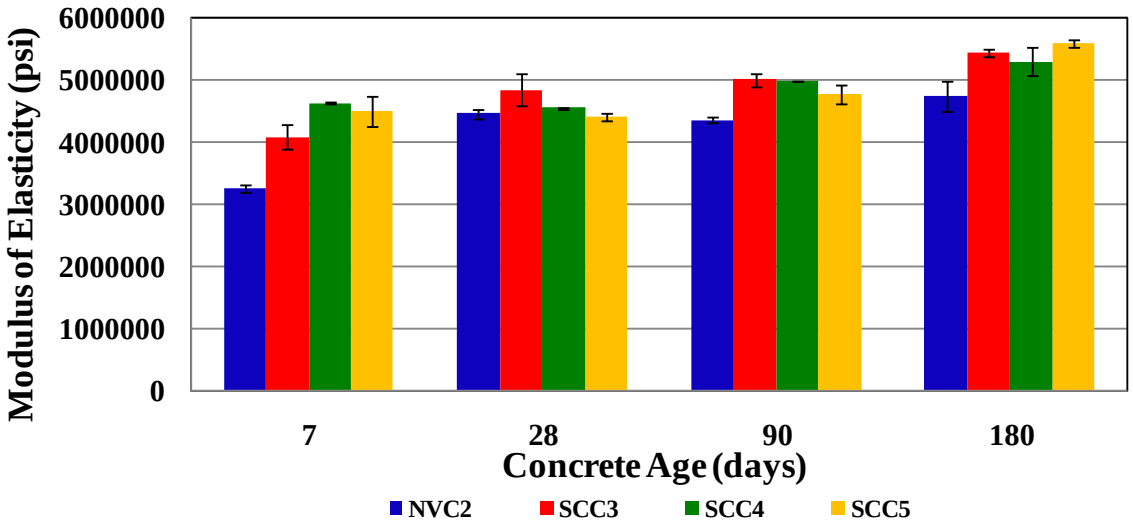

Figure 48: Comparison between the modulus of elasticity of NVC2, SCC3, SCC4 and SCC5.

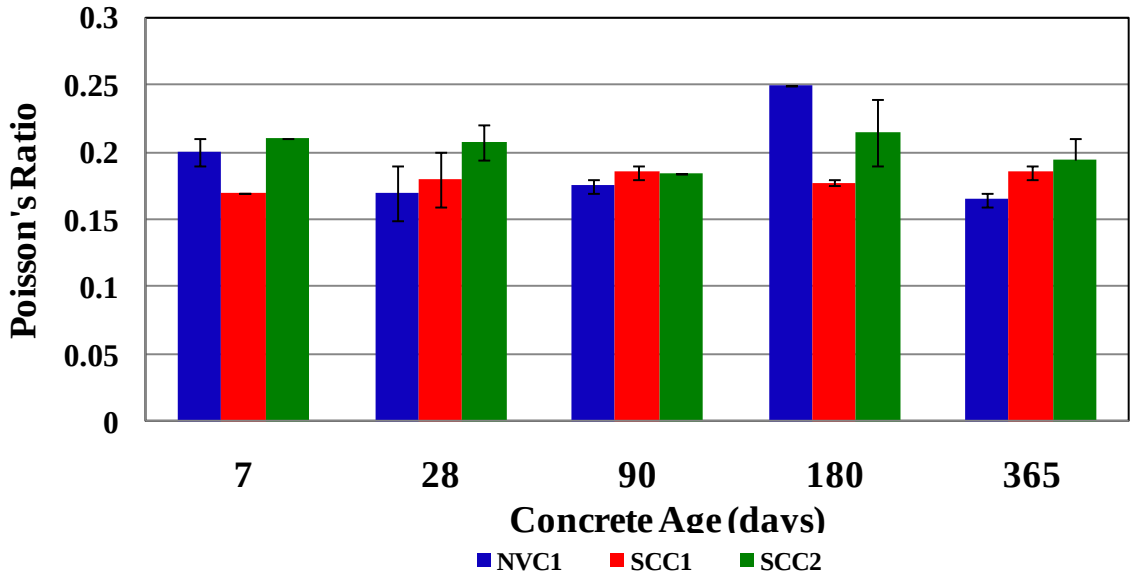

Figure 49: Comparison between Poisson's ratio of NVC1, SCC1 and SCC2.

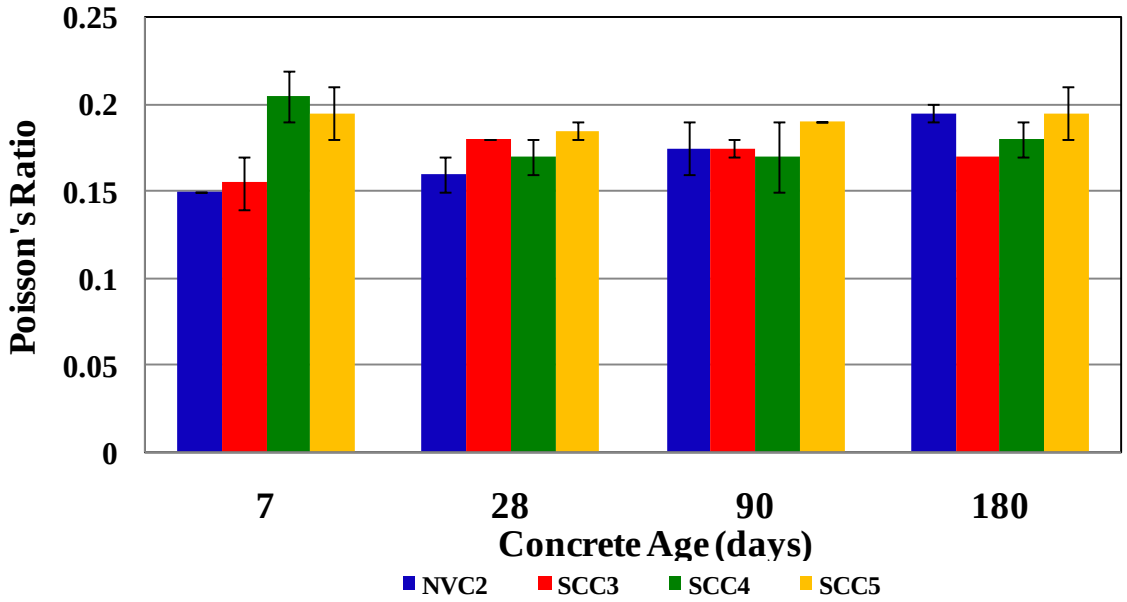

Figure 50: Comparison between Poisson's ratio of NVC2, SCC3, SCC4 and SCC5.

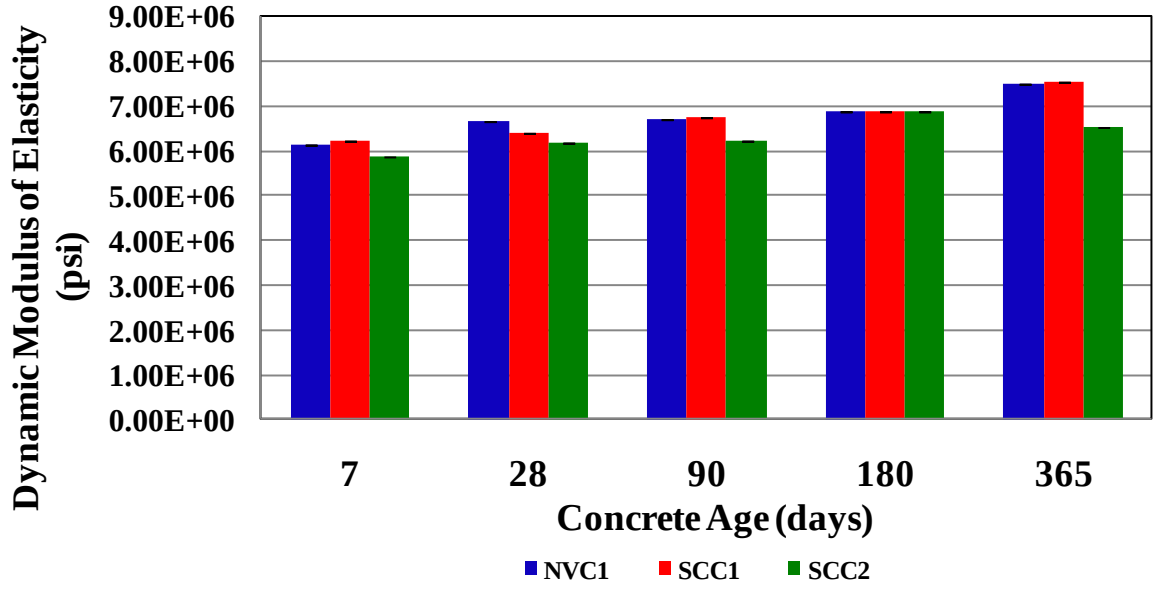

Figure 51: Comparison between the dynamic modulus of elasticity of NVC1, SCC1 and SCC2, measured using pulse velocity.

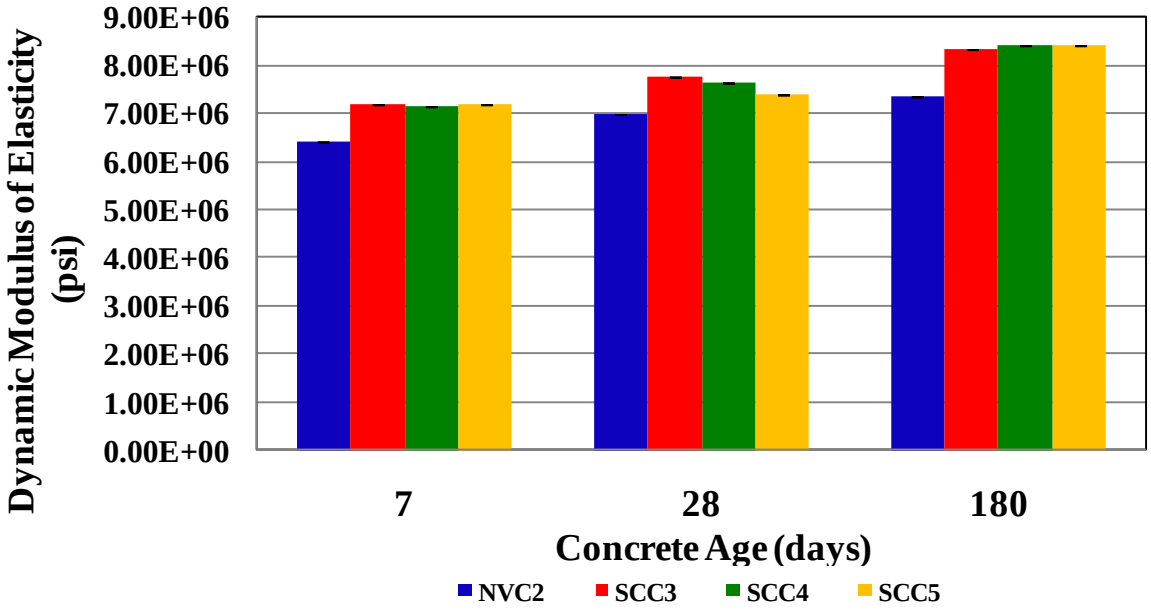

Figure 52: Comparison between the dynamic modulus of elasticity of NVC2, SCC3, SCC4 and SCC5 using pulse velocity

The placitas source concretes showed consistant compressive strength gain up to 180 days for NVC1 and SCC2, and 365 days for SCC1. The mean values of compressive strength are similar, and the variation of strength for each mix is similar. Modulus of rupture gains strength consistently through the year for all mixes, and is more variable in SCC1 and SCC2 than NVC1. NVC1 is stronger in modulus of rupture than SCC1 or SCC2. Static modulus of elasticity is noticably increasing for all mixes up to 180 days with similar variation between SCC1 and NVC1. Mean values are the close to each other for modulus of elasticity. SCC2 showed high variation for measurements collected at 180 days. Poisson's ratio can be interpreted to be consistantly 0.20, but is extreemly variable within given mixes at different times. Dynamic modulus of elasticity improved for SCC1 and NVC1 up to 365 days, and for SCC2 up to 180 days. Variation for dynamic modulus of elasticity was small, and the average values were similar.

The Griego source aggregate concretes showed similar variation in compressive strength between NVC2, SCC3, SCC4, and SCC5. NVC2 and SCC5 demonstrated consistent strength gain up to 180 days, and SCC3 and SCC4 up to 90 days. The mean strength of NVC2 was considerably and consistently lower than these SCC mixes because the water to total cementitious ratios are less in these SCC mixes. Modulus of rupture gained strength significantly up to 180 days for all mixes, with higher variation in SCC3, SCC4, and SCC5 than in NVC2. The MOR is higher in SCC3-5 than it is in NVC2, but the results are not as different from each other as they are in compressive strength. Static modulus of elasticity increased consistently up to 180 days for all mixes with similar variation between mixes. Mean values of the modulus of elasticity of NVC2 are slightly less but none the less close to modulus of elasticity SCC3, SCC4, and SCC5.

This can be attributed to NVC2's coarse aggregates contributing to higher modulus of elasticity. Poisson's ratio of NVC2 increases with time up to 180 days, and SCC3 increases up to 28 days but remains the same following this. SCC4 and SCC5 appear to have steady Poisson's ratio through time with values between 0.16-0.18. There is high variation for mean values of Poisson's ratio in all mixes, but the mean values of NVC2 are similar to SCC3-5. Dynamic modulus of elasticity increases steadily up to 180 days for all mixes. No data was collected for this parameter on 90 days for SCC mixes. Mean values of NVC2 are similar to SCC3-5, but slightly less with low variation between tests.

The two sample t test was used to compare the mean strength and durability properties of SCC with NVC. This was done to measure statistical differences between the mean values found from testing SCC and the mean values found from testing NVC assuming that the populations used to calculate these values followed the t-distribution. The advantage of implementing the t-distribution is that is much like the normal distribution, but can be used for smaller sample sizes [78] with variable sample populations between different mixes. SCC1 and SCC2 were compared to NVC1, and SCC3, SCC4, and SCC5 were compared to NVC2. The test result demonstrates whether the mean values of a given property are significantly different (SD) or not significantly different (NSD). The level of significance for samples with a population greater than 6 was $\alpha = 0.05$ (95% confidence interval) and for smaller sample populations $\alpha = 0.1$ (90% confidence interval). Equation 26 was used to calculate the t value where X_1 = mean value for NVC, X_2 = the mean value for SCC, δ = anticipated difference between two means, S_p = the pooled variance of the two samples combined, S_1 = variance in NVC, S_2 = variance of SCC, n_1 = population of NVC samples, and n_2 = the population of SCC

samples. The hypothesis for comparing SCC with NVC is that they have the same mean strength or durability properties (δ=0), and was accepted for - $t_{\alpha/2} < t < t_{\alpha/2}$.

$$t = \frac{\overline{X}_1 - \overline{X}_2 - \delta}{S_p \sqrt{\frac{1}{n_1} + \frac{1}{n_2}}} \tag{26}$$

$$S_p^2 = \frac{(n_1 - 1)S_1^2 + (n_2 - 1)S_2^2}{n_1 + n_2 - 2} \tag{27}$$

It was observed that there is not a significant difference between the mean results of NVC1, SCC1, and SCC2, but there were significantly different mean results found between NVC2, SCC3, SCC4, and SCC5.

Table 24: Two sample t test for comparing mean compressive strength of SCC1-2 to NVC1

SCC1	**7**	**28**	**90**	**180**	**365**
t test	0.106	-2.410	-2.448	-0.709	-1.697
$t_{\alpha/2=0.025}$	±2.776	±2.571	±2.776	±2.776	±2.776
Significance	**NSD**	**NSD**	**NSD**	**NSD**	**NSD**
SCC2	**7**	**28**	**90**	**180**	**365**
t test	3.656	1.504	-2.031	1.663	2.593
$t_{\alpha/2=0.025}$	±2.571	±2.571	±2.776	±2.776	±2.571
Significance	**SD**	**NSD**	**NSD**	**NSD**	**SD**

Table 25: Two sample t test for comparing mean compressive strength of SCC3-5 to NVC2

SCC3	**7**	**28**	**90**	**180**
t test	-12.263	-14.531	-15.827	-13.355
$t_{\alpha/2=0.025}$	±2.447	±2.571	±2.571	±2.571
Significance	**SD**	**SD**	**SD**	**SD**
SCC4	**7**	**28**	**90**	**180**
t test	-4.866	-9.987	-12.182	-15.055
$t_{\alpha/2=0.025}$	±2.447	±2.571	±2.571	±2.571
Significance	**SD**	**SD**	**SD**	**SD**

Table 26: Two sample t test for comparing bending strength (MOR) of SCC1-2 to NVC1

SCC1	**7**	**28**	**90**	**180**
t test	3.055	1.318	3.820	7.717
$t_{\alpha/2=0.05}$	±2.920	±2.920	±2.920	±2.920
Significance	**SD**	**NSD**	**SD**	**SD**
SCC2	**7**	**28**	**90**	**180**
t test	1.544	1.742	13.072	5.096
$t_{\alpha/2=0.05}$	±2.920	±2.920	±2.920	±2.920
Significance	**NSD**	**NSD**	**SD**	**SD**

Table 27: Two sample t test for comparing bending strength (MOR) of SCC3-5 to NVC2

SCC3	**7**	**28**	**90**	**180**
t test	-9.389	-9.174	-6.698	-11.422
$t_{\alpha/2=0.05}$	±2.920	±2.920	±2.920	±2.920
Significance	**SD**	**SD**	**SD**	**SD**
SCC4	**7**	**28**	**90**	**180**
t test	-4.430	-4.382	-10.631	-6.331
$t_{\alpha/2=0.05}$	±2.920	±2.920	±2.920	±2.920
Significance	**SD**	**SD**	**SD**	**SD**
SCC5	**7**	**28**	**90**	**180**
t test	-9.499	-23.596	-9.235	-12.030
$t_{\alpha/2=0.05}$	±2.920	±2.920	±2.920	±2.920
Significance	**SD**	**SD**	**SD**	**SD**

Table 28: Two sample t test for comparing static modulus of elasticity of SCC1-2 to NVC1

SCC1	**7**	**28**	**90**	**180**	**365**
t test	-2.140	0.690	-1.793	-4.594	-12.438
$t_{\alpha/2=0.05}$	±2.920	±2.920	±2.920	±2.920	±2.920
Significance	**NSD**	**NSD**	**NSD**	**SD**	**SD**
SCC2	**7**	**28**	**90**	**180**	**365**
t test	-4.621	-0.131	-3.265	0.246	0.038
$t_{\alpha/2=0.05}$	±2.920	±2.920	±2.920	±2.920	±2.920
Significance	**SD**	**NSD**	**SD**	**NSD**	**NSD**

Table 29: Two sample t test for comparing static modulus of elasticity of SCC3-5 to NVC2

SCC3	**7**	**28**	**90**	**180**
t test	-3.936	-1.386	-5.700	-2.733
$t_{\alpha/2=0.05}$	±2.920	±2.920	±2.920	±2.920
Significance	**SD**	**NSD**	**SD**	**NSD**
SCC4	**7**	**28**	**90**	**180**
t test	-20.235	-1.073	-13.798	-1.694
$t_{\alpha/2=0.05}$	±2.920	±2.920	±2.920	±2.920
Significance	**SD**	**NSD**	**SD**	**NSD**
SCC5	**7**	**28**	**90**	**180**
t test	-4.955	0.531	-2.577	-3.353
$t_{\alpha/2=0.05}$	±2.920	±2.920	±2.920	±2.920
Significance	**SD**	**NSD**	**NSD**	**SD**

Siddique [79] conducted research on powder type SCCs containing class F fly ash. The way that the materials were proportioned for Siddique's concretes is different from the way materials were proportioned for this Thesis. Approximately 30% more cement by mass is provided to his mixes. The fly ash percentages are based on the ratio of fly ash to total cementitious materials rather than fly ash to cement, and the dosage of superplasticizer is 2% instead of the 2.5% used for SCC in this Thesis. The lower dosages of superplasticizer added to his mixes can be attributed to the much higher amounts of fly ash which enhanced the workability in his mixes.

From the compressive strength results, we can observe in Figure 53 that the highest strength gains over time result from providing lower volumes of fly ash, which is in some cases contrary to the findings of this Thesis. This Thesis provides logical results

by demonstrating strength gain over time, but it is unclear whether higher strength gain comes from concretes containing less fly ash. Concretes containing more fly ash would typically react with more of the less desirable products of hydrated cement and convert them into the harder, stronger, and more durable products of hydrated cement. The Placitas source concretes appear to behave as Siddique's. This resemblance can be attributed to the similar water to cementitious ratios. The lower water to cementitious ratio, Griego and Sons source, concretes demonstrate higher strength gain with higher volumes of fly ash.

The relationship between modulus of rupture and compressive strength is different between SCC and NVC. SCC has the tendency to have higher flexural strength than NVC, so conventional relationships used today will underestimate the result for SCC. Figure 54 demonstrates a relationship between compressive strength modulus of rupture found by Domone in 2007 [42]. It can be seen that SCC is stronger than one would anticipate both in this Thesis, and from research by Domone. The higher results of MOR in SCC can be attributed to the smaller initial defects created by the transition zone between cement paste and aggregate. More stress is required to be provided before a crack can propagate and cause failure in SCC. The aggregate in SCC is smaller than in NVC, so once a crack begins to propagate, there is not as much energy consumed by displacing the path of the crack resulting in lower fracture toughness in SCC than in NVC.

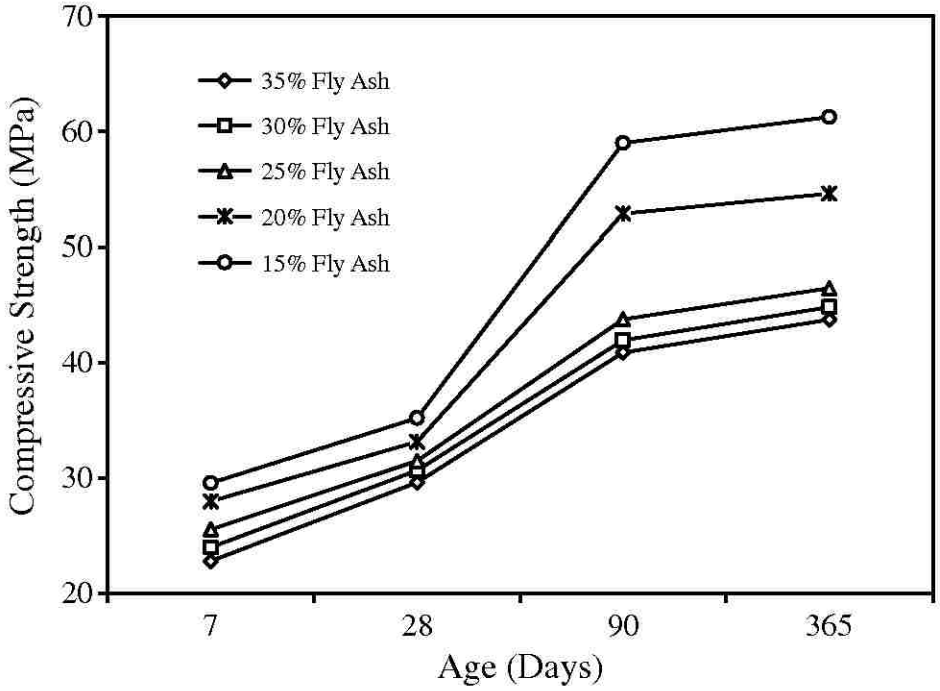

Figure 53: Compressive strength gain of SCC mixes with time (Siddique 2011).

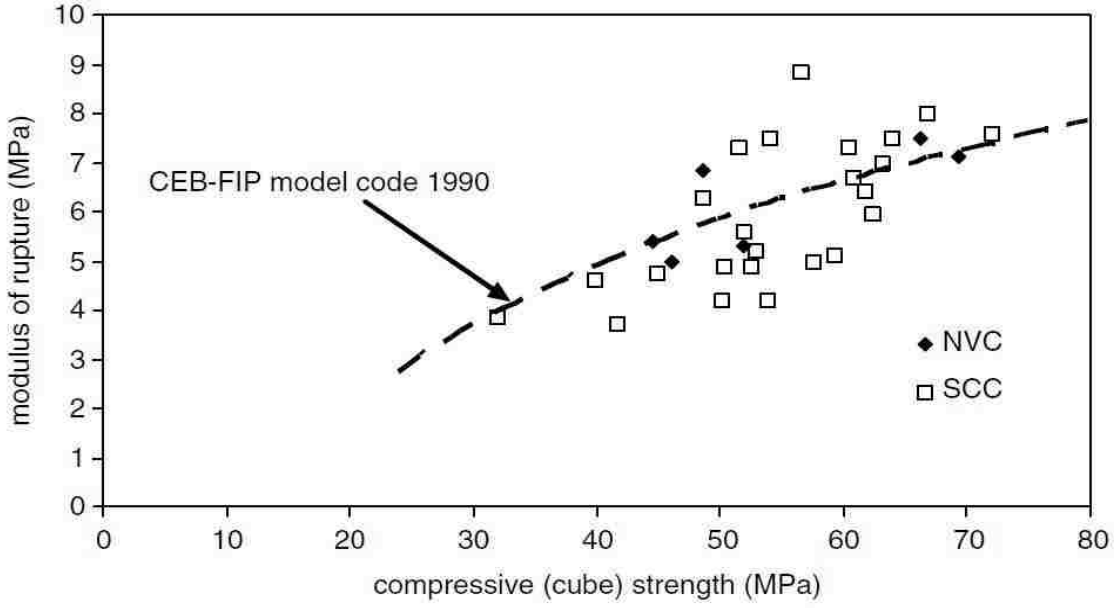

Figure 54: Relationship between MOR and compressive strength (Domone 2007)

4.3 Durability Test Results

Electrical current in RCPT tests for NVC1, SCC1, SCC2, NVC2, SCC3, SCC4, and SCC5 are shown in Figures 55, 56, 57, 58, 59, 60, and 61 respectively. Comparison of maximum electrical charge observed in RCPT test mixes is shown in Figure 62. Comparison of relative dynamic modulus of elasticity of NVC and SCC mixes with increased number of freeze-thaw cycles is shown in Figure 63. The durability factors for the mixes can be seen in Figures 64, and 65. Comparison of the expansion of mortar bars in NaOH solution incorporating various levels of fly ash can be observed in Figure 66 for Placitas Source and Figure 67 for Griego's source. Figure 68 shows the expansion of mortar bars containing no fly ash and a percentage of high range water reducer and viscosity modifying admixture equivalent to that in SCC mixes. Figure 69 implies that there is no significant difference on mortar bar expansion due to ASR when chemical admixtures are provided in respectively high proportions.

The freeze-thaw samples made with Placitas aggregate were damaged by an unknown number of freeze thaw cycles prior to measurements, and were older than 120 days of age when loaded into the freeze-thaw apparatus. Despite this, the Placitas samples outperformed the Griego and Sons samples in freeze/thaw durability.

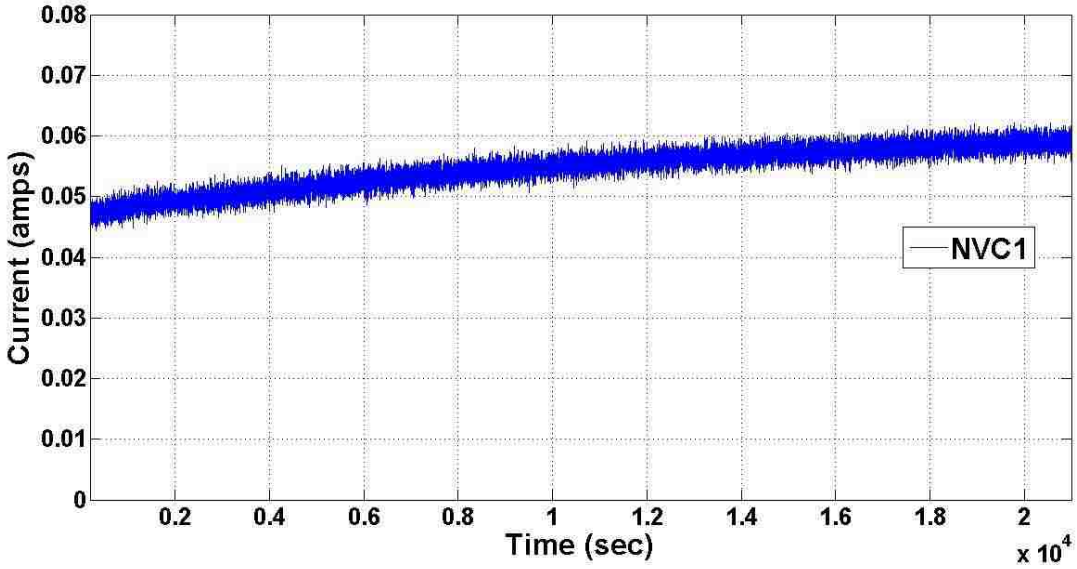

Figure 55: Electrical current in RCPT test for NVC1

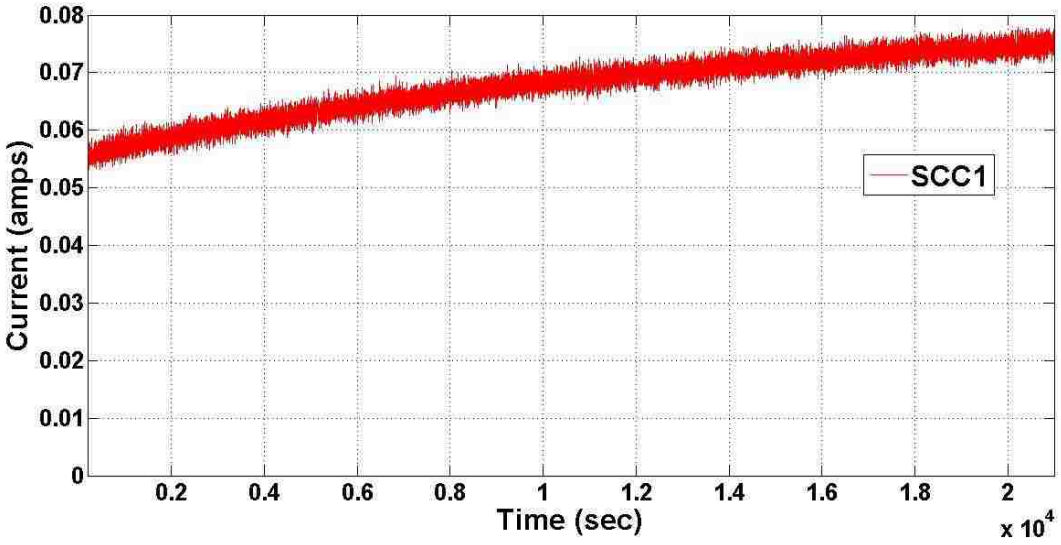

Figure 56: Electrical current in RCPT test for SCC1

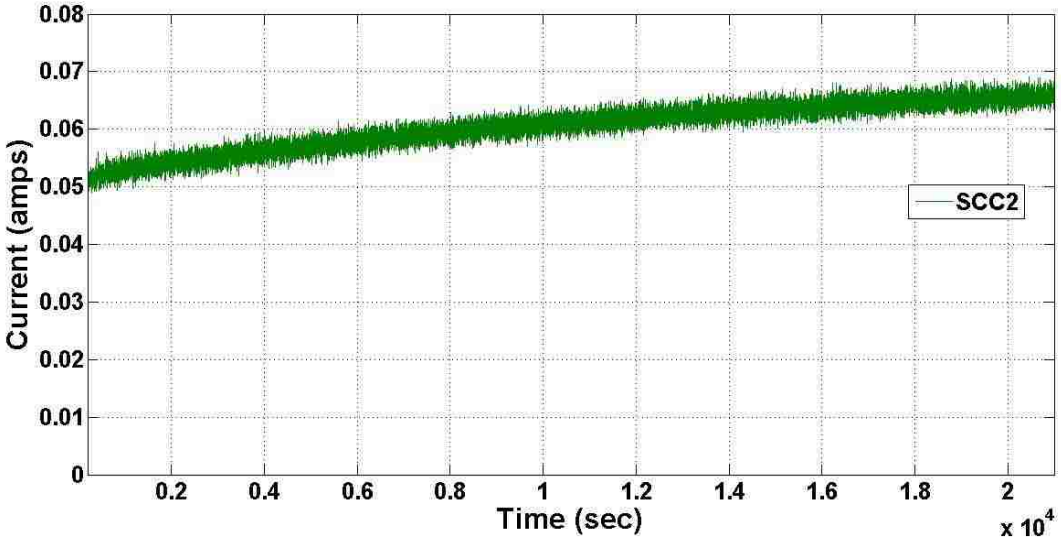

Figure 57: Electrical current in RCPT test for SCC2

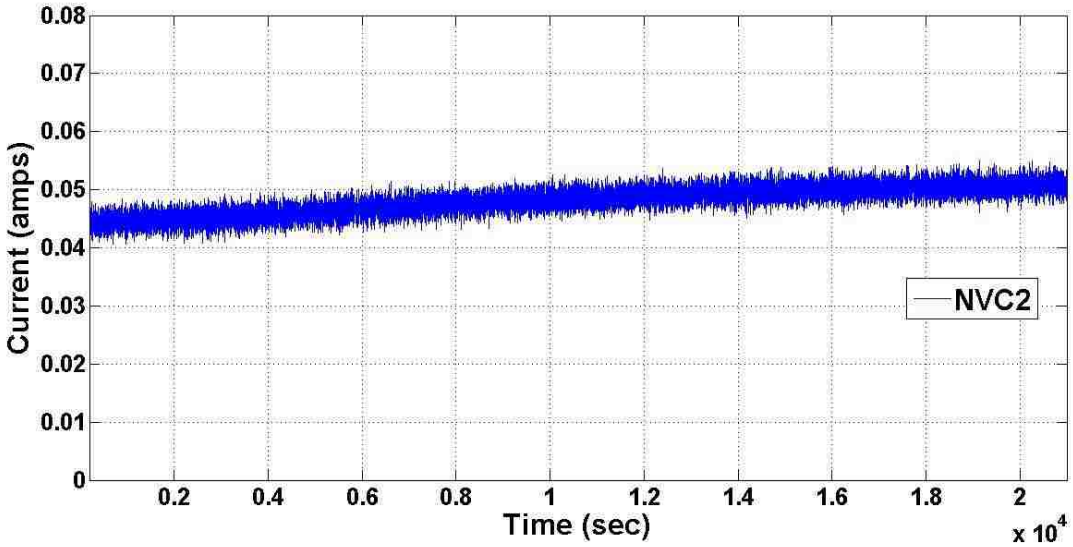

Figure 58: Electrical current in RCPT test for NVC2

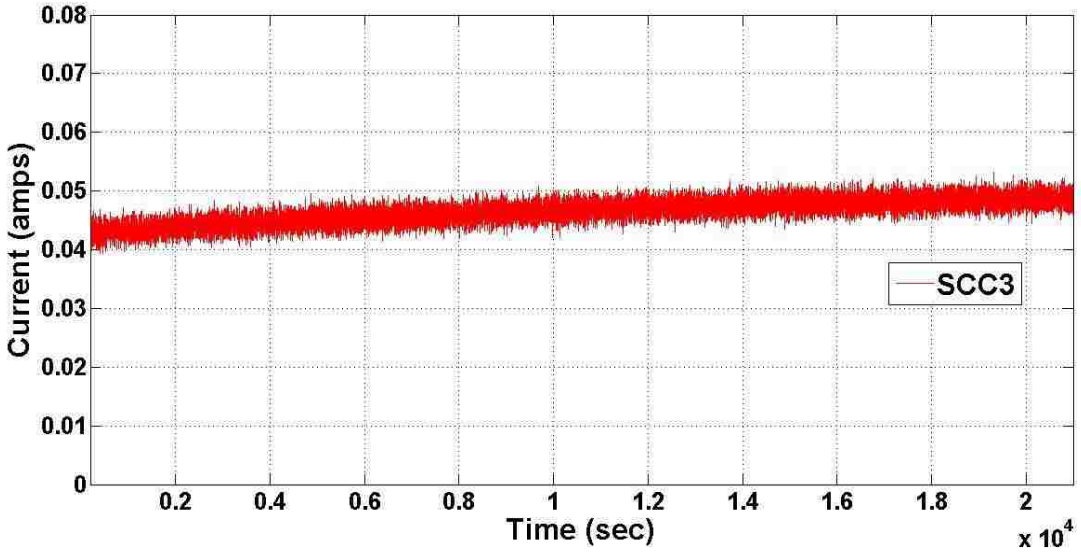

Figure 59: Electrical current in RCPT test for SCC3

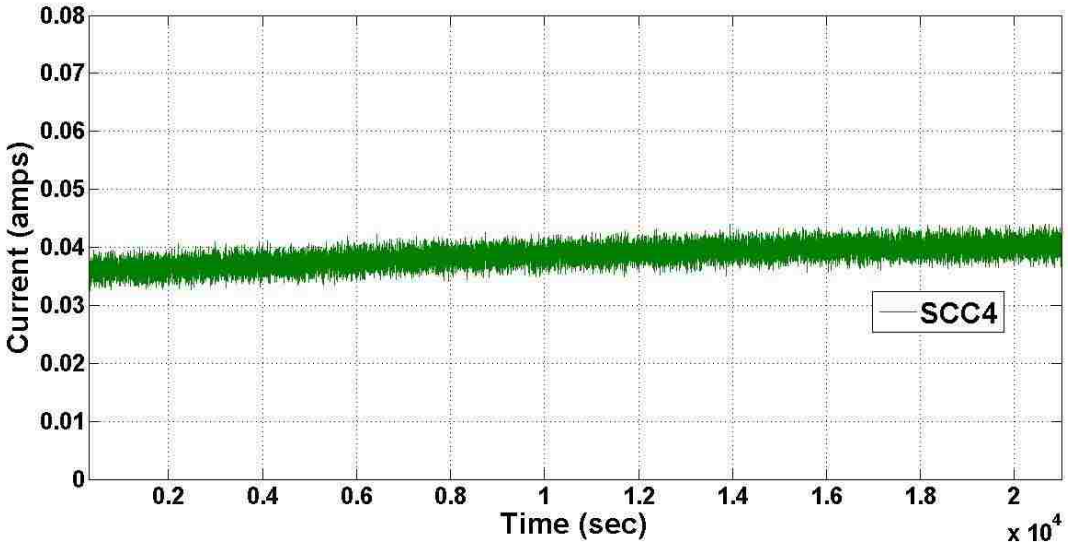

Figure 60: Electrical current in RCPT test for SCC4

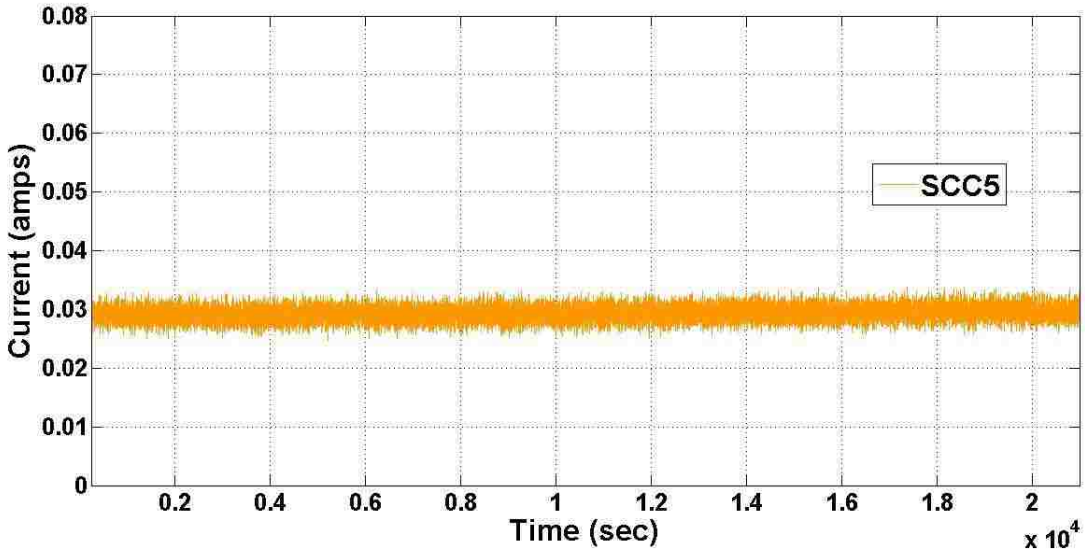

Figure 61: Electrical current in RCPT test for SCC5

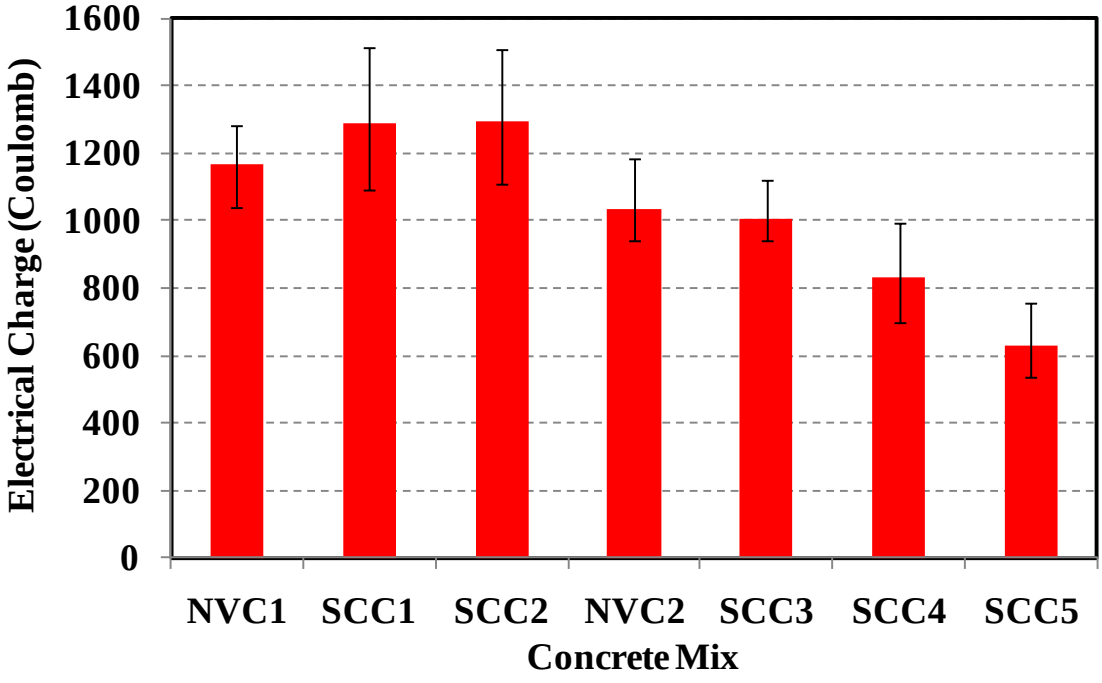

Figure 62: Comparison of maximum electrical charge for NVC1, SCC1, SCC2, NVC2, SCC3, SCC4, and SCC5

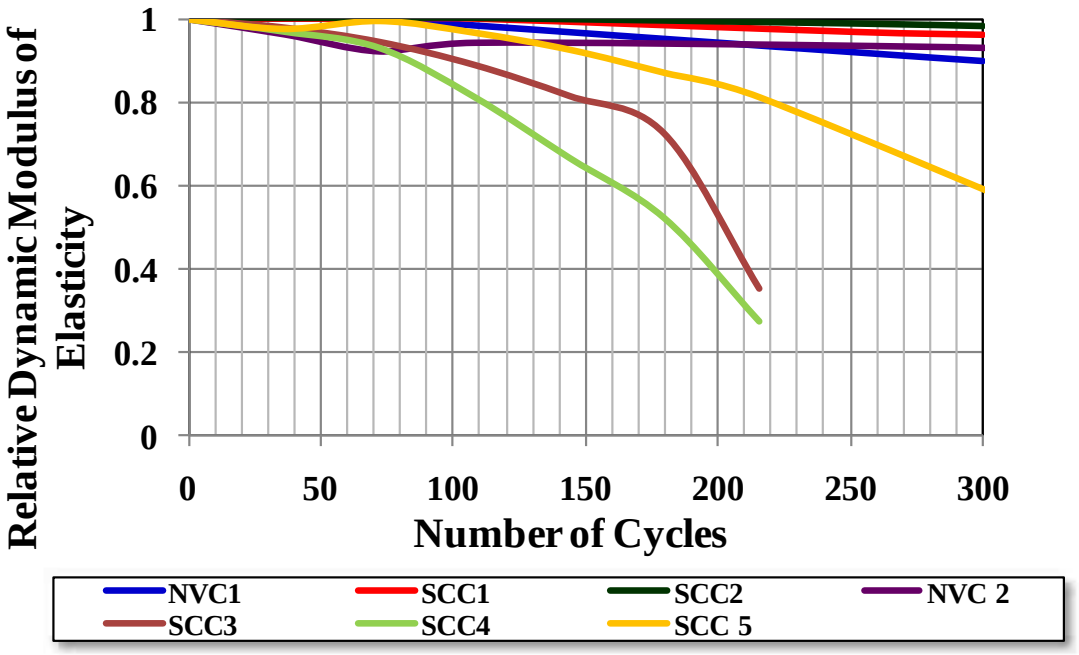

Figure 63: Relative dynamic modulus of elasticity versus number of freeze-thaw cycles for SCC, and NVC showing damage propagation due to freeze-thaw cycles.

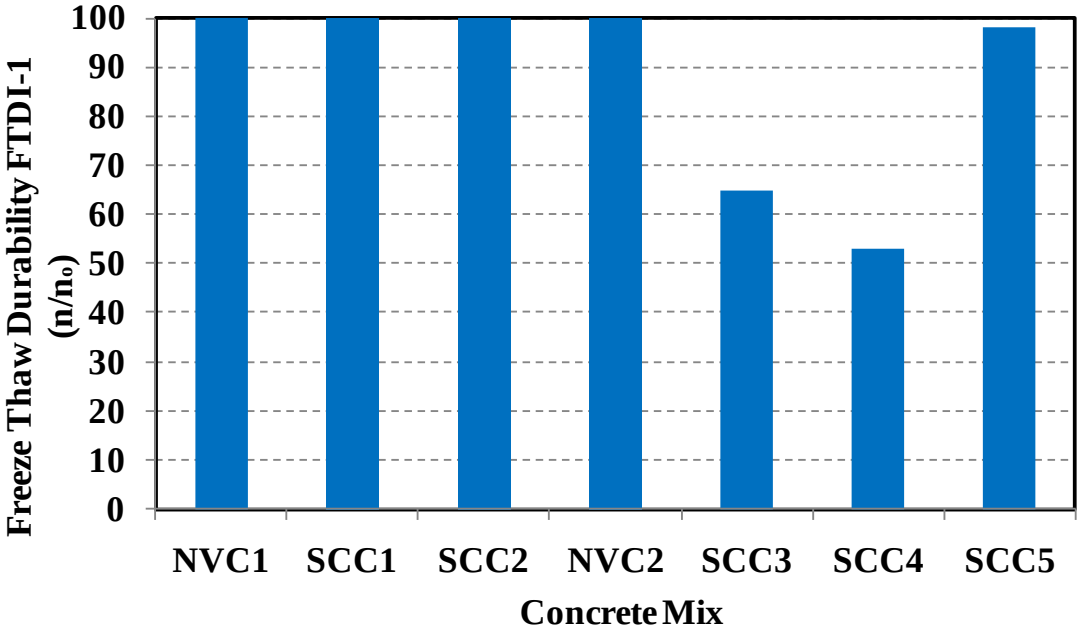

Figure 64: First freeze-thaw first durability index *FTDI-1* for NVC and SCC

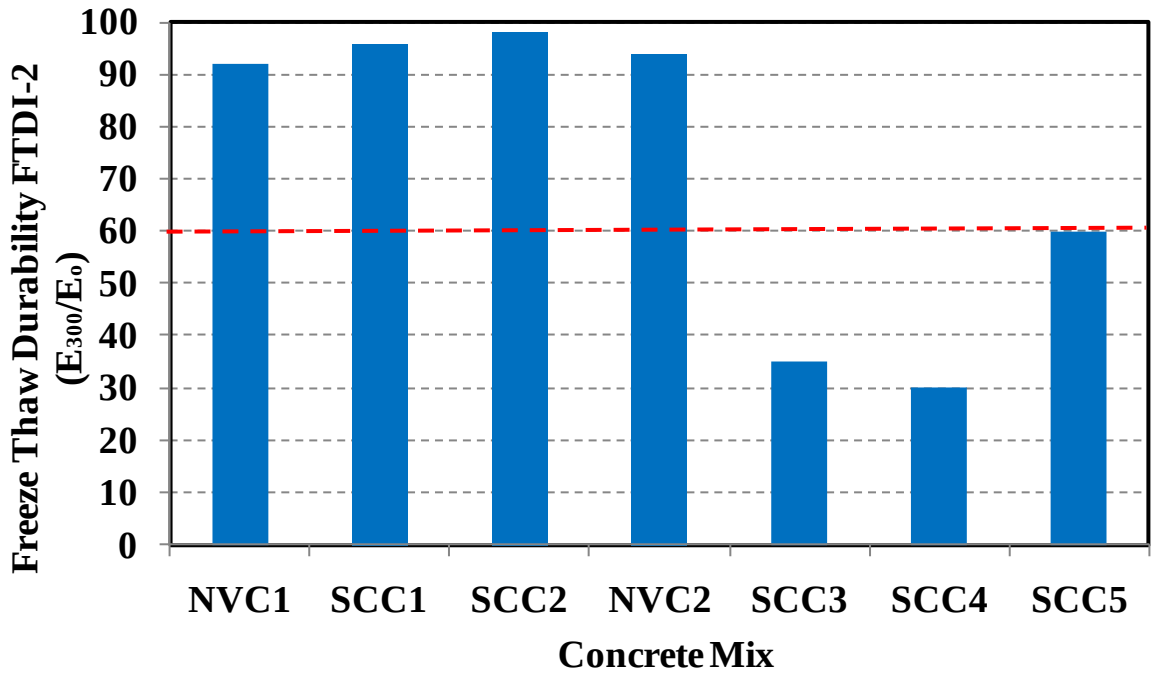

Figure 65: Second freeze-thaw second durability index *FTDI-2* for NVC and SCC

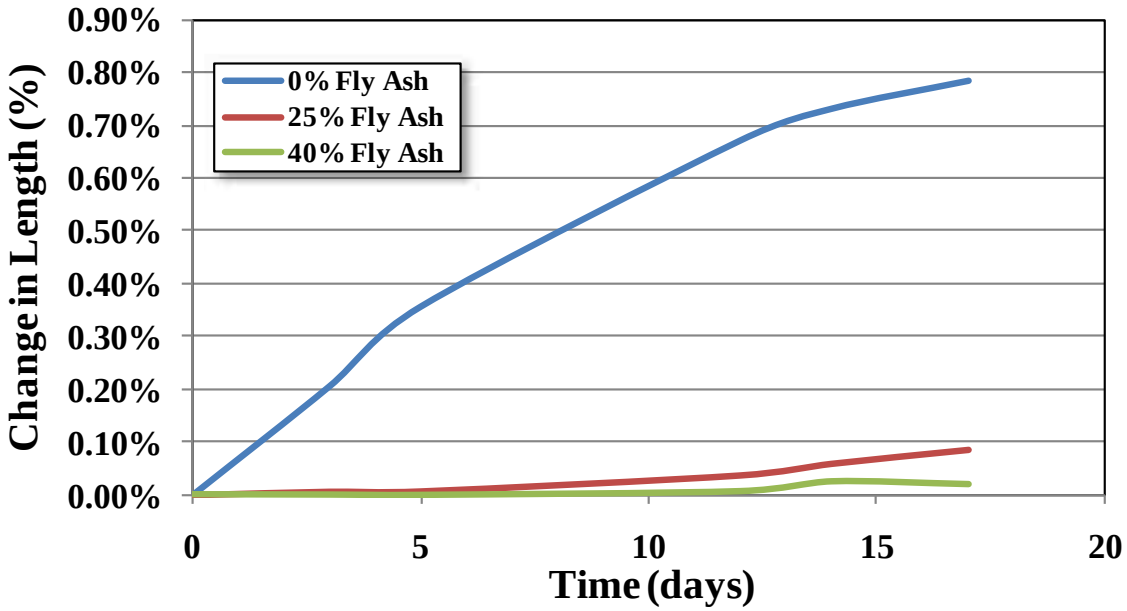

Figure 66: Expansion with time using the Placitas aggregate source.

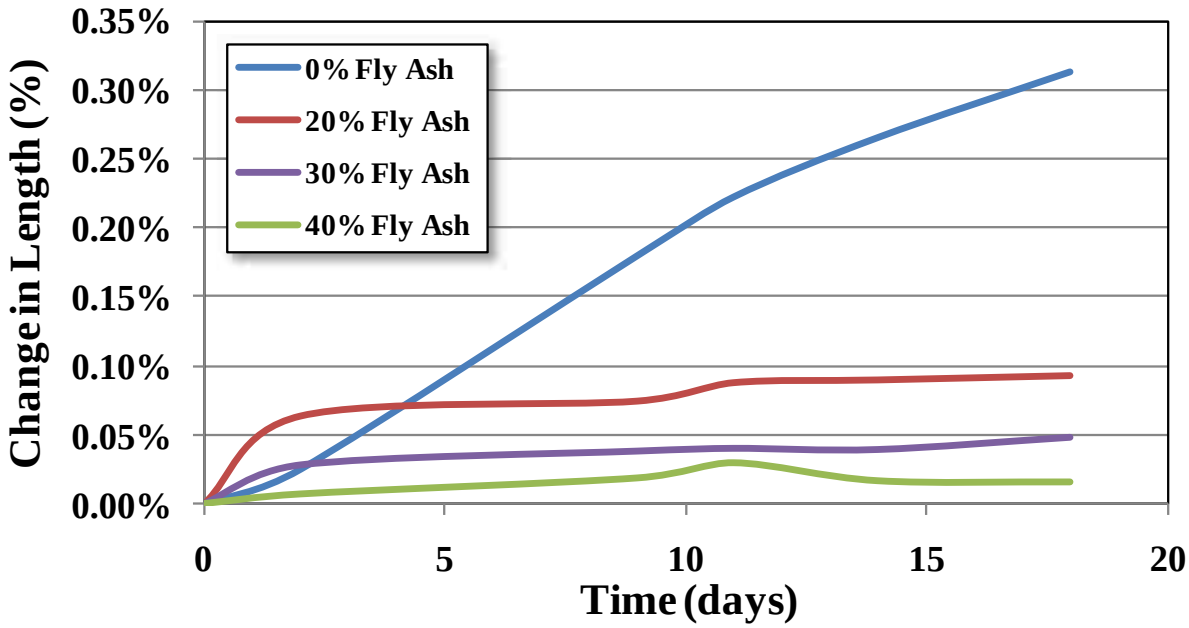

Figure 67: Expansion with time using the Griego and sons aggregate source.

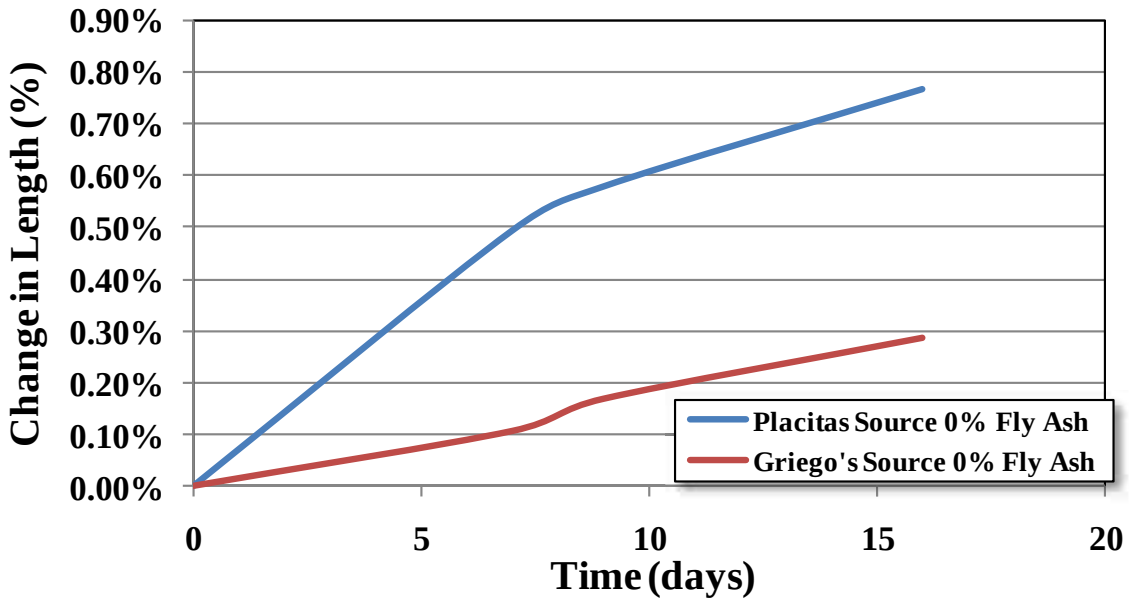

Figure 68: Expansion with time providing chemical admixtures used to make SCC.

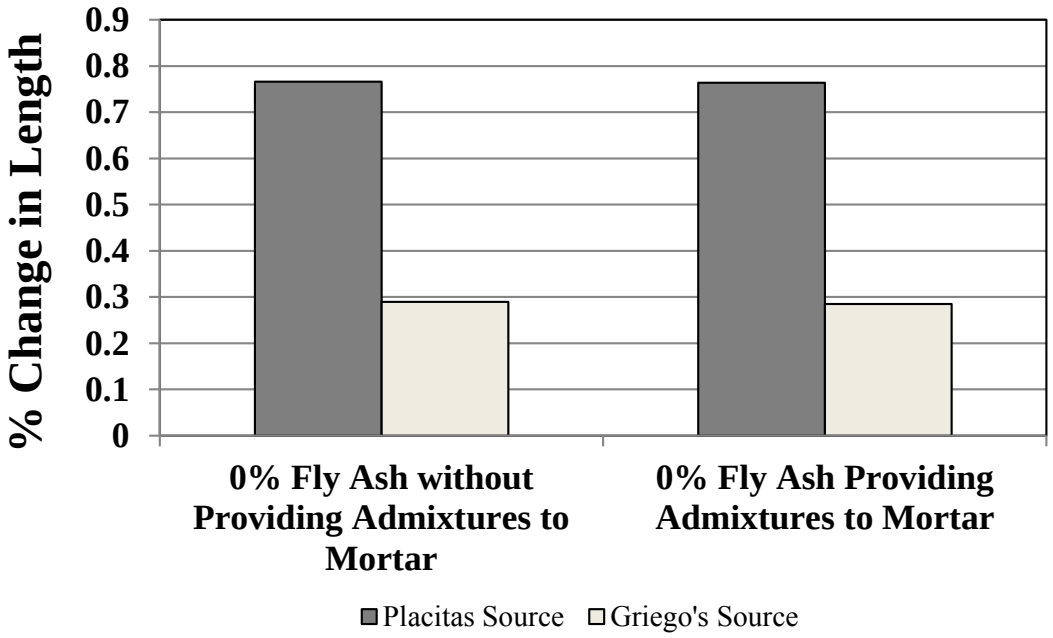

Figure 69: Comparison between ordinary mortar, and mortar containing admixtures used to make SCC.

The Rapid Chloride Ion Penetration Test RCPT results for the Placitas source concretes classify as having low to very low chloride ion permeability according to ASTM 1202. SCC1 and SCC2 have slightly higher permeability than NVC1, but the variation between the mixes is similar. These concretes show that current through the specimens increases over the six hour time interval. The results for the Griego source concretes classify NVC2 and SCC3 as low, and SCC4 and SCC5 as very low. Current through the Griego concretes is more constant with time. It appears that the permeability of the SCC mixes decreases as the amount of fly ash provided increases. Variation of test results is similar between NVC2, SCC3, SCC4, and SCC5. It has been determined that chloride ion penetration can decrease as the water to cementitious materials decreases, and SCC has typically shown lower chloride ion penetration than NVC [80].

It can be observed that chloride ion permeability increases as the amount of fly ash increases for concretes with high water to total cementitious materials ratios, but chloride ion permeability decreases as the amount of fly ash increases for concretes with low water to total cementitious materials ratios. Similar results have been reported by others [81].

Table 30 represents the statistical results found using the t test for comparing chloride ion resistance of NVC and SCC. The mean values of SCC1 and SCC2 are not significantly different (NSD) from NVC1 with 95% confidence. SCC3 and SCC4 were found to not be significantly different from NVC2, but the mean value for SCC5 is significantly different (SD) using a 95% confidence interval. The variation between the samples of the chloride ion resistance test is high. ASTM C1202 [72] recommends that the results of individual specimens for charge in coulombs should not differ from another by more than 42% when three or more samples are tested. This has been achieved for all of the test results found from multiple samples to determine the reported mean values of charge in coulombs.

Table 30: Two sample t test for comparing RCPT of SCC1-2 to NVC1 and SCC3-5 to NVC2

Mix	t test	$t_{\alpha=0.025}$	Significance
SCC1	-2.4121	±2.447	**NSD**
SCC2	-1.3178	±2.447	**NSD**
SCC3	0.30631	±2.776	**NSD**
SCC4	1.75105	±2.776	**NSD**
SCC5	3.98756	±2.776	**SD**

There are similarities between the RCPT results of this Thesis, and the results of Siddique [79]. The general consensus is that concretes containing a high volume of fly ash have low chloride ion penetration. The RCPT was conducted at 90 days for concrete

in this Thesis, and was conducted at 90 and 365 days by Siddique [79]. The chloride ion penetration decreasing with time is shown in figure 70.

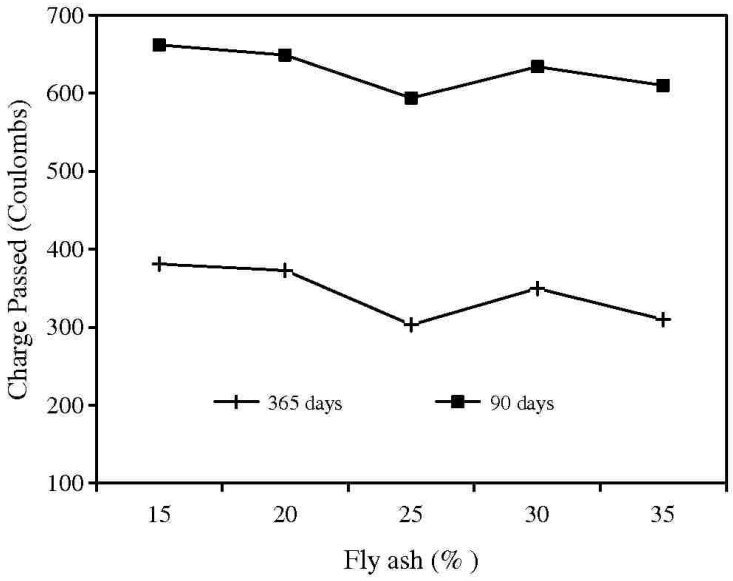

Figure 70: RCPT results for SCC containing different levels of fly ash [79]

Resistance to damage produced by freeze-thaw cycles appeared high for SCC2, SCC1, NVC1, and NVC2. NVC1 and NVC2 exhibited good freeze thaw durability as expected. SCC2 and SCC5 contained the highest levels of fly ash, and performed better than the other SCCs when compared to the mixes containing the same aggregate source. Nonetheless, SCC3, SCC4, and SCC5 have poor freeze thaw durability.

The durability of SCC was examined by Rudolf Hela [82]. It was demonstrated that there are issues in aerated SCC mixes because of incompatibilities between polycarboxylate based superplasticizers and air entraining admixtures. Moreover, the fresh, mechanical, and durability properties of SCC incorporating volcanic ash were examined by Hossain and Lachemi. The fresh concrete properties are similar to those presented in this Thesis, but no air entrainment was provided to those mixes [81]. The

characteristic compressive strengths and chloride ion penetration of the concretes produced using volcanic ash also have similar properties compared to the SCC mixes presented in this Thesis. From the work of Hossain and Lachemi, the freeze-thaw durability index (FDTI -2) ranged from 60 with water to total cementitious ratio of 0.45 to 80 with water to total cementitious ratio of 0.35. This indicates that there is a problem with the air structure in the Griego and Sons aggregate source concretes produced for this Thesis. It is apparent that the air void structure worked well for the Placitas source concretes, but the Griego and Sons source concretes have lower freeze/thaw durability than the concretes produced by Hossain and Lachemi [81] that contain no air entraining admixture. The difference in proportioning the batch water is believed to be the reason for the logical inconsistency in this Thesis. The discrepancies in freeze-thaw resistance of SCCs reported here shall lead to further investigations accompanied with air void analysis to correlate spacing factor measurements to freeze-thaw observations and to examine the effect of superplasticizer, and the possible incompatibility between superplasticizer and air entraining admixture. The spacing factor is a parameter related to the maximum distance found between air-voids within the cement paste [83]. If the distance between air-voids is large, the expansion of water due to freezing will develop high stresses within the concrete and cause damage. Further research is definitely needed to examine freeze-thaw properties of SCC.

The Placitas fine aggregate is more reactive than the Griego fine aggregate. When percentages of fly ash are provided, the expansion is reduced significantly. As the amount of fly ash is increased the expansion decreases as anticipated. The mortar bar expansion is the same when amounts of superplasticizer and VMA are added to the

mixing water. The same amounts of admixtures that were provided to SCC were provided to mortar to determine this.

4.4 Field Implementation in New Mexico

Over the last two decades, there has been an increase in the use of Self Consolidating Concrete because it can reduce unwanted voids within placements, and increases freedom in design of reinforced structures. Because of this, SCC can be implemented by the New Mexico Department of Transportation for applications in ordinary highway construction, and specialized transportation projects. SCC is defined greatly by its freshly mixed properties. SCC hardened properties are similar to those of NVC with some exceptions such as freeze thaw durability. Investigations showed that the Specification and Guidelines for Self-Compacting Concrete produced by the European Federation for Specialist Construction Chemicals and Concrete Systems (EFNARC) might be used to classify and aid in the design of SCC that will be used in the future. This classification can be performed based on three fresh concrete characteristics: slump flow, the mixture viscosity and the passibility. These three major fresh concrete characteristics can be measured in the field. The flowability is measured using slump flow, the viscosity of the mix is measured using T_{50} time and the passability is measured using the L-Box or the J-Ring. The J-ring test is the slump flow test incorporating obstacles mimicking reinforcement. A ring with variable spaced rebar simulating a reinforcement configuration is placed over the cone to fence the concrete contained in the cone. The cone is raised and the concrete flows from the inside of the ring to the outside of the ring. We then compare the diameter of the ordinary slump flow with the diameter of the slump flow passing through the J- ring to determine the passability. The J- ring

test is a good measure for field applications because it is compact and yields decent results. The L-box test method is also a measure of passing ability. It can be used in the field, but it is a large apparatus so it may be practical for lab use only. The three tests are described in the literature. Tables 31, 32 and 33 provide the three classifications based on EFNARC with modification to suite the imperial unit system.

Table 31: SCC flowability classification based on slump flow

SCC Classification	**Slump flow (inch)**	**Typical application**
SF1	20-25	Pump injecting concrete and small sections that do not permit horizontal flow
SF2	25-30	Applications require flowable concrete as walls and columns
SF3*	30-35	Highly congested reinforcement and structures with complicated shapes

* High possibility for segregation requires careful check of trial mix

Table 32: SCC viscosity classification based on T_{50}

SCC Classification	**Time to flow (seconds)**	**Typical application**
VS1 (Low Viscosity)*	≤ 2 seconds	Highly congested reinforcement
VS2 (High Viscosity)	2-7 seconds	Applications require flowable concrete as walls and columns

* High possibility for segregation requires careful check of trial mix

Table 33: SCC passability classification based on L-Box height ratio

SCC Classification	**L-Box Height Ratio**	**Typical application**
PA1 (High passability)	≥ 0.8	Highly congested reinforcement
PA2 (Low passability)	< 0.8	Applications require flowable concrete as walls and columns

When SCC is used, it is important to emphasize the necessary evaluation of form work for any structural application using SCC. NVC has internal friction helping reduce pressure exerted on forms. SCC will exert hydrostatic pressure on forms which may result in blowing the forms out during construction.

CHAPTER 5 CONCLUSIONS

In this Thesis, Mechanical and durability properties of self consolidating concrete (SCC) were investigated at the macro-scale. The differences and similarities between SCC and normally vibrated concrete (NVC) were examined and reported. It is shown that SCC can be made with the local New Mexico aggregate sources, and by incorporating class F fly ash.

5.1 Fresh, Mechanical, and Durability Characteristics

All SCCs achieved the requirements of flowability, viscosity, and passability without excessive bleeding, or visual segregation in fresh state. Moreover, all SCCs achieved the required air content and temperature requirements of the NMDOT. Trial batches showed the necessity to optimize the aggregate gradation to produce homogenous SCC mixes.

The hardened SCC showed mechanical properties in agreement of typical concrete by having similar results in compression, modulus of rupture (MOR), Young's modulus, Poisson's ratio, and pulse velocity. The high volume fly ash mixes continued to gain strength up to 180 days of age. Concretes with characteristic compressive strengths in excess of 7000 psi were easily achievable. SCC is observed to have between 20 to 40 percent strength gain from 7 to 28 days, where NVC demonstrates 15 to 25 percent. The other mechanical properties of SCC were acceptable and exceeded expectations compared with conventional NVC produced with the same materials as well.

Durability characteristics of SCC were acceptable and comparable to NVC. SCC with high volumes of fly ash demonstrated better durability properties than those containing less fly ash. The durability properties sometimes exceeded those of NVC.

The Placitas aggregate showed to be highly reactive and high volume fly ash mixes must be used to reduce this reactivity. The Griego and sons aggregate showed to be much less reactive compared with Plactias aggregate. There was also no effect of the admixtures used to produce SCC on the performance of the mortar bar test. The freeze-thaw durability experiments were not conclusive and there is a need to examine freeze-thaw of SCC in depth while considering the air void system.

5.2 Recommendations

It will be required to examine the air void system of self consolidating concretes prior to the implementation of SCC in exposed structures because freeze thaw durability is very important for accepting concrete mix designs in New Mexico. From this Thesis, it is recommended to produce SCCs with the grading provided, and viscosity modifying admixture (VMA) coupled with water cementitious materials ratio between 0.33 and 0.40. By implementing fatty acid based air entraining admixture [84], the problems encountered with freeze thaw durability may be solved.

5.3 Future work

SCC mixes with Griego and Sons aggregate showed significantly lower freeze/thaw durability compared with NMDOT standards. While the air contents measured in fresh state using the pressure method met the specifications, the distribution of air bubbles is unknown and the spacing factor needs to be determined. Further investigations shall be conducted in that field with focus on relating the air spacing factor to the freeze-thaw durability of SCC mixes.

REFERENCES

1. Concrete, T.E.G.S.C., *The European Guide lines for Self-Compacting Concrete*, BIBM, et al., Editors. 2004.
2. Ozawa, K., et al. *Developement of high-performance concrete based on durability design of concrete structures*. in *East Asia and Pacific Conference on Structural Engineering and Construction (EASEC-2)*. 1989.
3. Khayat, K.H. and D. Mitchell, *Self Consolidating Concrete for Precast, Prestressed Concrete Bridge Elements*, F.H.W.A. (FHWA), Editor. 2009, Transportation Research Board Washington, D.C.
4. Domone, P.L., *Self -compacting concrete: An analysis of 11 years of case studies* Cement & Concrete Composites, 2005. **28**(2): p. 197-208.
5. Brown, D.A., et al., *Evaluation of self-consolidating concrete for drilled shaft applications at lumber River Bridge project, South Carolina.* Transportation Research Record, 2007(2020): p. 67-75.
6. Okamura, H. and M. Ouchi, *Self-compacting high performance concrete.* Progress in Structural Engineering and Materials, 1998. **1**(4): p. 378-383.
7. Okamura and Ozawa, *Mix Design for Self Compacting Concrete.* Concrete Library of Japan Society of Civil Engineering 1995(25): p. 107-120.
8. Heirman, G., et al., *Integration approach of the Couette inverse problem of powder type self-compacting concrete in a wide-gap concentric cylinder rheometer Part II. Influence of mineral additions and chemical admixtures on the shear thickening flow behaviour.* Cement and Concrete Research, 2009. **39**(3): p. 171-181.
9. Billberg, P. and K.H. Khayat. *Use of Viscosity-Modifying Admixtures to Enhance Robustness of SCC*. in *The Third North American Conference on the Design and Use of Self-Consolidating Concrete*. 2008. Chicago, Illinios.
10. Khayat, K.H., *Viscosity-enhancing admixtures for cement-based materials - An overview.* Cement & Concrete Composites, 1998. **20**(2-3): p. 171-188.
11. Lachemi, M., et al., *Self-consolidating concrete incorporating new viscosity modifying admixtures.* Cement and Concrete Research, 2004. **34**(6): p. 917-926.
12. Stirmer, N. and I.B. Pecur, *Mix design for self-compacting concrete.* Gradevinar, 2009. **61**(4): p. 321-329.
13. Su, N., K.C. Hsu, and H.W. Chai, *A simple mix design method for self-compacting concrete.* Cement and Concrete Research, 2001. **31**(12): p. 1799-1807.
14. Leemann, A. and F. Winnefeld, *The effect of viscosity modifying agents on mortar and concrete.* Cement & Concrete Composites, 2007. **29**(5): p. 341-349.
15. *The European Guide lines for Self-Compacting Concrete*. 2005.
16. Bouras, R., M. Chaouch, and S. Kaci, *Influence of Viscosity-Modifying Admixtures on the Thixotropic Behaviour of Cement Pastes.* Applied Rheology, 2008. **18**(4): p. -.
17. Bonen, D. and S.P. Shah, *The effects of formulation on the properties of self-consolidating concrete*, in *Concrete Science and Engineering A Tribute to Arnon Bentur International RILEM Symposium* K. Kolver, et al., Editors. 2004, RILEM. p. 43-56.

18. Khayat, K.H., A. Ghezal, and M.S. Hadriche, *Factorial design models for proportioning self-consolidating concrete.* Materials and Structures, 1999. **32**(223): p. 679-686.
19. Hwang, S.D., K.H. Khayat, and O. Bonneau, *Performance-based specifications of self-consolidating concrete used in structural applications.* Aci Materials Journal, 2006. **103**(2): p. 121-129.
20. Lachemi, M., et al., *Influence of paste/mortar rheology on the flow characteristics of high-volume fly ash self-consolidating concrete.* Magazine of Concrete Research, 2007. **59**(7): p. 517-528.
21. Patel, R., et al., *Development of statistical models for mixture design of high-volume fly ash self-consolidating concrete.* Aci Materials Journal, 2004. **101**(4): p. 294-302.
22. ASTM, *ASTM C143 / C143M - 09 Standard Test Method for Slump of Hydraulic-Cement Concrete*. 2009, ASTM International: West Conshohocken, PA.
23. ASTM, *ASTM C1611 / C1611M - 09b Standard Test Method for Slump Flow of Self-Consolidating Concrete*. 2009, ASTM International West Conshohocken, PA.
24. Yang, E.H., et al., *Rheological Control in Production of Engineered Cementitious Composites.* Aci Materials Journal, 2009. **106**(4): p. 357-366.
25. Kasemchaisiri, R. and S. Tangtermsirikul, *Deformability prediction model for self-compacting concrete.* Magazine of Concrete Research, 2008. **60**(2): p. 93-108.
26. Boukendakdji, O., et al., *Effect of slag on the rheology of fresh self-compacted concrete.* Construction and Building Materials, 2009. **23**(7): p. 2593-2598.
27. El-Chabib, H. and M. Nehdi, *Effect of mixture design parameters on segregation of self-consolidating concrete.* Aci Materials Journal, 2006. **103**(5): p. 374-383.
28. Ghezal, A. and K.H. Khayat, *Optimizing self-consolidating concrete with limestone filler by using statistical factorial design methods.* Aci Materials Journal, 2002. **99**(3): p. 264-272.
29. Guneyisi, E. and M. Gesoglu, *Properties of self-compacting mortars with binary and ternary cementitious blends of fly ash and metakaolin.* Materials and Structures, 2008. **41**(9): p. 1519-1531.
30. Guneyisi, E., M. Gesoglu, and E. Ozbay, *Effects of marble powder and slag on the properties of self compacting mortars.* Materials and Structures, 2009. **42**(6): p. 813-826.
31. Sahmaran, M., I.O. Yaman, and M. Tokyay, *Transport and mechanical properties of self consolidating concrete with high volume fly ash.* Cement & Concrete Composites, 2009. **31**(2): p. 99-106.
32. Sonebi, M., *Applications of statistical models in proportioning medium-strength self-consolidating concrete.* Aci Materials Journal, 2004. **101**(5): p. 339-346.
33. Wu, Z.M., et al., *An experimental study on the workability of self-compacting lightweight concrete.* Construction and Building Materials, 2009. **23**(5): p. 2087-2092.
34. Khayat, K.H., J. Assaad, and J. Daczko, *Comparison of field-oriented test methods to assess dynamic stability of self-consolidating concrete.* Aci Materials Journal, 2004. **101**(2): p. 168-176.

35. Ng, I.Y.T., H.H.C. Wong, and A.K.H. Kwan, *Passing ability and segregation stability of self-consolidating concrete with different aggregate proportions.* Magazine of Concrete Research, 2006. **58**(7): p. 447-457.
36. Kwan, A.K.H. and I.Y.T. Ng, *Optimum superplasticiser dosage and aggregate proportions for SCC.* Magazine of Concrete Research, 2009. **61**(4): p. 281-292.
37. Sukumar, B., K. Nagamani, and R.S. Raghavan, *Evaluation of strength at early ages of self-compacting concrete with high volume fly ash.* Construction and Building Materials, 2008. **22**(7): p. 1394-1401.
38. Gesoglu, M. and E. Ozbay, *Effects of mineral admixtures on fresh and hardened properties of self-compacting concretes: binary, ternary and quaternary systems.* Materials and Structures, 2007. **40**(9): p. 923-937.
39. Sahmaran, M. and I.O. Yaman, *Hybrid fiber reinforced self-compacting concrete with a high-volume coarse fly ash.* Construction and Building Materials, 2007. **21**(1): p. 150-156.
40. Prasad, B.K.R., H. Eskandari, and B.V.V. Reddy, *Prediction of compressive strength of SCC and HPC with high volume fly ash using ANN.* Construction and Building Materials, 2009. **23**(1): p. 117-128.
41. Zhu, W. and J.C. Gibbs, *Use of different limestone and chalk powders in self-compacting concrete.* Cement and Concrete Research, 2005. **35**(8): p. 1457-1462.
42. Domone, P.L., *A review of the hardened mechanical properties of self-compacting concrete.* Cement & Concrete Composites, 2007. **29**(1): p. 1-12.
43. Andic-Cakir, O., et al., *Self-compacting lightweight aggregate concrete: design and experimental study.* Magazine of Concrete Research, 2009. **61**(7): p. 519-527.
44. Golaszewski, J., *Influence of Viscosity Enhancing Agent on Rheology and Compressive Strength of Superplasticized Mortars.* Journal of Civil Engineering and Management, 2009. **15**(2): p. 181-188.
45. Schindler, A.K., et al., *Properties of self-consolidating concrete for prestressed members.* Aci Materials Journal, 2007. **104**(1): p. 53-61.
46. De Schutter, G. and R.T. Committee, *Final report of RILEM TC 205-DSC: durability of self-compacting concrete.* Materials and Structures, 2008. **41**(2): p. 225-233.
47. Yazici, H., *The effect of silica fume and high-volume Class C fly ash on mechanical properties, chloride penetration and freeze-thaw resistance of self-compacting concrete.* Construction and Building Materials, 2008. **22**(4): p. 456-462.
48. Assie, S., *Durabilite Des Beton Autoplacants*, in *Laboratoire Matériaux et Durabilité des Constructions*. 2004, L'Institut National Des Sciences Appliquees De Toulouse: Toulouse. p. 249.
49. Assie, S., et al., *Durability properties of low-resistance self-compacting concrete.* Magazine of Concrete Research, 2006. **58**(1): p. 1-7.
50. Assie, S., G. Escadeillas, and V. Waller, *Estimates of self-compacting concrete 'potential' durability.* Construction and Building Materials, 2007. **21**(10): p. 1909-1917.
51. Nehdi, M.L. and M.T. Bassuoni, *Durability of self-consolidating concrete to combined effects of sulphate attack and frost action.* Materials and Structures, 2008. **41**(10): p. 1657-1679.

52. Persson, B., *Internal frost resistance and salt frost scaling of self-compacting concrete.* Cement and Concrete Research, 2003. **33**(3): p. 373-379.
53. Lowke, D., et al., *The potential durability of self-compacting concrete.* Beton-Und Stahlbetonbau, 2008. **103**(5): p. 324-333.
54. Shi, C.J. and Y.Z. Wu, *Mixture proportioning and properties of self-consolidating lightweight concrete containing glass powder.* Aci Materials Journal, 2005. **102**(5): p. 355-363.
55. ASTM, *ASTM C150 / C150M - 09 Standard Specification for Portland Cement* 2009, ASTM International: West Coshohocken, PA.
56. ASTM, *ASTM C618-05 Standard Specification for Coal Fly Ash and Raw or Calcined Natural Pozzolan for Use in Concrete*. 2005, ASTM International: West Conshohocken, Pa.
57. ASTM, *ASTM C136-06 Standard Test Method for Sieve Analysis of Fine and Coarse Aggregates*. 2006, ASTM International: West Conshohocken, PA.
58. ASTM, *ASTM C128 - 07a Standard Test Method for Density, Relative Density (Specific Gravity), and Absorption of Fine Aggregate*. 2007, ASTM International: West Conshohocken, PA.
59. ASTM, *ASTM C566 - 97(2004) Standard Test Method for Total Evaporable Moisture Content of Aggregate by Drying* 1997, ASTM International: West Conshohocken, PA.
60. ASTM, *ASTM C702 - 98(2003) Standard Practice for Reducing Samples of Aggregate to Testing Size.* 1998, ASTM International: West Conshohocken, PA.
61. ASTM, *ASTM C117 - 04 Standard Test Method for Materials Finer than 75 µm (No. 200) Sieve in Mineral Aggregates by Washing.* 2004, ASTM International: West Conshohcken, PA.
62. ASTM, *ASTM C33 - 11 / C33M - 11 Standard Specification for Concrete Aggregates.* 2003, ASTM International: West Conshohocken, PA.
63. ASTM, *ASTM C192 - 07 / C192M - 07 Standard Practice for Making and Curing Concrete Test Specimens in the Laboratory.* 2007: West Conshohocken, PA.
64. ASTM, *ASTM C1064 - 08 / C1064M - 08 Standard Test Method for Temperature of Freshly Mixed Hydraulic Cement Concrete.* 2008: West Conshohocken, PA.
65. ASTM, *ASTM C231 - 04 / C231M - 04 Standard Test Method for Air Content of Freshly Mixed Concrete by the Pressure Method.* 2004: West Conshohocken, PA.
66. ASTM, *ASTM C138 - 07 / C138M - 07 Standard Test Method for Density (Unit Weight), Yield, and Air Content (Gravimetric) of Concrete* 2007: West Conshohocken, PA.
67. ASTM, *ASTM C39 / C39M - 05e2 Standard Test Method for Compressive Strength of Cylindrical Concrete Specimens*. 2005, ASTM International West Conshohocken, PA.
68. ASTM, *ASTM C469 - 10 / C469M - 10 Standard Test Method for Static Modulus of Elasticity and Poisson's Ratio of Concrete in Compression.* 2002, ASTM International: West Conshohocken, PA.
69. ASTM, *ASTM C78 - 08 / C78M - 08 Standard Test Method for Flexural Strength of Concrete (Using Simple Beam with Third Point Loading).* 2008, ASTM International: West Conshohocken, PA.

70. ASTM, *ASTM C597 - 09 Standard Test Method for Pulse Velocity Through Concrete.* 2009, ASTM International: West Conshohocken, PA.
71. ASTM, *ASTM C617 - 09a Standard Practice for Capping Cylindrical Concrete Specimens.* 2009, ASTM International: West Conshohocken, PA.
72. ASTM, *ASTM C1202 - 09 Standard Test Method for Electrical Indication of Concrete's Ability to Resist Chloride Ion Penetration.* 2009, ASTM International: West Conshohocken, PA.
73. ASTM, *ASTM C666 - 03(2008) / C666M - 03(2008) Standard Test Method for Resistance of Concrete to Rapid Freezing and Thawing.* 2008, ASTM International: West Conshohocken, PA.
74. ASTM, *ASTM C215 - 08 Standard Test Method for Fundamental Transverse, Longitudinal, and Torsional Frequencies of Concrete Specimens* 2008, ASTM International: West Conshohocken, PA.
75. ASTM, *ASTM C1293 - 08b Standard Test Method for Determination of Length Change of Concrete Due to Alkali Silica Reaction.* 2008, ASTM International: West Conshohocken, PA.
76. ASTM, *ASTM C1260 - 07 Standard Test Method for Potential Alkali Reactivity of Aggregates (Mortar Bar Method).* 2007, ASTM International: West Conshohocken, PA.
77. ASTM, *ASTM C1567 - 08 Standard Test Method for Determining the Potential Alkali Silica Reactivity of Combinations of Cementitious Materials and Aggregate (Accelerated Mortar Bar Method)* 2008, ASTM International: West Conshohocken, PA.
78. Johnson, R.A., *Miller & Freund's Probability and Statistics for Engineers*. 7th Edition ed. 2007: Pearson Prentice Hall.
79. Siddique, R., *Properties of Self-Compacting Concretes Containing Class F Fly Ash.* Materials in Engineering. 2011. **32**: p. 1501-1507.
80. K. Audenaert, V.B., G. De Schutter, *Chloride Penetration In Self Compacting Concrete by Cyclic Immersion*, in *1st International Symposium on Design, Performance and Use of Self-Consolidating Concrete*, C.S. Zhiwu Yu, Kamal Henri Khayat, Youjun Xie, Editor. 2005, RILEM Publications: Changsha, Hunan, China. p. 355-362.
81. K. M. A. Hossain, M.L., *Fresh, Mechanical, and Durability Charachteristics of Self-Consolidating Concrete Incorporating Volcanic Ash.* Journal of Materials in Civil Engineering, 2010. **22**(7): p. 651-657.
82. Hela, R., *Durability of Self Consolidating Concrete (SCC)*, in *1st International Symposium on Design, Performance and Use of Self-Consolidating Concrete*, C.S. Zhiwu Yu, Kamal Henri Khayat, Youjun Xie, Editor. 2005, Rilem Publications: Changsha, Hunan, China. p. 347-354.
83. ASTM, *ASTM C457-08 Standard Test Method for Microscopical Determination of Parameters of the Air-Void System of Hardened Concrete* 2008, ASTM International: West Conshohocken, PA.
84. Khayat, K.H., *Optimization and performance of air-entrained, self-consolidating concrete.* ACI Materials Journal, 2000. **97**(5): p. 526-535.